MIKRONIEK

PROFESSIONAL JOURNAL ON PRECISION ENGINEERING

2018 (VOL. 58) ISSUE 5

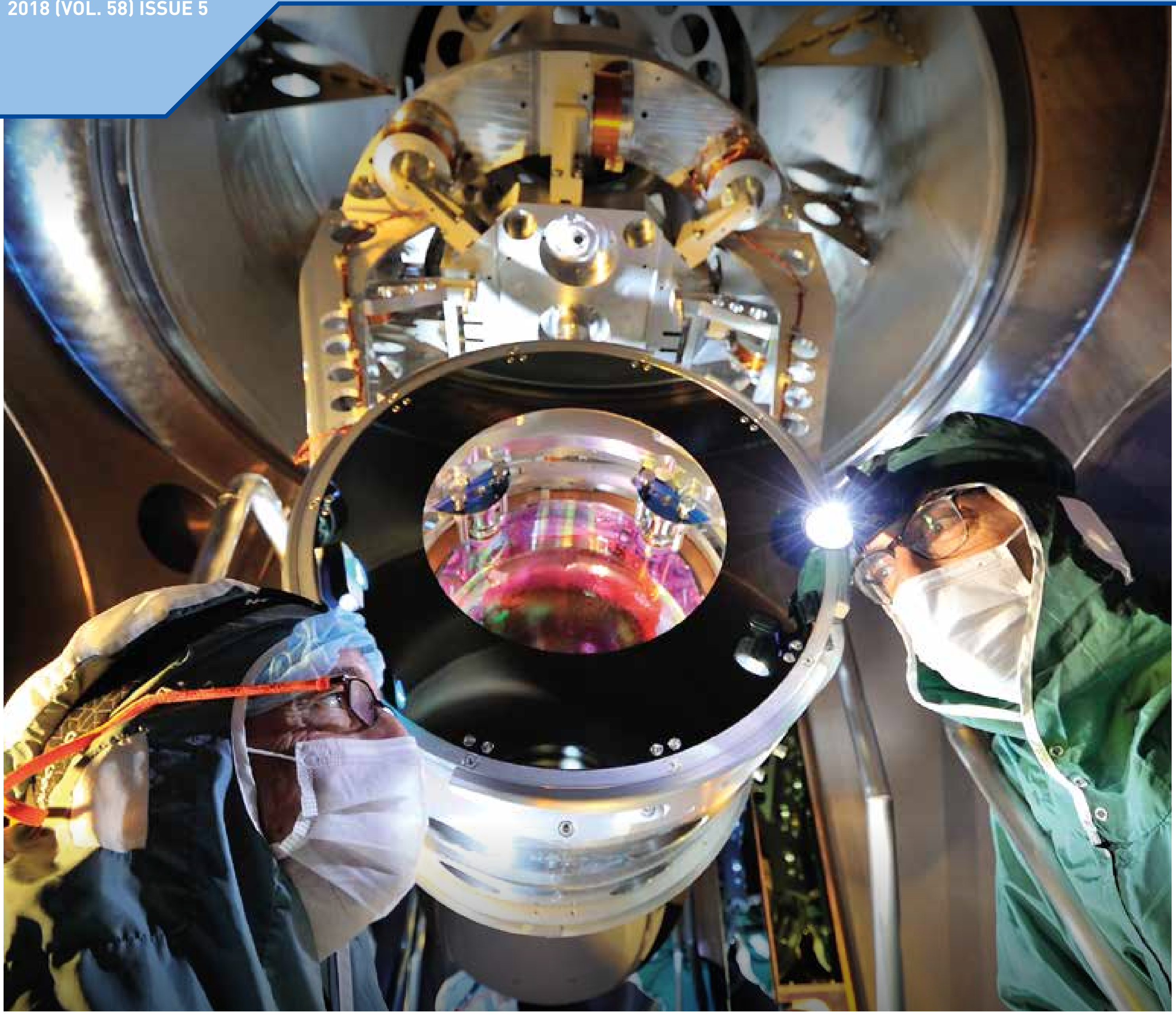

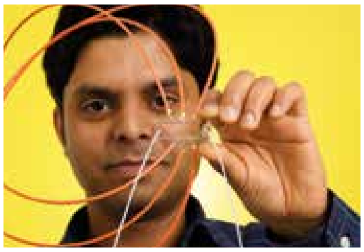

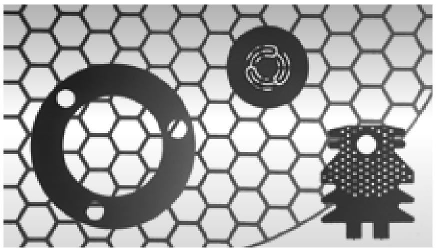

- THEME: BIG SCIENCE
- PRECISION FAIR 2018 PREVIEW
- MICRO-OPTOFLUIDICS
- SWISS WATCH FEATURING DUTCH PRECISION

DSPE

MIKRONIEK IS A PUBLICATION OF THE DUTCH SOCIETY FOR PRECISION ENGINEERING WWW.DSPE.NL

PUBLICATION INFORMATION

Objective
Professional journal on precision engineering and the official organ of DSPE, the Dutch Society for Precision Engineering. Mikroniek provides current information about scientific, technical and business developments in the fields of precision engineering, mechatronics and optics. The journal is read by researchers and professionals in charge of the development and realisation of advanced precision machinery.

DSPE
YOUR PRECISION PORTAL

Publisher
DSPE
Annemarie Schrauwen
High Tech Campus 1, 5656 AE Eindhoven
PO Box 80036, 5600 JW Eindhoven
info@dspe.nl, www.dspe.nl

Editor
Hans van Eerden, hans.vaneerden@dspe.nl

Advertising canvasser
Gerrit Kulsdom, Sales & Services
+31 (0)229 – 211 211, gerrit@salesandservices.nl

Design and realisation
Drukkerij Snep, Eindhoven
+31 (0)40 – 251 99 29, info@snep.nl

Subscription
Mikroniek is for DSPE members only.
DSPE membership is open to institutes, companies, self-employed professionals and private persons, and starts at € 80.00 (excl. VAT) per year.

Mikroniek appears six times a year.

ISSN 0026-3699

The main cover photo (representing an input mirror of Advanced Virgo, suspended from a super-attenuator) is courtesy of Maurizio Perciballi. Read the article on page 5 ff.

IN THIS ISSUE

THEME: BIG SCIENCE

28

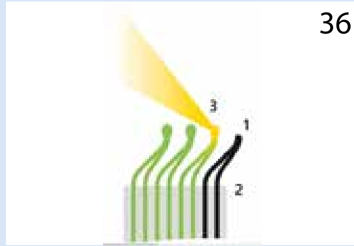

36

FEATURES

BIG SCIENCE, BIG OPPORTUNITIES

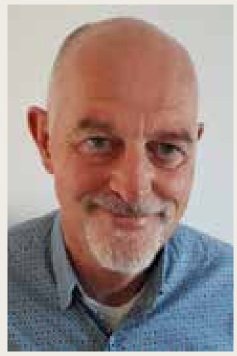

A lot has changed since Galileo Galilei pointed his simple telescope at the sky and discovered Jupiter's four largest moons around 1609. It's possible to regard this event as the start of what we now call modern science. In some respects, you could also think of it as the start of 'Big Science'. New discoveries are made and new insights gained on the basis of observations. Instruments are required for the purposes of these observations, as are specialists capable of designing and building them. Galileo was dependent on a lens-maker in the Low Countries for his telescope.

That principle hasn't changed, as we still need new instruments to be able to make new discoveries, as well as physicists and engineers to design and build them. Nevertheless, the instruments are getting ever bigger, more expensive and technologically complex. This is certainly the case in astronomy, or in particle physics. A telescope like the one used by Galileo no longer suffices if we're looking to discover planets around stars other than our own sun.

The first European organisations for the joint development, construction and operation of large-scale research facilities were set up in the 1950s and 1960s: CERN, for nuclear research; ESO, for large astronomical observatories on earth; and the European Space Agency ESA. The Netherlands was in the vanguard of all these initiatives and is still continuously contributing to further developments. Large particle accelerators, vast telescopes containing mirrors several dozen meters in diameter, and large scientific satellites are too expensive to be funded by a single nation. European cooperation – and in many cases global cooperation – is the order of the day.

Thus ensuring that Big Science continues to produce spectacular scientific results and data that can be worked on for years to come, ultimately leading to Nobel Prizes. The Netherlands funds the facilities in conjunction with other European nations, and a proportion of this contribution is recouped in the form of assignments awarded to high-tech industry. Hence Big Science is a firm route to innovation, even if the path to practical applications for society is sometimes long and those applications are usually not predictable.

What is clear, however, is that groundbreaking science is increasingly reliant on industry. In order to bridge the gap between science and high-tech industry, industrial liaison officers (ILOs) are active within scientific institutes. They draw companies' attention to the opportunities that exist in terms of capitalising on possible assignments (tenders) from Big Science organisations, and give some of the guidance when it comes to securing those assignments. Thus contributing to improving the 'geographic return' on our national contributions.

It's far from easy, though; the scientific community is a demanding customer, and when developing entirely new, complex technology companies are running more risks than usual, sometimes spanning many years too. And so the onus is on the government to create facilities to mitigate the risks, thereby giving considerable impetus to innovation driven by curiosity. The Dutch ILO-net – which is the network of ILOs and part of the Netherlands Organisation for Scientific Research (NWO) – is doing its utmost to reinforce the connection between the business community and Big Science, along with a large number of other parties active in this area. This issue of Mikroniek gives several examples of the challenges being worked on at present ...

Gerard Cornet
Policy officer SRON, coordinator ILO-net
g.cornet@sron.nl, www.bigscience.nl

Note
The Netherlands contributes around 150 million euros each year for the construction of large-scale infrastructure through its membership of CERN, ESO, ESA and several other Big Science organisations. The aim is to 'earn back' at least 70% of that amount in the form of assignments put to Dutch industry.

HOW TO MEASURE SUB-Å DISPLACEMENTS ON THE EARTH-JUPITER DISTANCE

Recent joint observations of gravitational waves from binary black hole and neutron star mergers have demonstrated the potential of a global network of interferometers. The unprecedented accuracy in the source localisation, achieved with a network of only three detectors, has made multi-messenger astrophysics a reality. This article gives an overview of the measurement principle and instrumentation of the detectors, with a focus on the thermal compensation system needed to achieve the highest possible sensitivity in the coming years.

ALESSANDRO BERTOLINI AND ERIC HENNES

The discovery of gravitational waves (GWs) originating from merging black holes in 2015 and 2016 [1] [2] with the two LIGO detectors in the USA was awarded the 2017 Nobel Prize in Physics. During the first joint observations with the Virgo detector near Pisa in Italy (Figure 1) in 2017, another GW signal from a binary black hole merger was observed by all three interferometers [3], the first significant GW signal ever recorded by Virgo.

Three days later, the merger of two neutron stars was detected for the first time [4]. About seventy electromagnetic telescopes, both space-borne and Earth-based, also observed the event; each in its own wavelength range varying from X-rays to radio waves. This allowed for the second identification ever of a kilonova, a brief burst of electromagnetic radiation that is characteristic for the synthesis of heavy-element nuclei. Presently, both LIGO and Virgo are being further upgraded towards the next joint observation period starting in early 2019. Their final versions, coined Advanced Virgo [5] and Advanced LIGO, will be simply called Virgo and LIGO, respectively, hereafter.

Detector operation principle

Gravitational waves arise during events in the cosmos in which large masses undergo extreme accelerations. They cause ripples in space-time that propagate outward at the speed of light, and were conceived by Einstein in 1916 as a direct result of his general theory of relativity [6]. GWs are transverse waves that stretch the space along one axis while squeezing it along the perpendicular axis (and vice versa). They can be observed by measuring the distance between test masses in free-fall, which is just what a Michelson interferometer is suitable for (Figure 2a). Here, the mirrors and beam splitter serve as test masses.

1

Aerial photo of Virgo, the gravitational-wave detector with its 3-km-long arms.

AUTHORS' NOTE

Alessandro Bertolini and Eric Hennes are both working at Nikhef (Dutch National Institute for Subatomic Physics) on the instrumentation of gravitational-wave detectors.

a.bertolini@nikhef.nl
e.hennes@nikhef.nl
www.nikhef.nl

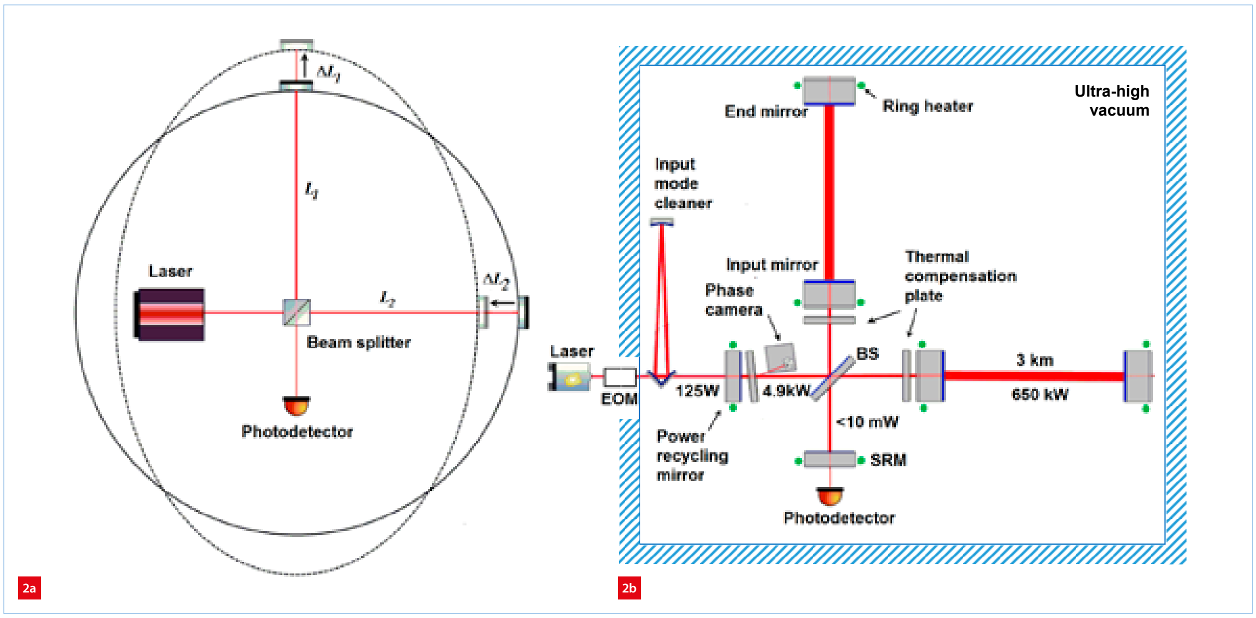

Gravitational wave-detection principle.
(a) Effect of a GW that passes perpendicular to a Michelson interferometer. It deforms the space in such a way that one arm becomes shorter and the other longer, as a result of which the intensity of the light on the photodetector is modulated.
(b) A somewhat detailed optical layout of Virgo. The laser beam first passes the electro-optic modulator (EOM), followed by a 144-m triangular resonator, the so-called input mode cleaner. It filters out jitter noise and all laser modes other than the Gaussian TEM_{00} mode. Each interferometer arm consists of a 3-km-long optical resonator formed by an input mirror (which is also output) and an end mirror. This effectively increases the arm length by a factor of 280 (see text for explanantion). Thanks to the Power Recycling and Signal Recycling mirrors (PRM and SRM), the signal-to-noise ratio of the photodetector signal is further enhanced. Almost all components are placed in ultra-high vacuum and equipped with vibration isolation. On several locations a small quantity of light is tapped to measure the position and orientation of the mirrors to an accuracy of 1 nm and one nrad, respectively.

A GW impinging on the surface of the interferometer makes one arm longer by ΔL_1, for example, while the other arm becomes shorter (ΔL_2) and vice versa. The degree of space strain at any time is defined as $h(t) = (\Delta L_1 - \Delta L_2)/L$, where $L = L_1 = L_2$ is the length of the interferometer arms. As a consequence, the two reflected light beams recombining at the beam splitter show a mutual phase shift $\varphi = 4\pi Lh/\lambda$, where λ is the laser wavelength; λ = 1,064 nm for both LIGO and Virgo. φ is measured as a change in intensity of the light on the photodetector according to:

$$P_{out} = \frac{P_L}{2}\left[1 + \cos\left(\varphi_0 + \frac{4\pi L}{\lambda}h\right)\right] \qquad (1)$$

Here, P_L is the laser power. In practice, the detectors are operated close to the dark-fringe condition ($\varphi_0 \approx (2n + 1)\pi$, with n an integer), in order to suppress as much as possible the effect of laser power fluctuations that could mimic a signal.

Increasing the signal strength

The amplitude of GWs is inversely proportional to the distance to the source. The expected GW strain h from distant sources is therefore very small, in the order of 10^{-22} m/m, which is less than 1 Å on the Earth-Jupiter distance. To enhance the detector response, the interferometer arms are replaced by Fabry-Pérot optical resonators, called arm cavities, in which the photons travel back and forth many times before recombining at the beam splitter (Figure 2b). In this way, we benefit from the long timescale of the signal phase, milliseconds, compared to the round-trip time of the light in the arms (~20 μs).

At Virgo, the input mirrors (Figure 3) have a transmission coefficient of T_s = 1.4%, enhancing the arm length effectively by a factor of $4/T_s$ = 280 to L_{eff} = 840 km. For a GW of frequency f_{GW} the phase shift per unit of GW strain h is given by:

$$\frac{d\varphi}{dh} = \frac{4\pi L}{\lambda}\frac{L_{eff}/L}{\sqrt{1+(f_{GW}/f_c)^2}}, \; f_c = c/2\pi L_{eff} \qquad (2)$$

Equation 2 is valid for $\lambda_{GW} >> 2L$, or in this case, $f_{GW} << 50$ kHz and shows that the amplification factor L_{eff}/L (280 for low frequencies) gradually decreases above the cut-off frequency, f_c = 57 Hz, down to 1.6 at around 10 kHz.
A second way to enhance the signal strength is to increase the light power on the beam splitter. This is realised with the same laser source, as follows. In the dark-fringe state all the light energy is reflected back towards the laser. If we place an extra mirror, the Power Recycling Mirror (PRM), between the laser and the beam splitter (Figure 2b), most of this light is reinjected into the interferometer.

The position of the PRM is chosen such that the reinjected light interferes constructively with the 'fresh' light from the

3

Input mirror of Advanced Virgo, suspended from a super-attenuator. The mirror is the last element of a chain of horizontal and vertical vibration isolators, all housed in a 10-m-high ultra-high vacuum tower. The black ring in front of the mirror is a light baffle, meant to prevent stray light to re-enter the interferometer. On the photo Maurizio Perciballi (left) and Ettore Majorana. (Photo: Maurizio Perciballi)

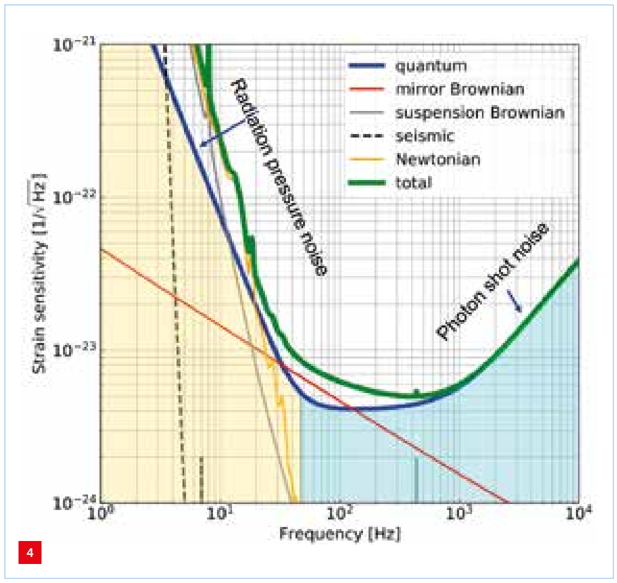

4

Expected noise budget of Advanced Virgo, shown as the amplitude spectral density, ASD(f), of the various contributions to the noise in the measuring signal. The unit (1/√Hz) indicates that the value of ASD(f) is the RMS of the noise signal per unit bandwidth, i.e. when measured with an analyser having a bandwidth of 1 Hz.

laser. In this way, another optical resonator arises: the Power Recycling Cavity. For Virgo the achieved power cycling in this cavity is almost 40 times the entrance power.

Another technique, signal recycling, will be used to further increase the response of the interferometer to GWs. This is done by placing another mirror, the Signal Recycling Mirror, between the beam splitter and the photodetector (Figure 2b). Just as for power recycling, this forms an optical resonator in combination with the rest of the system, as a result of which the signal is enhanced even further.

Detector control by laser beam modulation

In order to keep the position and orientation of all mirrors nicely aligned during operation, linear and angular steering actuators are constantly controlling their position and orientation. The required control signals are generated by sending the laser beam, before injecting it into the interferometer, through an electro-optic modulator (EOM). This results in several sidebands at selected frequencies such that each of them is resonant or anti-resonant in one or more cavities. Demodulating the cavity beams provides the required error signals on all mirrors.

Noise sources and their suppression

Figure 4 shows contributions to the amplitude spectral density $ASD(f)$ of the detector noise. A GW signal with frequency f and strain amplitude h is measurable if $h >> ASD(f) / \sqrt{t}$, with t the time duration of the signal. We discuss some noise sources.

Quantum noise

The resolution of the detector is fundamentally limited by the quantum nature of light. The number of photons per unit time that reaches the photodetector obeys a Poisson distribution with mean $\langle N \rangle = P_{out} /(\hbar\omega)$ and standard deviation $\sqrt{\langle N \rangle}$. Here, ω is the angular frequency of the photons and $\hbar$ the reduced Planck's constant. This results in a contribution to the GW strain noise, called shot noise, with a level linearly increasing with frequency (Figure 4), and inversely proportional to the light power impinging on the beam splitter.

A second type of quantum noise is generated by the multiple reflections of photons in the arm cavities. Each photon carries momentum $2\pi\hbar/\lambda$, and transfers momentum $4\pi\hbar/\lambda$ to the mirror on each reflection. Collectively, the photons exert a force on the mirror. Due to the random timing of the reflections, this force shows a fluctuation with an RMS amplitude proportional to the square root of the optical power circulating in the arms. The mirrors are suspended on a chain of pendulums to satisfy the free-fall condition as closely as possible. Above the natural frequency of the suspension, these force fluctuations give the mirror a white acceleration noise.

As a result of this second type of noise, the position of the mirror and with it the measurement signal, h, exhibits a noise spectrum with an amplitude proportional to $1/f^2$ (Figure 4). This so-called radiation pressure noise limits the sensitivity of the detector at low frequencies.

Note that at larger optical power, the signal-to-noise ratio increases for shot noise, but decreases for radiation pressure noise.

Figure 4 shows that below and above 40 Hz (the frequency regions marked in yellow and light blue, respectively) the quantum noise is dominated by radiation pressure and shot noise, respectively. Regarding the total noise, Figure 4 also shows that quantum noise limits the sensitivity of the current detectors above about 150 Hz. Below this frequency the noise is dominated by thermal fluctuations in the mirror coating (down to 30 Hz). Thermal fluctuations elicit internal dissipation processes that, in turn, generate a Brownian motion of the mirrors. At lower frequencies, thermal noise in the suspension wires and Newtonian noise (see below) are limiting factors. Thanks to the vibration isolation, the seismic noise is negligible above ~4 Hz.

Seismic noise

Microseismic vibrations above 10 Hz exhibit amplitudes of an order of magnitude of 1 nm. Maybe not much, but still ten orders of magnitude too strong to measure the mirror displacements induced by a GW (10^{-19} m). Fortunately, seismic vibrations in all degrees of freedom can be successfully suppressed by suspending all mirrors and other optic components (except the laser) from vibration isolators consisting of complex multi-stage and multi-dimensional mechanical filters [7] [8].
Seismic vibrations have another effect on the mirrors: they cause fluctuations in the local gravitational acceleration (g), both in size and direction, which in turn generate force fluctuations on the mirrors. This Newtonian noise (NN) can be mitigated by placing arrays of seismometers around the mirrors so that the seismic profile of the environment can be determined. This enables the estimation of the NN forces on the mirror and consequently their effect on the measured signal. This contribution can then be subtracted from the GW signal using suitable algorithms [9]. The GW group at Nikhef in Amsterdam is leading the efforts to develop this system for the next upgrade of Virgo [10].

Towards larger optical power and sensitivity

One of the upgrade activities at Virgo is the gradual increase of the injected laser power from 13 to 125 W, thus reducing the shot noise by a factor of three. That is no mean feat, as the beam intensity in the power recycling and arm cavities will increase up to 5 and 650 kW, respectively.

Effect of thermal expansion
The fraction of light power absorbed in the test masses, i.e. the mirrors at each end of the arm cavities, is about 0.5 ppm. Despite this state-of-the-art low figure, it is not negligible. At the highest input laser power up to 400 mW of heat is deposited in each of these mirrors, mainly in the reflective coating, near the optical axis. This causes axial and radial temperature gradients up to several Kelvin (see Figure 5a). The corresponding non-uniform material thermal expansion will alter the curvature of the high-reflectivity surfaces, causing loss of concentricity in the arm cavities.

Thermo-optic effect
A much larger effect of the thermal gradients arises in the Power Recycling Cavity (PRC), whre the beam passes each Input Mirror substrate twice per circulation.
The corresponding non-uniform change in the material refractive index n ($dn/dT \neq 0$) changes the optical path length (OPL) through the mirrors according to:

$$\Delta OPL_M(x,y) = 2\frac{dn}{dT}\int_0^{t_M} \Delta T(x,y,z)\,dz = \Delta OPL_{uniform} + \Delta OPL_{spatial}(x,y) \quad (3)$$

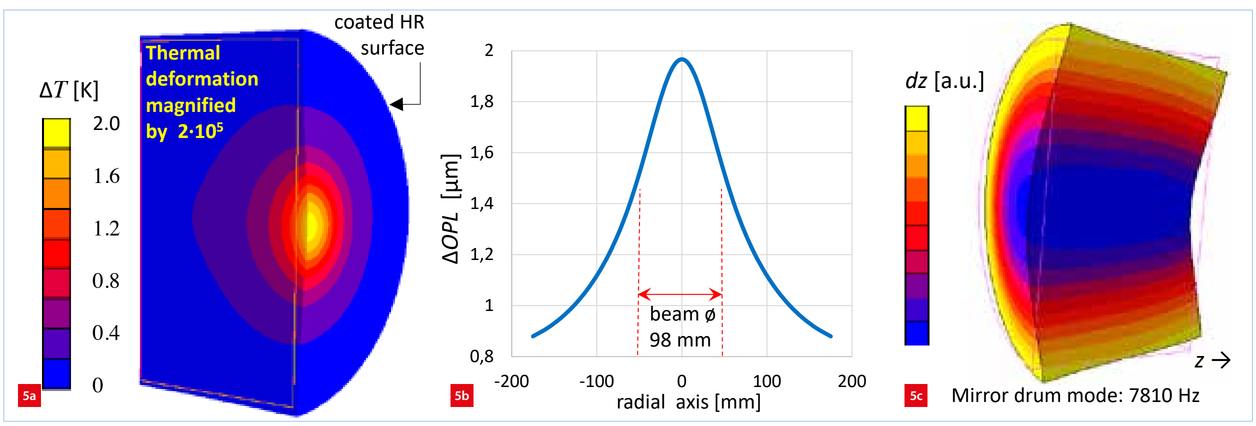

Effect of light absorption in an input mirror at full interferometer power.
(a) Temperature distribution inside the mirror. The 2.5-kW PRC beam is incident from the left side, passing the 20 cm thick substrate, and is internally reflected from the coated right face. The 650-kW arm cavity beam is incident from the right side. The deformation due to thermal expansion is at most 60 nm.
(b) Corresponding optical path length increase (ΔOPL) due the thermo-optic effect. It has a uniform and a spatially varying contribution of about 0.9 µm and 1.1 µm, respectively, the last of which creates a thermal lens with a focal length of about 5 km. Compare this to the radius of curvature of the coated surface, 1.5 km, equal to half of the arm length.
(c) The global temperature increase, here ~0.2 K, is inferred from the measured mirror's drum mode frequency shift (~0.88 Hz/K) with mHz precision.

Here, z is the optical axis coordinate, t_M is the mirror thickness, and $\Delta T(x,y,z)$ its temperature increase distribution. At full laser power both contributors to ΔOPL may raise up to a micron, i.e. one wavelength (see Figure 5b). The uniform term in Equation 2 can be corrected by the linear alignment control, for instance by moving the Power Recycling Mirror slightly towards the beam splitter.

The spatial term in Equation 2 is responsible for the so-called thermal lensing: it disturbs the passing wavefront profile, and this has consequences for both the laser carrier and some of the resonant sidebands. The carrier is resonant in all cavities, the sidebands are resonant in the PRC cavity only. For both carrier and sidebands the electromagnetic field entering the interferometer is prepared by the injection system in an almost pure TEM_{00} Gaussian mode, with size and divergence parameters precisely matching the fundamental resonant mode of both PRC and arm cavities.

While raising the laser power, the aberrations due to thermal lensing will spoil this match, causing a significant fraction of the power in the PRC cavity to leak out from the fundamental mode into higher-order optical modes. The lower carrier power directly increases the shot noise contribution to the detector's sensitivity (see section on quantum noise), while the reduced sideband power deteriorates the interferometer's control signals, putting its stability at risk. Moreover, the interference between the two arms of the detector becomes noisy due to the significant light power, stored in higher-order modes (so-called junk light), that reaches the interferometer photodiode.

Thermal compensation system

In Virgo a Thermal Compensation System (TCS) is provided to correct for all these effects [11]. The TCS consists of several types of wavefront sensors and non-contacting thermal actuators. The sensors measure the spatial profile of optical path length distortions, $\Delta OPL(x,y)$, the actuators introduce extra *OPL* profiles such that the distortions are cancelled, except for some uniform contribution.

Thermal lensing actuators

The main thermal actuator is realised by placing a thin glass plate, called compensation plate (CP), in front of each Input Mirror (see Figure 2b). A suitable compensating thermal lens is created by shining the plate with an annularly shaped CO_2 laser beam profile, the wavelength of which, $\lambda = 10$ µm, is strongly absorbed by the glass (see Figure 6a).
The outer section of the plate heats up, increasing the path length through the plate at larger radii, thus compensating the increased path length in the central part of the mirror. The ring shape is obtained by passing the original Gauss beam from the CO_2 laser through an axicon-type lens.

More complexly pixelated compensation patterns can be achieved by selectively scanning the CO_2 beam over the CP surface, such that the average intensity of the laser can be adjusted pixel by pixel. This allows to correct any distortion profile, including those caused by so-called 'cold' defects in the mirrors. Cold defects are imperfections in the surface profile and local variations in the refractive index due to non-perfect production and polishing of the mirror substrates.

In principle, these corrections can also be achieved by locally heating the mirror itself with the CO_2 laser beam. However, this method was discarded for Virgo as it would inject to much mirror displacement noise caused by intensity fluctuations of the CO_2 laser.

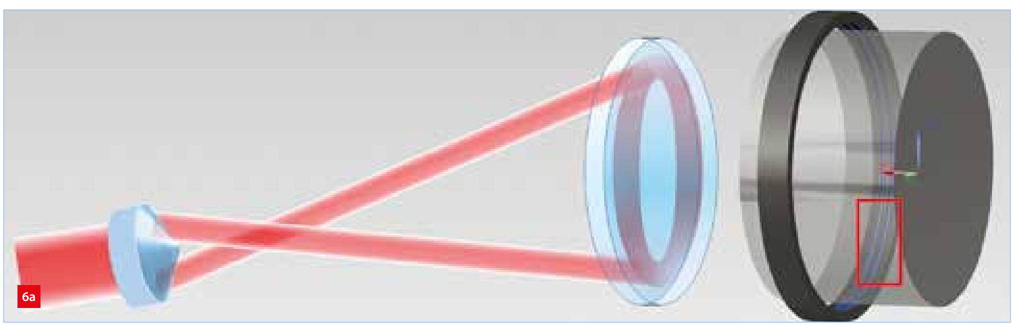

Thermal lensing actuators.
(a) Construction sketch of an annular CO_2 laser beam with a conically shaped axicon lens, shining on a 30-mm-thick compensation plate in front of the 42-kg Virgo Input Mirror (ø 350 mm, thickness 200 mm), thus establishing a negative-focus lens. The mirror is surrounded by a ring heater.
(b) Photo of a ring heater section (red box on the left) as viewed from the mirror barrel, showing two heating wires wound around a glass tube, all inside the thermal shield.

A second type of thermal actuator, a ring heater, is installed around all four test masses (Figure 2b and 6). The ring heater is an infrared-light radiator consisting of a coil of manganin wire wound on a glass support and a reflector to enhance the efficiency. Unlike the CP, it heats (part of) the mirror itself, not only changing the substrate path length profile by thermal lensing, but also the mirror surface radius of curvature (ROC) by thermal expansion. The last effect allows correction of both 'cold' and 'hot' ROC mismatches. Thanks to the TCS the radii of curvature of the test masses can then be tuned and kept constant within a meter over the nominal 1.5 km, independent of the power circulating in the interferometer.

Wavefront sensors

Measurement of the wavefront distortion introduced by each arm cavity mirror is realised by using Hartmann sensors [12] (Figure 7). The image reflected by the mirror, illuminated with an auxiliary low-coherence light-probe beam, is projected onto a mask with an array of pin holes; the position of the image of each pin hole, a light spot, on a CCD camera placed behind the plate, linearly depends on the local angle of incidence of the wavefront of the incoming beam. Once a reference image, e.g. in cold conditions, has been acquired, thermally induced distortions can be observed with nanometer-level accuracy. In Virgo, six Hartmann sensors are installed to measure distortion on all test masses, on the input mirrors even on both sides.

Complementary to the Hartmann sensors is the phase camera that allows to spatially image the intensity and phase distribution of each frequency component of the laser field circulating in the Power Recycling Cavity (PRC), both carrier and sidebands (Figure 8). The operation is based on spatially overlapping a reference light beam, sampled from the injection system, with a light beam sampled at (x,y) from the PRC beam profile. The two beams interfere and their beating power is measured by a fast photodetector. The amplitude and phase of each beat note, corresponding to carrier and sidebands, are then extracted by means of digital signal processing in an FPGA.

Images of the total profile are generated by scanning the sampled beam over a pin-hole placed in front of the photodetector. The phase camera is not able to distinguish contributions from individual optics, but – unlike the Hartmann sensors – it is sensing the interferometer beam itself, and performs absolute measurements. In Virgo, three phase cameras are installed, designed and built by Nikhef [13].

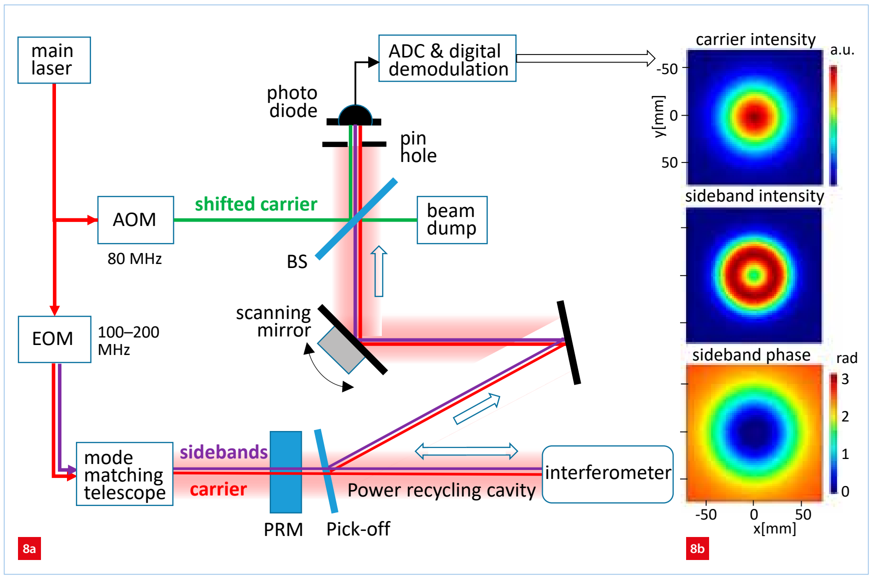

The phase camera.
(a) Optical scheme. The electro-optic modulator (EOM) generates sideband pairs. The acousto-optic modulator (AOM) shifts the carrier frequency, enabling to distinguish the sidebands of each pair after demodulation. The pick-off plate reflects the beam of interest towards a piezo-driven scanning mirror that sweeps the beam over the pin-hole in front of the photodiode. The beating diode signal is digitised and demodulated to generate intensity and phase images of all components.
(b) Typical intensity and phase contour plots, simulated using Oscar, a code toolbox for optical cavities by J. Degallaix.

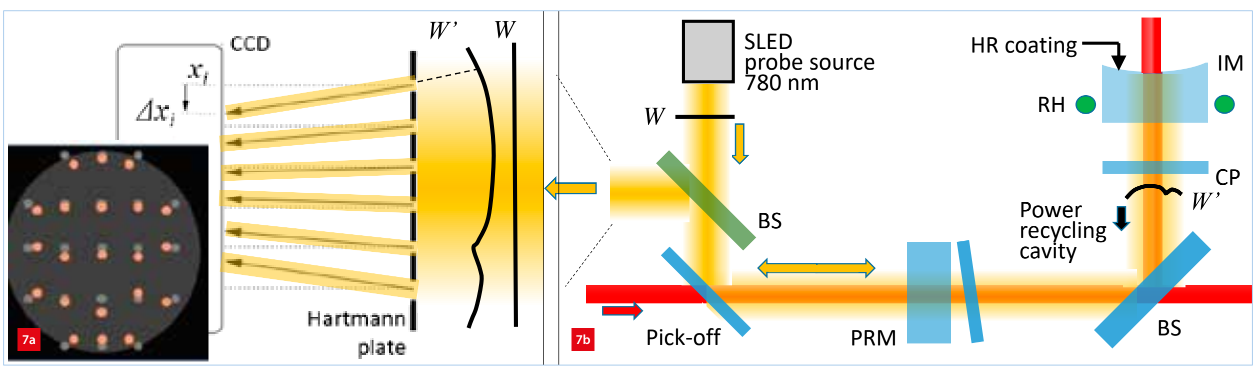

Principle of wavefront distortion measurement.
(a) Sketch of a Hartmann sensor. A well-defined flat wavefront W is imaging, by diffraction, every pin hole i (ø 150 µm) in the perforated Hartmann plate (30 x 30 holes) on position (x_i,y_i) of a CCD camera. A disturbed wavefront W' will shift the images by ($\Delta x'_i$,$\Delta y'_i$), from which the corresponding optical path length change (ΔOPL) is derived.
(b) A probe source beam is sent along the main laser beam, enters the power recycling cavity and is directed towards a Virgo Input Mirror (IM). After transmission through the IM substrate and reflection on its coated, high-reflective back side, it is sent to the Hartmann sensor. This allows to measure distortions caused by the combined thermal lensing and expansion of the IM and its compensation plate. The optical scheme relies on carefully selected transmission and reflection properties which are dependent on both wavelength and angle of incidence.

Looking ahead

In the coming years, the worldwide network of interferometers will be expanded with the Japanese detector KAGRA and a LIGO detector in India. The sensitivity of LIGO and Virgo will be further improved to make optimum use of the existing facilities. For example, intensive R&D campaigns have started to improve the mirror coatings, and to realise so-called squeezed light injection, an advanced trick to selectively reduce the phase or amplitude components in the quantum noise (which satisfy Heisenberg's uncertainty principle) as a function of the frequency.

With granted financial support from the European Community, the Province of Limburg, Nikhef and others, a large R&D facility called ETpathfinder will be founded in Maastricht, the Netherlands, hopefully next year.

The results of all these efforts pave the way for the third generation of detectors such as the underground Einstein Telescope (ET) [14], with which the inflation of the universe shortly after the Big Bang will come within reach.

REFERENCES

[1] C. van den Broeck, *NTvN* 83-01, 2017.
[2] J. van den Brand, *NTvN* 83-05, 2017.
[3] B.P. Abbott, et al., *Phys. Rev. Lett.* 119, 141101, 2017.
[4] B.P. Abbott, et al., *ApJL* 848, L12, 2017.
[5] F. Acernese, et al., *arXiv*:1408.3978v3, 2014.
[6] A. Einstein, *Ann. der Phys*. 49, 769, 1916.
[7] S. Braccini, et al., *Astroparticle Phys.*, vol. 23, 557-565, 2005.
[8] M.G. Beker and E. Hennes, *Mikroniek* 52(4), 2013.
[9] M.G. Beker, et al., *Gen. Relativ. Grav.* 43, 623-656, 2011.
[10] S. Koley, et al., *First Break* 35, 71-78, 2017.
[11] A. Rocchi, et al., *J. Phys.: Conf. Ser.* 363, 012016, 2012.
[12] A.F. Brooks, et al., *Opt. Express*, vol. 15, no. 16, 2007.
[13] L. van der Schaaf, et al., *J. Phys.: Conf. Ser.* 718, 072008, 2016.
[14] *www.et-gw.eu*


Precision Systems
KMWE
Precision Components
Always on the cutting edge of excellence
SLM 280
• Machining
• Assembly
• Additive Manufacturing
• Sheet Metal Fabrication
• Thermal Spraying
• Engineering
in
f
You Tube
visit us at booth 49
www.kmwe.com

INSTRUMENTATION FOR SPACE

Space travel has always been very appealing to people. With the Leiden Instrument Makers School (LiS) located in the heart of the Dutch aerospace community, it was obvious for LiS to take this up. With the help of an investment from the Regional Investment Fund and contributions from local government, (research) institutions and the business community, the 'Instrumentation for Space' programme was set up to train students who are specialised in designing and building instrumentation for space travel and astronomy.

1 *The Dutch lunar rover with Oliver Bentley (LiS student, middle), Jerre Sweers (SSI, right) and Maneesh Verma (SSI & TU Delft, left).*

In the past it turned out that students after graduation often still needed a long-term training course to learn to deal with all the requirements that are customary in the space industry. With the extra attention paid to these aspects, the LiS and its partners hope to deliver students who can be deployed almost immediately or at least with much less internal training.

The specialisation will take shape through an optional module, small additions to the regular programme and extra attention to the procedures applicable in space travel during space- and astronomy-related graduation projects. In addition, the partners have promised to regularly provide assignments that can be carried out by LiS students.

Lunar rover

An example of such an assignment is the construction of the Dutch lunar rover (Figure 1), which is to be launched in 2019, in collaboration with Delft University of Technology (TU Delft) and Stellar Space Industries (SSI). The components of the engineering model were made by LiS students, and the intention is that this will also be the case for the flight model.

Aerospace specialists

The expertise of specialists at various aerospace companies and institutions, such as Airbus, ISIS, Lens R & D, NLR, NOVA, SRON, SSI and TNO, is used for the development of the elective module. Experts from these parties will not only help with the development of education, but they are also supposed to give guest lectures, so that the curriculum that the students are presented with will stay up-to-date. It is expected that the optional module will be offered in 2019 for the first time to the students of the LiS.

EDITORIAL NOTE

This contribution was received from LiS.

INFORMATION
WWW.LIS.NL

FROM FIRST LIGHT TO THE ASSEMBLY OF GALAXIES

The James Webb Space Telescope (JWST), the largest space observatory ever constructed, is awaiting the journey to its final destination, to unravel some of the biggest mysteries of astronomy. With 6.5 meter the primary mirror of JWST exceeds the collective imaging area of the famous Hubble Space Telescope by almost a factor of 7, thus increasing resolution significantly. JWST is extra special because of its dedicated infrared observing capabilities. This article focuses on the Dutch JWST content in the Mid Infrared Instrument.

GABBY AITINK-KROES

The evolution of space observatories is slow but impressive. The famous Hubble Space Telescope (HST) was launched in 1990 and just recently put on hold because of gyroscope failure. Its successor, the James Webb Space Telescope (JWST), is to be launched in 2021. Over this period of thirty years, the diameter of the primary mirror has changed from 2.5 to 6.5 meter, yielding a nearly sevenfold increase of the collective imaging area (Figure 1).

JWST is a joint international mission (NASA/ESA/CSA) involving scientists and engineers from all over Northern America and Europe. On board, the Integrated Science Instrument Module (ISIM) is the heart of the observatory, housing the four science instrument of JWST (Figure 2). Each instrument has its dedicated function targeting a specific wavelength range. This combination offers images and spectra at several resolutions for various fields of view at a wavelength range from 0.6 to above 25 micron. The instruments are mounted into a dedicated support which is then mounted to the JWST support structure, behind the primary mirror.

AUTHOR'S NOTE

Gabby Aitink-Kroes worked for over twenty years as a mechanical systems lead engineer at NOVA-ASTRON; the NOVA Optical InfraRed Instrumentation group of ASTRON, the Netherlands Institute for Radio Astronomy, based in Dwingeloo, the Netherlands. Recently, she joined the Netherlands Institute for Space Research, SRON.

g.aitink-kroes@sron.nl
www.astron.nl/nova

The following instruments are on board:
- The combined Fine Guidance Sensor/Near-InfraRed Imager and Slitless Spectrograph – FGS/NIRISS
- The Near-Infrared Camera – NIRCam
- The Near-Infrared Spectrograph - NIRSpec
- The Mid-Infrared Instrument – MIRI

Mid Infrared Instrument

From the Dutch perspective, the prime instrument on board is the Mid Infrared Instrument (MIRI), which as the name suggests is specifically targeting the mid-infrared wavelength range. MIRI is being built by: ESA, the MIRI consortium (a collaboration of nationally funded European institutes), the Jet Propulsion Laboratory (JPL) and NASA's Goddard Space Flight Center (GSFC). It provides imaging and spectroscopy over the 5-28 micron wavelength range by dedicated modules.
In the Netherlands, NOVA-ASTRON, together with TNO and SRON developed, designed and realised part of the spectrometer. MIRI comprises two main modules: MIRIM and MRS (Figure 4).

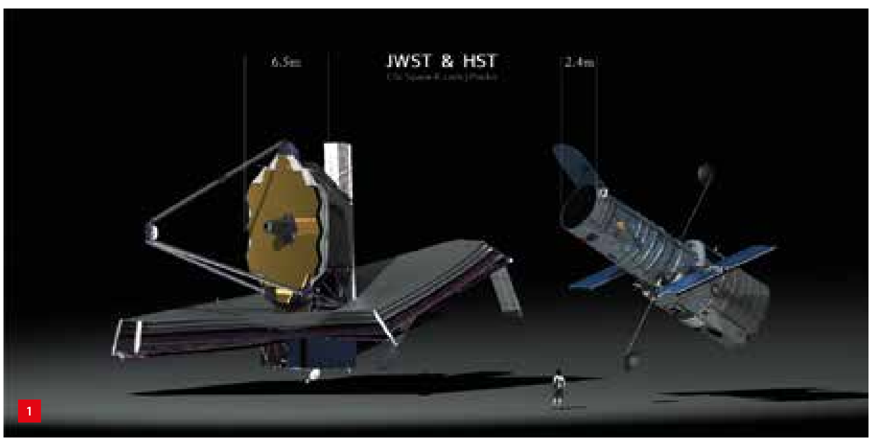

1 *The Hubble Space Telescope (HST) versus the James Webb Space Telescope (JWST). (Image: NASA)*

2 *JWST's Integrated Instrument Science Module with its instruments: MIRI (left, wrapped in aluminium-coated multi-layer insulation), in the centre NIRCam at the front and GFS in the back, and NIRSpec (right). (Image: NASA)*

Astronomy – Science with JWST

Astronomy – the knowledge of the universe – is one of the oldest natural sciences, dating back to antiquity. Modern astronomy started with Galilei, who was the first to use technology for sky observations. He pointed a self-built version of the 'kijker' at the sky. The Dutch spectacle maker Lippershey tried to obtain the first patent for this two-lens telescope a little earlier in 1609. This was soon followed by the rapidly increasing size and quality of the telescopes thus improving on resolution, contrast and reduced observing times. An impressive suite of revolutionary scientific instruments allows observations to cover a wide wavelength range from the ultra-short gamma rays to very long radio waves. In a relatively short time this has offered new insights and discoveries that revealed the diversity and extent of the universe.

The James Webb Space Telescope (JWST) is being built to specifically target the infrared wavelength and aims at unravelling some of the biggest mysteries of astronomy through four main science targets:

- First light & reionisation:
  Understanding the emergence of the first sources after the 'dark ages of the universe' is critical as they act as seeds for the later formation of larger objects, such as galaxies.
- Assembly of galaxies:
  Observing galaxy formation and evolution and comparing the faintest, earliest galaxies to today's enormous array of different galaxies in size and shape. Trying to understand how galaxies assemble over billions of years.
- Star birth & protoplanetary systems:
  Understanding how stars and planets are created by observations of planets and left-over debris around (young) stars. Trying to understand how they evolve and release the heavy elements they produce back into space for recycling into new generations of stars and planets.
- (Exo) planets & origins of life:
  Observing the atmospheres of extrasolar planets, and perhaps even finding the building blocks of life elsewhere in the universe. In addition to other planetary systems, also studying objects within our own solar system.

Galaxy, star and planet formation particularly take place inside dense gas and dust regions. The longer wavelength of infrared light makes it possible to see what happens inside (and behind) these regions as it penetrates through the clouds, contrary to visible wavelengths (Figure 3).
Far away galaxies emit radiation at shorter wavelengths, but will be observed in the infrared region. This is because of the Doppler Effect; as the cosmos expands the signal is elongated in wavelength, causing the so-called 'red shift'.

The 'pillars of creation' in the Eagle nebula.
(a) In visible wavelengths. (Image: NASA/ESA/Hubble Heritage Team (STScI/AURA)/J. Hester, P. Scowen (Arizona State University).
(b) In infrared wavelengths. (Image: NASA/ESA/Hubble Heritage Team (STScI/AURA)).

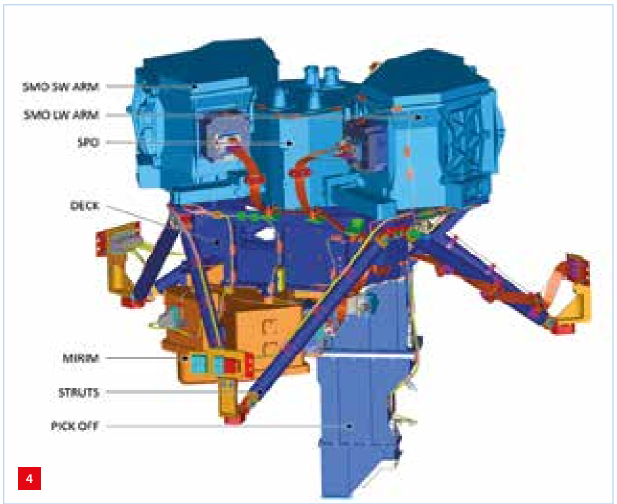

The Mid InfraRed Instrument (MIRI) with the spectrometer (top), the deck that connects the modules to the CRFP struts (middle), and the imager and pick-off mirror assembly (bottom). (Image: MIRI consortium)

MIRI Image Module (MIRIM)
The camera module provides wide-field broadband images that will continue the astrophotography that has made Hubble famous. The spectrograph module will enable medium-resolution spectroscopy to provide new physical details of the distant objects it will observe. The specially developed arsenic-doped silicon detectors provide yet unknown levels of sensitivity and are used in both the imaging as well as the spectroscopic module.

Medium Resolution Spectrograph (MRS)
The MRS is an Integral Field Unit (IFU) grating spectrograph. The IFU allows extended objects to be studied in more detail. The image is cut into several slices, these slices are laid out side by side in one long line that is offered to the spectrograph as a single (pseudo) slit. Each slice (also called slitlet) is then optically dispersed by a grating and imaged side by side onto the detector. This results in separate spectra for each discreet part (strip) of the extended objects.

In order to cover the full wavelength range with a minimum of observations the MRS consists of four channels used simultaneously, each covering in total one fourth of the full wavelength range. Per channel, one single exposure samples one third (called a sub-spectrum) of the specific range. So a full 5-28 μm spectrum requires three exposures, providing in total 12 sub-spectra (3 exposures x 4 channels). For each sub-spectrum a dedicated grating is provided

Structurally, the MRS is divided into two subsystems: the Spectrometer Pre-Optics (SPO) and the Spectrometer Main Optics (SMO). The previously discussed IFU is part of the pre-optics. The pre-optics also splits the light in four specific wavelength ranges, using dichroics on a rotating selection mechanism. This mechanism also selects the corresponding gratings to disperse the light. The main optics consists of the collimators and camera systems for the four channels.

Spectrometer Main Optics (SMO)
In the Netherlands, NOVA-ASTRON together with TNO and SRON developed, designed and realised the SMO. The early interaction between the optical and mechanical design together with high-level design choices resulted in a very compact and seemingly simple layout.

The SMO has two arms (Figure 5): SMO-SW for the short-wave channels 1 and 2, and SMO-LW for the long-wave channels 3 and 4. The very low optical *f*-ratio (close to 1) and the shared optics allow a minimum number of components and a very compact design. The two arms are each other's mirror image with respect to the mirror plane (dotted line) through the mechanism (GWA) axes.

This mirror symmetry and the symmetry through the centre plane (centre line) of the camera optics allow the camera mirrors and central support to be identical. The FF top, bottom and baffles are mirror images. Because the arms are very similar one arm was fully designed and tested while the other arm followed with little effort after proof of design, providing advantages in design effort and hence cost and schedule.

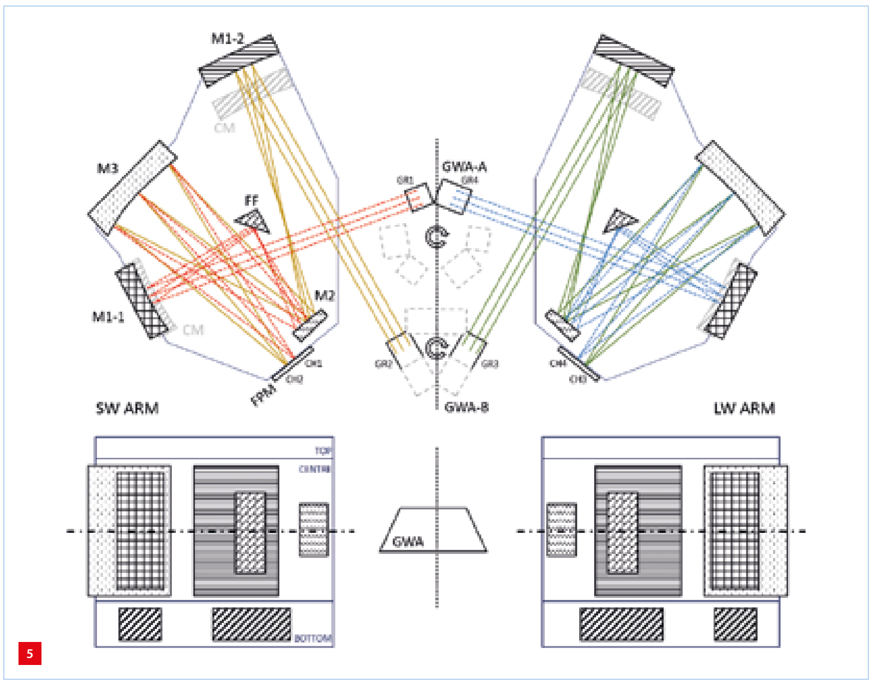

The SMO layout showing the SW arm (left) and LW arm (right) , from the top and the front. Two channels reside in each box. Each channel has its own collimator mirror (CM) in the bottom and a separate first mirror (M1-1 and M1-2) of the three-mirror anastigmat camera system in the central support. The 'FF' folds one channel onto the shared last two mirrors (M2 and M3) of the camera system and the detector (FPM). So, a channel enters the SMO at bottom level and is reflected by its CM onto the GWA at central level. The dispersed beam is then imaged onto the FPM by the camera system. The two 3-position grating wheels GWA-A and GWA-B contain the 2x3 gratings, one for each sub-spectrum, in the SPO on top of the selection mechanism. (Image: NOVA-ASTRON, UK-ATC)

Design solutions

Cryogenics

Any object having a temperature emits energy in the form of electromagnetic radiation. In order to minimise the instrumental radiation emission interfering with the infrared measurements, a cryogenic operating temperature of 7 K is required, which added interesting challenges to the instrument design.

Cooling the observatory is one problem, facing the effects of the cooling itself on the performance is another. In general the material properties (thermal expansion coefficient (*CTE*), heat capacity, E-moduli, refractive indices, etc.) of various materials change differently and in a (highly) nonlinear fashion during cooling. These varying material properties not only cause geometrical changes. The *CTE* differences between the various materials can cause misalignments, deformations and even breakage. In addition, other optical differences are caused by changes in the refractive indices.

The basic build material of MIRI and thus the SMO is aluminium (more specifically EN-AW 6061); while for the other instruments an exotic material with a high stiffness-to-mass ratio was selected. Within the MIRI consortium there is extensive experience with the use of aluminium and this was considered a low(er) risk. This 6061 alloy is very suitable for use in cryogenic instrumentation due to its high long-term stability and can be used for structures as well as mirrors. Although it is one of the metals with the highest *CTE* its relatively low density and workability allow very mass-efficient designs. Special heat treatment like precipitation hardening and intermediate artificial ageing steps were used to increase strength and remove most of the internal stresses.

Kinematic mounts

Optical mounts should provide and maintain highly accurate but stress-free mounting in all circumstances. Special kinematic mountings constrain exactly six degrees of freedom (DoFs) of rigid-body motion of the mirror. Effectively, the optical surface is decoupled and thus unsusceptible to material stresses, non-flatness of mechanical interfaces and differential thermal shrinkage. To release or constrain specific DoFs most commonly a set of three symmetric leaf springs or pivot hinge constructions at the circumference are used. The hinges could be integrated in the mirror and/or support structure. This type of hinges provides a minimum of hysteresis and wear.

To survive the launch loads the first natural frequency of a fully mounted mirror had to be above 200 Hz. The fully kinematic mounts as used in the past were not stiff enough.

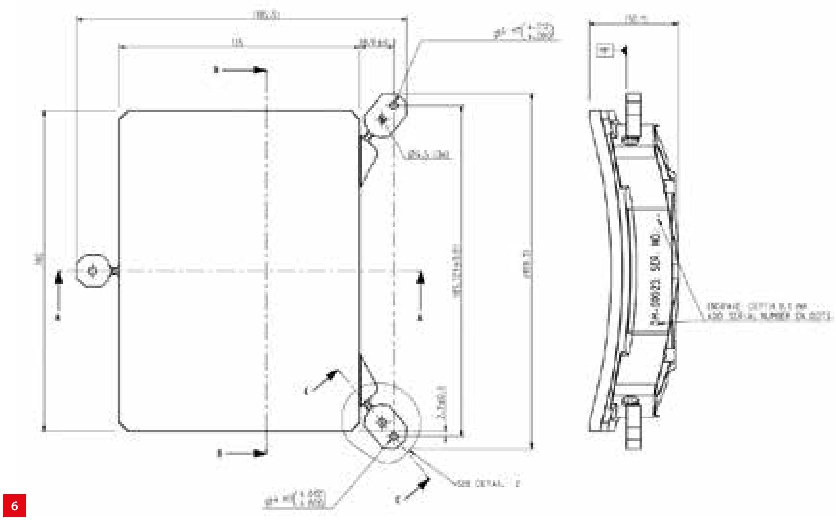

6

The SMO MIRI mirror with quasi iso-static mounting lugs. (Image: NOVA-ASTRON)

The simplest solution was to remove the radially oriented translation DoF per mounting point. This resulted in a local pivot point at each lug-to-mirror connection allowing each lug to rotate freely (Figure 6). However, this left the mirror overconstrained. The similar material of the mirror and the support structure, the slow cool down and the accurate machining were considered sufficient to allow this quasi-static mounting scheme. All in all the first natural frequency of the mounted mirror was lifted to a very comfortable 1,200 Hz.

Accuracy and alignment

Contrary to the traditional practice of alignment during assembly, for the SMO a 'no-adjustment' philosophy is adopted. Components are positioned by means of the accurately machined mounting and alignment features and no active alignment will take place. A much more stable instrument is provided, without risks of wandering adjustments and a significant reduction in assembly and test time is achieved.

Parts, mirrors and also each arm are mounted onto accurate surfaces and positioned by means of two dowel pins that reside in their respective dowel holes in the support (Figure 7). Two matching dowel holes are provided in the counterpart (mirror/arm) that slide over the pre-mounted pin. In theory this is again overconstrained, however when the dowel holes are accurately located, a relatively simple H7/h6/H7 fit for each pin is sufficient for effortless mounting and accurate positioning as well. It needs to be said that all pins function as locator only and not as sheer pin. The mounting screw provides sufficient pre-loading so that friction suffices, even during launch.

Separately manufactured interfaces contribute to the total error of a system, so the number of interfaces within the

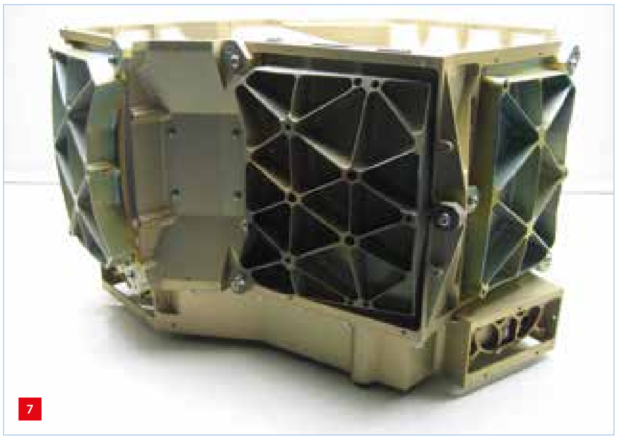

7

The SW arm. The open-back light-weighted mirrors are mounted with three bolts and two pins each. The largest optics are assembled onto the central support (from left to right: M1-2, M3 and M1-1) and the two (identical) collimator mirrors in the bottom (left and right). (Image: NOVA-ASTRON)

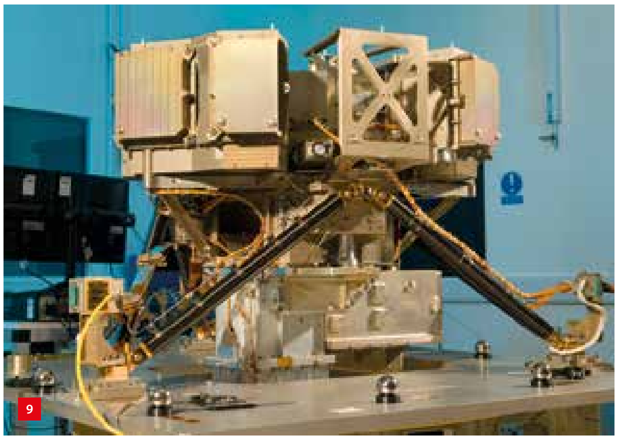

9

MIRI with the spectrometer (top), the deck that connects the modules with the CRFP struts (middle), and the imager and pick-off mirror assembly (bottom). (Image: MIRI consortium/STFC/RAL Space)

instrument was kept as low as possible. This concerns not only the interfaces in the final instrument, but also intermediate interfaces, e.g. with manufacturing tooling needs to be counted. The final interfaces are created in a single fixture, on a 5-axis milling machine, onto the pre-assembled structure (and pinned for re-assembly) to allow maximum accuracy. Interfaces are located at the outside circumference for accessibility, which was also very convenient during assembly and integration. Figure 7 shows the mirrors mounted at the circumference of the structure.

Analyses

The overall alignment performance depends strongly on the properties of both the optical and the mechanical design. The optical sensitivity analysis determined the effect of individual component misalignment (in all six DoFs) on the final image position and quality. However, the maximum feasible component misalignments were determined by means of mechanical tolerance analysis, while finite-element analysis determined the effects of environmental loading. The circle was closed in the end-to-end analysis, by merging the optical and mechanical effects in one analysis.

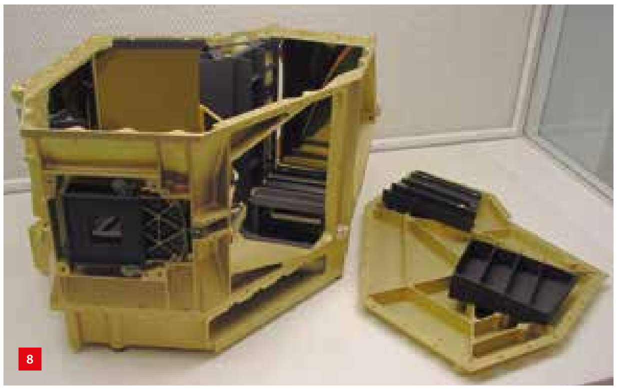

8

The SW arm in the cleanroom. The top is removed for visibility. The mirror surfaces are clearly visible as well as the baffles that were coated to reduce light scattering inside the arm. (Image: NOVA-ASTRON)

Conclusion

After manufacturing, it took only two days to fully assemble each arm (Figure 8). A test programme verified the image location as well as the focus position at ambient conditions for all the four images. This verification was repeated after each qualification test, like vibration testing, thermal cycling and zero-g testing. Each verification showed accurate alignment and no image deterioration at all.

After the SMO was assembled with the rest of MIRI testing under cryogenic conditions was performed. This again showed no changes with respect to the earlier tests. The images were located exactly on their nominally designated location. This ultimately proved the strength of the no-adjustment philosophy, not only for the SMO modules but for MIRI as a whole. Figure 9 shows the MIRI flight model after assembly, ready for take-off.

Appendix: The full JWST story in brief

The sheer size of the JWST observatory, together with the special remote location and particular operational wavelength range drove the many technologically challenges that were faced. Not just the complexity of the folding and the lightweight, but also the special operational requirements due to its wavelength coverage, posed several challenges on the design. New ideas were explored and adopted at both the telescope and instrument level.

At a special place

Observing from Earth is limited due to the atmosphere. Radiation is filtered, distorted and overpowered. This means that only a very limited piece of the electromagnetic spectrum can be observed from the Earth's surface. Professional observatories are mostly located at higher altitude (thinner atmosphere), at places with less air turbulence and shielded from human interference.

Avoiding the atmosphere is also a solution. JWST will therefore be located at a stable location behind the moon orbit; 1.5 million km away from earth. Here, the combined gravity of Sun, Earth and Moon results in a 1-year orbit around the Sun, just like Earth exhibits (for reference: Hubble resides at a humble 570 km altitude). At this position, JWST has an undisturbed view into deep space and a continuous line of sight to Earth, which is advantageous for communication purposes.

Complexity

JWST faces very demanding requirements. Besides the brutal transport through launch, the observatory needs to survive a huge range of temperatures. Crucially, a telescope's sensitivity is directly related to the size of the mirror area. Unfortunately, JWST in its fully deployed state is far too large to fit in any spacecraft. Folding and lightweighting (Figure 10) are needed to allow transport by even the world's largest available rocket, ESA's Ariane 5A.

JWST overview. (Images: NASA/Chris Gunn)
(a) The flight telescope structure with the backplane that holds the primary mirror segments.
(b) The fully assembled telescope of JWST fully folded.

(Un)folding

JWST is held together by a special foldable structure made from low-density graphite composite material. A special trussed design provides stiffness and strength at a very low total mass. The primary mirror is formed by 18 hexagonal beryllium mirror segments mounted onto the backplane of the telescope structure. Each segment measures ~1.3 m, from flat to opposite flat. The material choice and the lightweight open backplane structure reduce the mass of each segment to only 20 kg. For comparison, this is only one-tenth of the mass of Hubble's mirror per unit area. Six actuators per segment provide fine alignment of each mirror segment after launch, a seventh actuator at the centre is used to adjust the curvature.

Passive cooling

Although space is quite cold, the influence of radiation from external heat sources like Sun and Earth is tremendous. In order to get and keep the observatory cold enough, the telescope is protected by its own big parasol. A tennis-court-size, 5-layer sunshield provides permanent shading (Figure 11), each layer blocking and deflecting heat away from the telescope. This allows the telescope to 'passively' cool down to approximately 40 K. At the Sun-facing side the solar panels, all communication equipment and the heat-generating components are located.

The unfolded 5-layer sunshield, measuring 21.2 m in length and 14.2 m in width. The Sun-facing side of each layer is coated with high-emissivity silicon for radiation blocking. The other side is coated with pure aluminium to bounce the energy away from in between the layers. The shield will be folded up to stow away for launch. At the cold side a temperature of 40 K can be reached by just shading. (Image: Northrop Grumman)

Active cooling

Unfortunately, the 40 K achieved by the passive cooling is not sufficient for the mid-infrared wavelength. Further cooling to 7 K is required, so additional cooling is provided by a two-step process: a Pulse Tube pre-cooler brings the temperature down to 18 K, and a Joule-Thomson Loop heat exchanger knocks it further down to 7 K.

Conclusion

The instruments, telescope, sunshield and spacecraft have been assembled, integrated and tested extensively. Test campaigns at operational conditions (in an extremely large vacuum cryogenic tank) typically last for three months, while scientists perform scheduled experiments around the clock. Currently, the launch of JWST is set for 2021, although at this stage any mishap can cause further delay. This is because, unlike Hubble, the JWST cannot be repaired and its functioning must be 'first time right'.

‘FLYING BRAIN’

The ‘crew’ of the Horizons Mission, which embarked this summer for the International Space Station (ISS), has the CIMON astronaut assistant (Crew Interactive Mobile Companion) on board. This scientific project is the first artificial intelligence (AI) application for the ISS. The free-flying technology demonstrator is intended to support astronauts during routine work by, for example, displaying procedures or offering solutions to problems. CIMON is driven by Faulhaber servo motors.

The mission companion is intended to, among other things, lighten the load during daily routine work and to function as an early warning system in the event of technical problems. CIMON’s screen displays a friendly face, its voice and the AI make it a ‘colleague’ to the crew members, with whom it can engage in a true dialogue. The artificial assistant was developed on behalf of the Space Agency in the German Aerospace Center (DLR) by Airbus in Friedrichshafen.

Free-floating

The astronaut assistant of the CIMON project is approximately the same size as a medicine ball and weighs about five kilogrammes. In zero gravity, if floats freely in space and, on command, flies to the astronaut who needs its help. It moves by means of fourteen small propellers which transport it to the desired position and keep it there. They are driven by brushless DC servo motors of the 0824 series from Faulhaber and controlled with speed controllers of the SC1801 series. The motors were selected on account of their reliability and longevity with very small dimensions, low weight and low energy consumption.

Experimenting

The Horizons Mission of the German ESA astronaut Alexander Gerst will last from June to December 2018. The AI of the technology demonstrator was developed using, among other things, voice samples and photos of him. Gerst will perform three tests with the mission companion: the astronaut and his assistant will experiment with crystals, together solve the Rubik’s cube and perform a complex medical experiment in which CIMON will announce the individual steps and serve as an ‘intelligent’ flying camera. While Gerst will return to earth at the end of the mission, the artificial helper will remain on board and lend assistance during future missions.

EDITORIAL NOTE

This contribution was based on a press release from Faulhaber.

INFORMATION

WWW.DLR.DE
WWW.NASA.GOV/MISSION_PAGES/STATION
WWW.FAULHABER.COM

1 Faulhaber supplied brushless DC servo motors from its 0824 series (inset) for CIMON, the artificial crew member of the ISS. (Photos: DLR/T. Bourry/ESA, Faulhaber)

DYNAMICS OF THE 'BIGGEST EYE ON THE SKY'

The preparations for the design and construction of the Extremely Large Telescope (ELT) are in full swing. One of the most critical components of this enormous telescope is its segmented primary mirror (M1), for which TNO, in collaboration with VDL, has designed the mechanical segment support in the period 2015-2016. The dynamic performance of the structure has been validated experimentally.

GERT WITVOET, JAN NIJENHUIS AND LUKAS KRAMER

Introduction

The new mechanical segment support (M1SS) design [1] is based on the previous M1SS prototypes developed in 2009-2010 [2], but includes several enhancements to further improve its performance. Specific design drivers were, among others, the serviceability of the M1SS, the introduced surface form error at the segment, and the increased target values for the structural eigenfrequencies. The latter defines the dynamic performance of the structure (including the ~178-kg segment), which needed to be validated experimentally.

From the latest M1SS design one engineering model (EM) and six qualification models (QMs) have been manufactured recently, which have been tested intensively to verify their performance. Here, the test procedure employed to validate the dynamic behaviour, the dynamic tests and the results for one of the QMs are presented.

Test hardware and objectives

The primary mirror of the ELT will consist of 798 hexagonal segments, each 1.4 m wide, which together should form one smooth optical surface. The M1SS is the mechanical structure connecting the segments to the underlying telescope structure, but in such a way that the mirror segments never touch, and their optical surfaces are hardly effected by the change in gravity field when the telescope is rotating. Moreover, the M1SS should facilitate the use of active Position Actuators (PACTs) [4], with which each segment can be positioned in piston, tip and tilt directions.

Figure 1 shows a picture of one of the QMs of the ELT M1SS, which consists of a fixed frame (FF) and a removable segment assembly (SA). The structure holds a dummy segment with realistic mass and inertia on 27 support pads which, via a whiffletree construction consisting of two layers of tripods, is connected on three locations to a moving frame (MF). This MF is connected in 6 degrees of freedom (DoFs) to the FF, which interfaces with the telescope structure; the A-shaped folded leaf springs hold the three horizontal DoFs between FF and MF, the PACTs constrain the three vertical DoFs. Since the active PACTs are not part of the M1SS project, these actuators have been replaced by dummy PACTs in Figure 1.

Dynamic design targets

Given its purpose, the dynamic performance of the M1SS is defined by how well it can keep the segment in place with respect to the telescope structure below, which can be expressed in terms of structural eigenfrequencies. In the actual telescope these eigenfrequencies will of course largely depend on the dynamic properties of the telescope structure and the PACTs, but these are outside the scope of this project. To be able to zoom in on the performance of the M1SS itself and eliminate these unknowns, the telescope structure (or back structure) is therefore assumed to be infinitely heavy and stiff, and the PACT infinitely stiff.

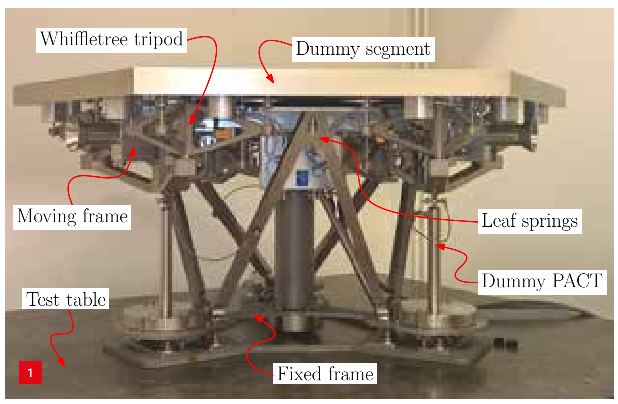

Picture of the test set-up, consisting of a 178.3-kg dummy segment on top of the M1SS, supported by stiff dummy PACTs. The whole set-up is mounted on a weakly supported 3-ton test table.

AUTHORS' NOTE

Gert Witvoet, Jan Nijenhuis and Lukas Kramer all work in the Optomechatronics department of TNO Technical Sciences in Delft, the Netherlands. Gert Witvoet is also a part-time assistant professor in the Control Systems Technology group at Eindhoven University of Technology, the Netherlands.

gert.witvoet@tno.nl
www.tno.nl/en/focus-areas/industry/expertise-groups

With these assumed boundary conditions, and based on the experience with the previous M1SS prototype [2], the following improved set of design targets have been formulated regarding the eigenfrequencies of the structure (consisting of both the M1SS and a mirror segment):

- the clocking mode, i.e. the rotation of the segment around the z-axis, should be higher than 30 Hz;
- the two lateral modes, i.e. the motion of the segment along the x- and y-axis, should be higher than 52 Hz;
- the tip and tilt modes, i.e. the segment rotation around the x- and y-axis, should be higher than 55 Hz;
- the piston mode, i.e. the segment translation along the z-axis, should be higher than 66 Hz;
- the first spurious mode, i.e. the seventh mode of the structure, should be higher than 85 Hz.

Note that the design challenge was to meet these values while the vast majority of the mass and inertia is located in the mirror segment, which typically weighs around 178 kg and is located roughly 0.67 m above the telescope structure. The objectives of the dynamic tests were to measure the first seven eigenfrequencies of the system, identify to which of the above mentioned modes they belong, and hence validate whether the above design targets are met by the QMs.

Test boundary conditions

As mentioned above, the dynamic behaviour of a system highly depends on the boundary conditions. For the dynamic tests to be representative, there are three particular elements of interest that effect the boundary conditions, namely the mirror segment, the back structure and the axial stiffness of the PACT.

An actual mirror segment was not available during the tests, hence an aluminum dummy segment has been manufactured, including dummy edge sensors, whose mass and inertia were carefully matched with the actual mass and inertia of a reference ELT mirror segment. The mass of this dummy segment, including interface pads, focus compensation, lateral support and dummy edge sensors, was validated by measurement to be 178.3 kg, which differs only 0.14% from the targeted value. This has been considered a negligible difference.

The characteristics of the back structure, i.e. the 'fixed world' below the M1SS, is equally important. Without any back structure or a very light structure the eigenfrequencies will be significantly higher, which is not representative for the actual use of the M1SS. Or if the M1SS is mounted on an arbitrary flexible structure, the dynamics of this structure will be visible in the measured mode shapes of the M1SS.

To minimise these effects, during the tests the M1SS is mounted on a softly supported heavy stiff structure; in this case a 3-ton steel table, with a first deformation mode of around 140 Hz (much higher than the frequency range of interest), which is suspended on soft air mounts yielding suspension modes of about 1.5 Hz in all 6 DoFs. This situation resembles the 'infinitely heavy and stiff' back structure assumption as good as practically possible.

An infinitely stiff PACT boundary condition cannot be accomplished in reality; instead, axially stiff dummy PACTs have been used during the tests, which are essentially very stiff steel bars. Since these dummy PACTs are very straightforward, their axial stiffness could accurately be estimated by finite-element model (FEM) calculations to be 143 N/µm. This is much higher than the expected stiffness of the M1SS whiffletree, and hence as close as we can practically get to an 'infinitely stiff PACT interface'.

Methodology

To observe the dynamic behaviour of a mechanical structure as in Figure 1, in essence one needs to apply a force at an arbitrary location k and measure its response (translation, velocity or acceleration) at another location l. It is known that the transfer function between these points is the result of a modal superposition [3]:

$$H_{k,l}(s) = \sum_{i=1}^{\infty} \frac{\phi_{k,i}\phi_{l,i}}{s^2+2\beta_i\omega_i s+\omega_i^2} \quad (1)$$

Here, ω_i and β_i are the eigenfrequency and damping of the i-th mode, and $\phi_{j,i}$ is the j-th element of the i-th mode shape Φ_i. Since $\phi_{k,i}\,\phi_{l,i} = \phi_{l,i}\,\phi_{k,i}$ reciprocity holds, which implies that $H_{k,l}(s) = H_{l,k}(s)$, in other words, excitation and measurement locations can be swapped, yielding exactly the same transfer function. This reciprocity is utilised in the roving hammer technique, where the measurement location l is fixed, and the system is excited with an impact hammer on multiple locations k; then only $\phi_{k,i}$ in Equation 1 varies with k, which thus enables identification of multiple elements of the mode shape Φ_i. Below, this technique will be discussed in more detail.

Frequency response measurements

The procedure starts with obtaining reliable frequency response functions (FRFs) from the system. To this end the M1SS has been excited on various locations by hammer impacts and the resulting motion has been measured by accelerometers.

To correctly classify the modes later on (as clocking, lateral, tip/tilt or piston) one needs to be able to at least reconstruct the rigid-body motion of the segment at each mode, which implies that the segment needs to be excited on six strategic locations; these roving hammer locations, and their directions, are illustrated in Figure 2. This figure also shows the accelerometer locations (orange squares):

- sensor 1: on the side of the segment, measuring in $+y$-direction;
- sensor 2: on top of the segment, measuring in $+z$-direction;
- sensor 3: on top of the table, measuring in $+z$-direction;

In principle only one single accelerometer (and sufficient excitation locations) would suffice to reconstruct the mode shapes, but for redundancy reasons three accelerometers are used here. There is no a priori guarantee that all relevant modes are sufficiently observed by a single sensor, hence by generating three independent data sets we can average the results to improve the reliability.

Each measurement consists of ten identical hammer impacts on location k, which are averaged in the frequency domain to cancel out random effects. For each impact both the force $u_k(t)$ and resulting accelerations $y_l(t)$ are traced during and after the impact (for 10 s). The averaged FRF is then calculated via:

$$H_{k,l}(j\omega) = \frac{\sum_{i=1}^{10} S_{u_k y_l}(j\omega)}{\sum_{i=1}^{10} S_{u_k}(j\omega)} \qquad (2)$$

Here, S_{u_k} and $S_{u_k y_l}$ are the (windowed) auto- and cross-power density per impact.

Mode shape estimation

A first estimate of the actual eigenfrequencies can of course directly be read from the resonance locations in one of the measured FRFs $H_{k,l}(j\omega)$ (which is accurate up to the frequency resolution of the Fourier transform used in the analysis). To determine the mode shapes further data processing is needed. To do so, we make a parametric least-squares fit for each measured FRF between 25 and 75 Hz, consisting of six modes (since only six modes can be observed in this frequency range), which is of the form:

$$\bar{H}_{k,l}(s) = \sum_{i=1}^{6} \frac{c_{k,i}^{l}}{s^2+2\beta_i\omega_i s+\omega_i^2} \qquad (3)$$

Note that since there is no co-located actuation and sensor measurement defined (see Figure 2), we always have $k \neq l$ and hence for each sensor location l we can only identify the product $c_{k,i}^{l} = \phi_{k,i}\,\phi_{l,i}$ instead of the individual $\phi_{k,i}$ and $\phi_{l,i}$ in Equation 1. Still, for each of the three independent accelerometer measurements l, we can store all the modal factors $c_{k,i}^{l}$ for mode number i in a vector $C_i^l \in \mathbb{R}^6$ to obtain the i-th mode shape at the 6 hammer excitation locations. By first scaling each C_i^l with a factor α_l (in this case such that the maximum value of each C_i^l is close to unity and their mutual differences are minimal in least squares sense) we can then obtain the averaged mode shape:

$$C_i = \frac{1}{3}\sum_{l=1}^{3} \alpha_l C_i^l \qquad (4)$$

With this C_i we can geometrically reconstruct the rigid-body motions of the segment at mode shape i. Visualisation of the motion of the segment on each mode allows for its classification in clocking, lateral, tip/tilt or piston mode.

In total 18 transfer function fits $\bar{H}_{k,l}(s)$ are made, for 3 accelerometers times 6 excitations, which all yield slightly different values for ω_i and β_i. All these values are averaged to obtain a more reliable estimate of the true eigenfrequencies. Moreover, the spread in these values gives an indication of the variance on this estimation.
Note that the above procedure is only applied to the first six modes of the system. The seventh eigenfrequency (first spurious mode) is only read from the FRFs, hence no modal reconstruction is made.

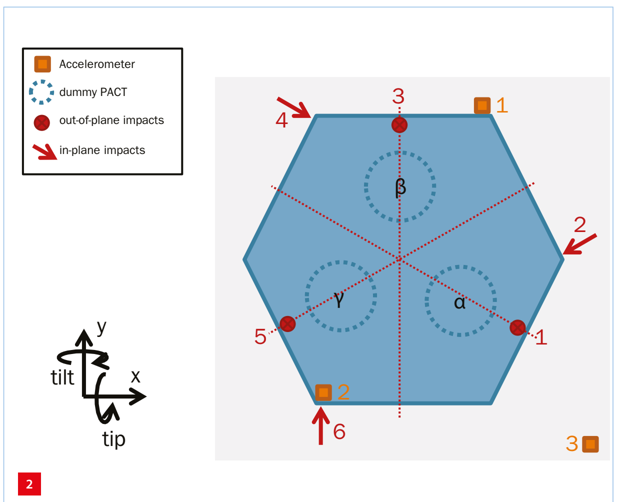

Visualisation of excitation and measurement locations during the dynamic tests. Sensor 1 and 2 are mounted on the segment, sensor 3 on the test table; sensor 1 measures in +y-direction, sensor 2 and 3 in +z-direction.

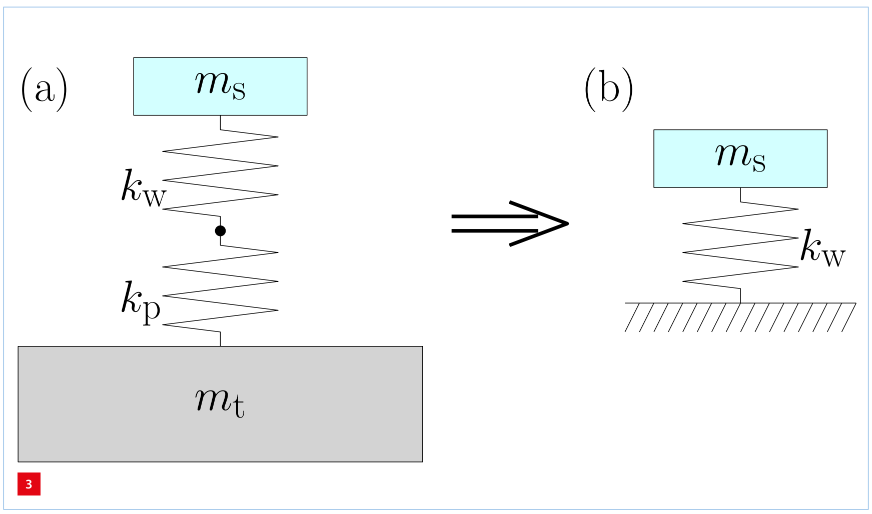

Simplified schematic representation of the actual test set-up (a), compared to the targeted configuration (b) with infinite k_p and m_t, which has also been used in FEM.

Piston/tip/tilt corrections

Although the testing boundary conditions have been carefully selected, the finiteness of both the dummy PACT stiffness k_p and the table mass m_t will affect the measured eigenfrequencies, especially for the piston, tip and tilt modes. The test set-up is schematically illustrated in Figure 3a, while the situation with ideal boundary conditions as defined in the section on test boundary conditions is shown in Figure 3b. Indeed, both configurations are only identical when $k_p = m_t = \infty$.

Hence, to allow for a fair assessment of the compliance of the measured piston/tip/tilt eigenfrequencies, and to allow for a comparison with FEM, the measured results with finite k_p and m_t have to be corrected, which is done analytically in this case.

For the piston mode the correction factor can be obtained via the ratio of the definitions of the eigenfrequencies f_p and $f_{p,\infty}$ of both cases in Figure 3, which yields:

$$\left.\begin{aligned} f_p &= \frac{1}{2\pi}\sqrt{\frac{k(m_s+m_t)}{m_s m_t}} \\ f_{p,\infty} &= \frac{1}{2\pi}\sqrt{\frac{k_w}{m_s}} \end{aligned}\right\} \Rightarrow \qquad (5)$$

$$f_{p,\infty} = f_p \cdot \sqrt{\frac{3k_p}{3k_p - k}} \cdot \sqrt{\frac{m_t}{m_s + m_t}}$$

Here, k_w is the (unknown) total whiffletree stiffness, k_p is the stiffness of an individual PACT, and k is the effective stiffness in Figure 3a which satisfies $1/k = 1/k_w + 1/(3k_p)$.

As mentioned in the section on test boundary conditions, the segment mass m_s = 178.3 kg, while the test table $m_t \approx 3 \cdot 10^3$ kg, meaning that the mass correction term is about 0.972 (–2.8%). To compute the stiffness correction we need to calculate k from the measured eigenfrequency f_p, i.e.

$$k = (2\pi f_p)^2 \frac{m_s m_t}{m_s + m_t} \qquad (6)$$

Since $3k_p >> k$ and given that $k_p = 143 \cdot 10^6$ N/m, the correction is about 1.042 (+4.2%). Combined, this implies that the measured piston eigenfrequencies should be corrected with approximately +1.2%.

The tip/tilt corrections can be done similarly. The rotational stiffness of the segment on the PACTs and the whiffletrees depends on the effective support radius (or arm lengths), but under the assumption that these radii are identical for k_p and k_w they disappear in the correction terms. In that case we obtain:

$$f_{tt,\infty} = f_{tt} \cdot \sqrt{\frac{3k_p}{3k_p - k}} \cdot \sqrt{\frac{J_t}{J_s + J_t}} \qquad (7)$$

Here, J_s and J_t denote the inertias of the segment and the test table, respectively. Hence, the stiffness correction is the same as for the piston mode. Unfortunately, the inertia correction cannot be determined exactly, since J_t is direction-dependent due to the rectangular shape of the table. However, using FEM it has been estimated that the table inertia is at least 35 times higher than the segment inertia, which yields a worst-case inertia correction term of 0.986 (–1.4%). Combined, this implies that the measured tip/tilt eigenfrequencies f_{tt} should be corrected with at least +2.7%.

Results

The results of the application of the methodology outlined above will be presented in detail for one QM. All 18 frequency responses (6 for each of the 3 sensors) from the roving hammer tests are shown in Figure 4 (top). These FRFs thus represent three independent measurements of the dynamic response of six independent points on the segment (see Figure 2).

All resonances duplicate very well across different sensors and excitation locations, hence the eigenfrequencies reproduce very well. These plots clearly show two distinct modes around 30 and 70 Hz, while around 55 Hz four modes clutter together.

To classify the mode shapes of the identified resonances, first parametric fits of all FRFs as in Equation 3 have been derived, whose frequency responses (between 25 and

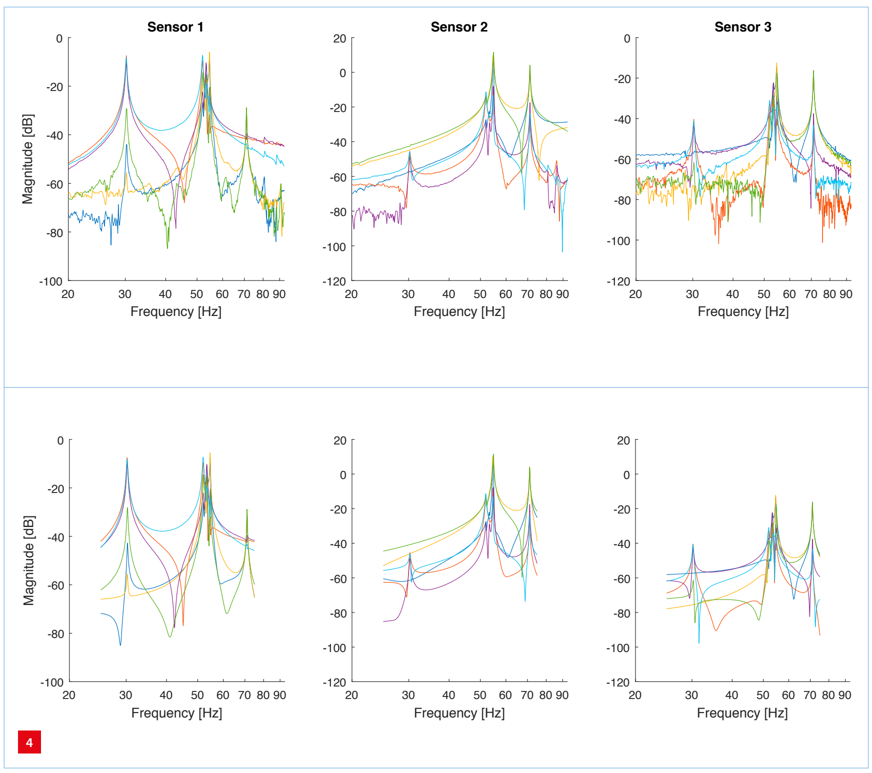

All 3 x 6 measured FRFs (top), and the frequency responses of the corresponding parametric fits (bottom).

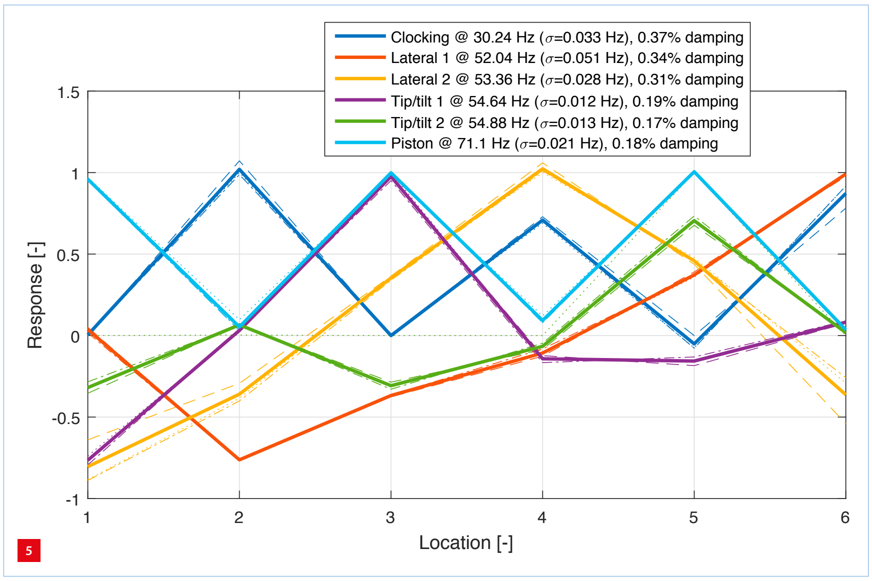

Representation of the identified mode shapes, depicting amplitude as a function of excitation location. The legend shows the eigenfrequencies and estimated damping per mode.

75 Hz) are shown in Figure 4 (bottom). The large resemblance between the top and bottom plots demonstrates the high quality of these fits. From these fits the mode vectors C_i^l have been constructed and their average C_i has been determined, as described above.

These obtained mode shapes are represented in Figure 5; the numbers along the *x*-axis represent the excitation locations (and associated directions) as indicated in Figure 2. Each color represents a mode; the thin dashed, dotted and dashed-dotted lines are the results per accelerometer $\alpha_l C_i^l$, the solid thick lines are the averages over the accelerometers C_i. The spread between the individual thin lines is quite small, again demonstrating the reliability of the procedure.

Realising that the odd location numbers in Figure 5 represent vertical segment motions and the even numbers horizontal ones, it is quite straightforward to classify the first and the sixth mode. The first mode is the clocking mode, since it has roughly the same displacements at the horizontal locations and hardly no vertical displacements at all. The sixth mode is clearly the piston mode, since it has nearly no horizontal displacements and roughly the same displacements at the vertical locations.

The other four modes however experience a huge amount of interaction, since their eigenfrequencies are quite close to each other. Consequently, lateral modes have tip/tilt components and vice versa. The easiest way to discriminate between the modes is then to visualise the mode shape graphically, which is done in Figure 6. In these plots the

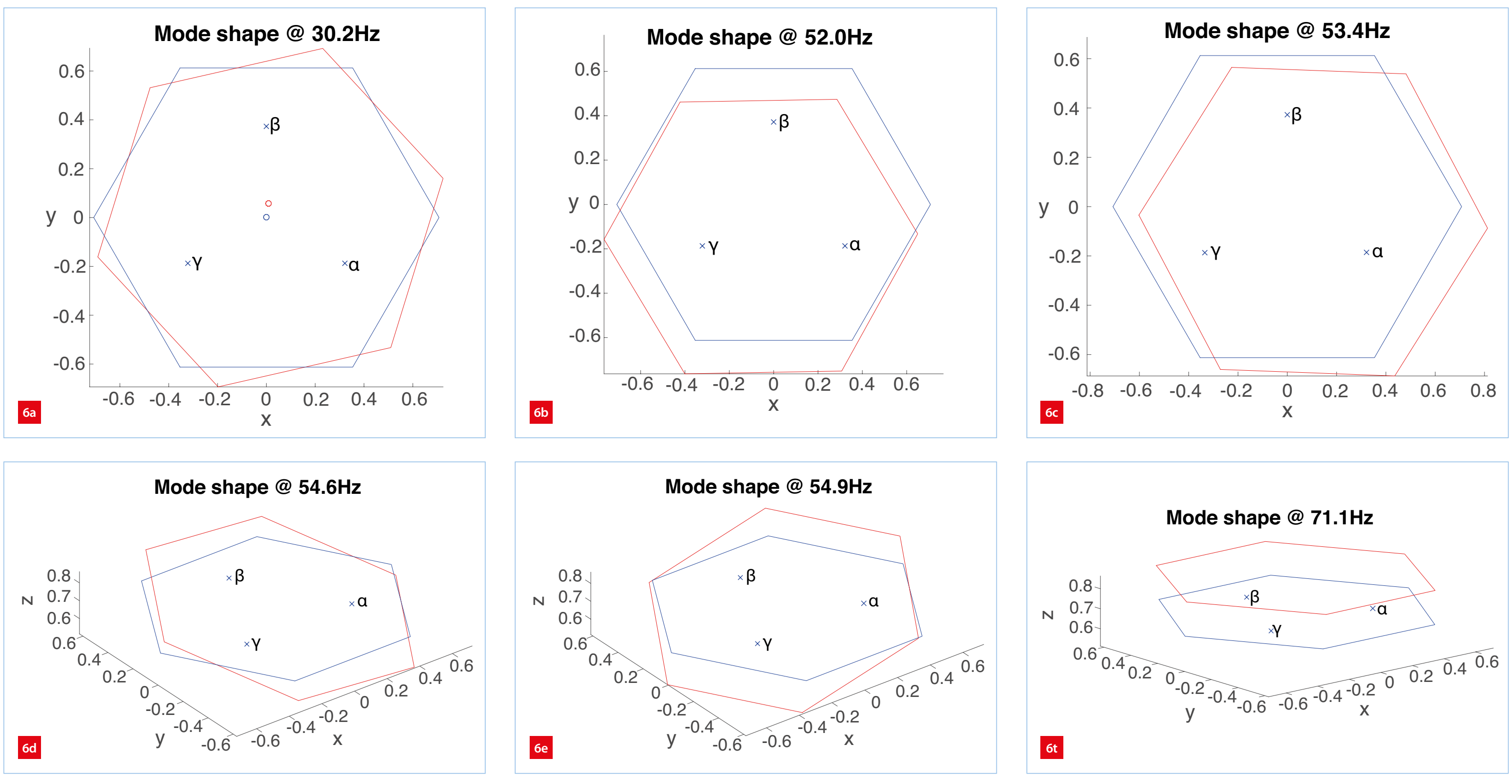

Visualisations of the first six mode shapes.
(a) First mode: clocking.
(b) Second mode: lateral.
(c) Third mode: lateral.
(d) Fourth mode: tip/tilt.
(e) Fifth mode: tip/tilt.
(f) Sixth mode: piston.

blue hexagonal represents the zero position of the segment, the red one is the deformed situation at the mode shape; the small crosses indicate the radial positions of the PACTs. From these plots it is clear that mode 2 and 3 are lateral modes (note that their translation axes are roughly perpendicular to each other), while mode 4 and 5 are tip/tilt modes (where the rotation axes are again roughly perpendicular).

The red disc in Figure 6a indicates the centre of rotation of the clocking mode, which is not in the centre of the segment but closer to one of the PACTs (PACT β in this case). This is due to the presence of the clocking strut [1], which increases the rotational stiffness of the M1SS. During the tests this clocking strut was indeed mounted close to PACT β.

After applying the correction factors discussed above to the piston, tip and tilt modes, our analysis thus yields the following results:
- the clocking mode is located at 30.2 Hz;
- the two lateral modes are at 52.0 and 53.4 Hz;
- the tip and tilt modes are at 56.1 and 56.4 Hz;
- the piston mode is located at 72.0 Hz.

As already indicated in Figure 5, the reliability of these eigenfrequency values is quite high. The worst case 3σ uncertainty (on the second mode in this case) is only $3 \cdot 0.051 = 0.15$ Hz. Moreover, the analysis also returned modal damping values, as shown in the legend of Figure 5. Quite interestingly, the horizontal modes show a statistically significantly larger damping than the vertical ones, the former being > 0.3%, whereas the latter are < 0.2%.

The measurement results have been summarised in Table 1, including the corrections on the piston/tip/tilt eigenfrequencies. When comparing the determined modes with the design objectives, it is clear that the QM is compliant. The table also shows the FEM predictions which were calculated earlier in the project, which differ less than 10% for every mode. Part of this difference can be attributed to details of specific welding connections in stiffness-critical locations and their associated modelling uncertainty. The first spurious mode can be observed at 80.8 Hz, just below the design target of 85 Hz. However, this mode is much smaller than the first six modes, and thus only plays a minor role at segment level. The tests have been repeated on other QMs as well, yielding very similar and equally compliant results.

Table 1
Summary of the results. All values are in Hz.

Mode	Target	FEM	Measurement
Clocking	30	31.7	30.2
First lateral	52	57.3	52.0
Second lateral	52	58.3	53.4
First tip/tilt corrected	55	60.2	54.6 56.1
Second tip/tilt corrected	55	60.5	54.9 56.4
Piston corrected	66	76.8	71.1 72.0
First spurious	85	86.6	80.8

Conclusions

In this paper we have presented the testing procedure for the validation of the dynamic performance of the QMs for the primary mirror support structure for the ELT. By careful selection of the boundary conditions during testing, we have been able to zoom in on the actual performance of the M1SS itself. By employing a roving hammer excitation technique to identify the system's frequency response and applying an accurate least-squares-based parametric fitting tool to the FRFs, we not only identified the resonance frequencies, but also determined the mode shapes at segment level, thereby allowing classification of these modes into rigid-body segment motions, and hence comparison with design targets and FEM calculations.

This procedure has successfully been applied to various M1SS QMs. The results of these analyses show that all QMs are compliant with the design targets on the eigenfrequencies of the first six modes of the structure. This successfully validates the dynamic behaviour of the ELT M1SS design by TNO-VDL. Over the next few years VDL will manufacture all ELT segment supports based on this design, thereby supplying one of the essential components of the 'biggest eye on the sky'.

REFERENCES

[1] Nijenhuis, J., Heijmans, J., den Breeje, R., Hazelebach, R., de Vreugd, J., Crowcombe, W., Naron, D., Fritz, E., Borghi, G., Navarro, R., Sillari, L., Sambenedetto, E., Eder, J., and Kamphues, F., "Designing the primary mirror support for the E-ELT", *Proc. SPIE* 9906, 990616, 2016.

[2] Nijenhuis, J., Hamelinck, R., Braam, B., and Cayrel, M., "Meeting highest performance requirements for lowest price and mass for the M1 segment support unit for E-ELT," *Proc. SPIE* 7733, 77332H, 2010.

[3] Ewins, D.J., *Modal testing: theory, practice, and application*, Research Studies Press, 2nd ed., 2000.

[4] Witvoet, G., den Breeje, R., Nijenhuis, J., Hazelebach, R., and Doelman, N., "Dynamic analysis and control of mirror segment actuators for the european extremely large telescope", *Journal of Astronomical Telescopes, Instruments, and Systems* 1(1), 019003 (2015).

FAST AND FLEXIBLE ANALYSIS OF ASPHERES

Testing the shape accuracy of aspherical lenses is a considerable challenge to the manufacturer. It requires measuring the tiniest deviations in shape in the nanometer range and, at the same time, making short measuring and set-up times possible. The solution is to use a new type of interferometry employing multiple tilted wavefronts. As part of the overall system, a hexapod takes over several positioning functions.

JÜRGEN SCHWEIZER AND DORIS KNAUER

Aspherical lenses have rotationally symmetrical optics around the optical axis, whose radius of curvature changes radially with the distance from the centre. This allows optical systems to achieve high image quality, while the number of elements required decreases, which saves on both costs and weight. Several methods have been established for checking their shape accuracy.
For example, interferometers with computer-generated holograms (CGHs) generate an aspherical wavefront in the desired shape and therefore make it possible to determine the deviation of the lens. The CGHs need to be created individually for each test object shape and are therefore only economical for series production.

Interferometric measuring of aspheres in circular sub-sections is another possibility. Each partial measurement is combined to a full-surface interferogram. The process is very flexible compared to CGHs and is also suitable for the production of prototypes and smaller series. However, 'stitching' the circular rings is often very time consuming, as in the case of steeper optics only smaller circular interference pattern rings can be captured and therefore many interference patterns have to be stitched together.

In addition to this non-contact interferometric measuring, tactile and 'quasi-tactile' measuring is possible. However, for polished surfaces this is not the best choice due to the risk of scratching.

Tilted wavefront technology

For this reason, Mahr relies on a new instrument for precise, fast, flexible measuring of different aspheres directly on the production line, without CGH, classical stitching or tactile contacting. In contrast to existing systems that need several minutes to do the measuring, the MarOpto TWI 60 (Tilted Wave Interfometer), needs only 20 to 30 seconds to measure the entire surface. The next test object can be measured while the previous one is being evaluated. The system is so robust that it is possible to set it up directly in a production environment and it can measure aspheres as well as freeforms (Figure 1).

The new measuring system works just like a 'normal' interferometer. However, it does not immediately acquire the entire test object optically in one single image, but in several subapertures that are active at different times, which yields better quality interference patterns in the case of optics with steep surfaces, such as aspheres and freeforms. If the individual geometrically distributed subapertures

1 *It's not only possible to measure aspheres, but also so-called freeforms. (Source: Docter Optics SE)*

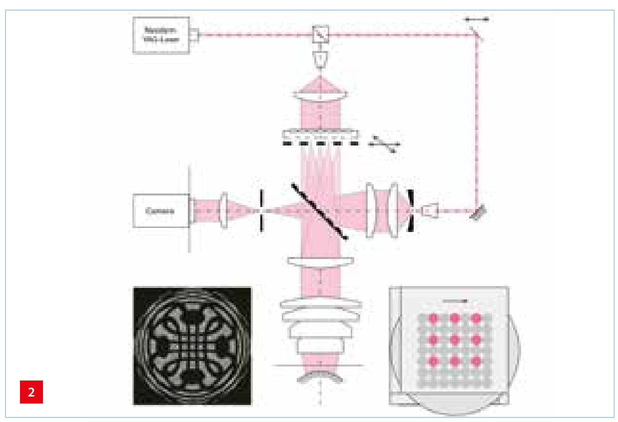

2 *The individual subapertures are spread out and actively switched. This allows the various tilted wavefronts to hit the inspection optics so that the resulting interference patterns do not overlap. (Source: Mahr)*

AUTHORS' NOTE

Dr.-Ing. Jürgen Schweizer is in charge of product management marketing at Mahr, and Dipl. Geogr. Doris Knauer is global campaign manager Industrial Automation at Physik Instrumente (PI). Mahr is a globally operating group of companies with headquarters in Göttingen, Germany, in the field of production measuring technology. PI is market leader for precision positioning technology concerning standard and OEM products with piezo or motor drives.

d.knauer@pi.de
www.mahr.com
www.physikinstrumente.com

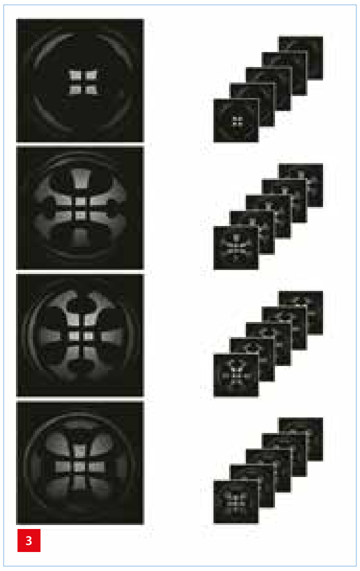

The individual interference patterns are combined to a single pattern.

are actively switched then different tilted wavefronts hit the inspection optics without overlapping interference patterns. An undisturbed interference pattern of a local part of the test object surface is obtained from each subaperture and the entire surface of the test object can be measured within a short time (Figure 2).

Finally, the individual interference patterns are combined to form a topography of the test object's surface. This represents the surface of the (aspherical) test object and can be evaluated accordingly (Figure 3). The deviation of the actual shape from the nominal shape is important. The design of the TWI is flexible with respect to varying surface geometry of test objects. There is no need to change the TWI set-up or even interrupt the production process at all. Even segmented and off-axis aspheres, toroid, and freeform optics can be measured quickly with high lateral resolution and measuring uncertainties under 50 nm.

The referencing process

For referencing and calibrating the TWI a highly accurate sphere with known geometrical specifications is moved for each subaperture to a specific position and then measured by this subaperture. Due to the complex optical beam path and in contrast to conventional systems, these types of interferograms are more sophisticated (Figure 4).
The wavefronts generated from the individual subapertures are combined to an overall wavefront. Finally, all measurements are evaluated and an algorithm is used to correct the systematic measurement deviations across all subapertures.
As all kinds of positioning errors of the calibration sphere affect the correction algorithm of the respective subaperture, the calibration sphere needs to be positioned very exactly. A maximum lateral position error of 5 µm with a repeatability below 0.5 µm is required.

In order to meet the high demands on the positioning mechanism in the TWI, Mahr after careful testing decided to use the H-824 hexapod from PI (Physik Instrumente).

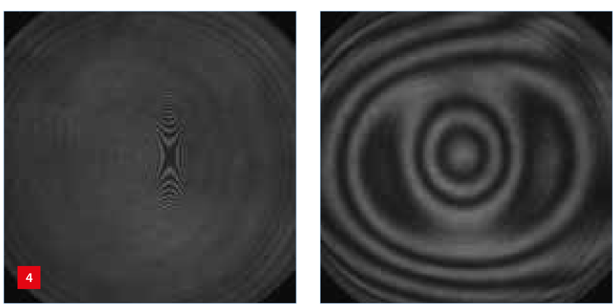

Interferograms of a subaperture from the calibration sphere. (Source: Mahr)

The H-824 hexapod positions the calibration sphere and also the test object before the measuring process starts. (Source: PI)

This hexapod also positions the test object in five degrees of freedom before the actual measuring process starts (Figure 5). Both the nominal and actual position need to be matched exactly. For example, deviations in tilt may not exceed 60 µrad.

Parallel-kinematic positioning system

Of course, hexapods, or parallel-kinematic positioning systems, are predestined for this, because they are able to position in all degrees of freedom with high accuracy and travel along trajectories with high precision. In the case of hexapods and in contrast to serial kinematics, all six actuators act directly on the same platform (Figure 6). This allows a more compact design than stacked systems. Because hexapods move only one platform, the overall mass is also less, which results in high dynamics in all motion axes.

In contrast to a stacked system, hexapods are also distinguished by improved path accuracy, higher repeatability, and flatness. Another essential characteristic is the freely definable rotation or pivot point, which means it is possible to define various coordinate systems that, for example, refer to the position of the workpiece or tool.

PI's high-performance C-887 digital controller takes care of controlling the hexapod. It specifies the positions in Cartesian coordinates, and applies all transformations to the individual drives. The innovative measuring system has proven itself in practice. TWI 60 systems are currently being used at the PTB (Physikalisch-Technische Bundesanstalt) in Braunschweig, Germany, as well as by a number of well-known manufacturers of aspheric precision optics.

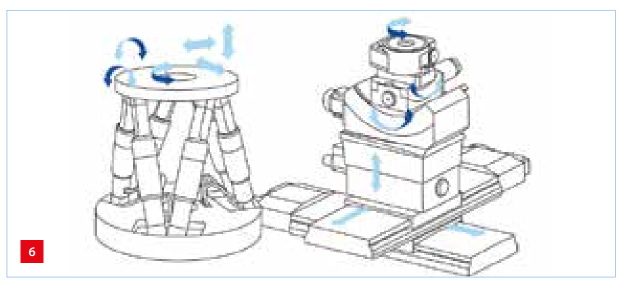

In contrast to serial kinematics, the actuators in parallel-kinematic systems act directly on the same platform. (Source: PI)

SWISS WATCH FEATURING DUTCH PRECISION

A method is introduced to design compliant micro transmission mechanisms which double the motion frequency of a cyclic input motion. Compliant embodiments are generated based on exploiting the singularity in a double-slider mechanism, which provides building blocks with a frequency-multiplication factor of two. It is shown that the proposed building blocks can be concatenated for higher frequency-multiplication ratios. To validate the building block approach, a compliant micro transmission mechanism is presented which quadruples the frequency of a cyclic rectilinear input motion.

DAVOOD FARHADI MACHEKPOSHTI, JUST L. HERDER, GUY SEMON AND NIMA TOLOU

Introduction

Displacement, force, and operation frequency are the main criteria for selecting an actuator for an application, while also size, cost, efficiency, and power supply have a great impact on the final choice. In many cases, actuator specifications do not match the requirements of a given application. In such cases a power transmission mechanism may be needed.

For instance, among different micro-actuators, thermal micro-actuators can offer high forces and displacements. However, they are limited to low operating frequencies as compared to other actuation schemes [1]. These actuators can be applied for more applications if a micro power transmission can be integrated to transform the low frequency of the input motion into an output motion with higher frequency.

Gear trains are the only examples of transmission mechanisms that have been used in mechanical and micro-electromechanical systems (MEMS) to multiply the motion frequency. However, gears are rigid-body mechanisms which generally give rise to many drawbacks, including friction, backlash, wear, and the need for assembly, lubrication, and maintenance. Besides, it is difficult to achieve a continuous rotational bearing with the existing MEMS fabrication technology.

Recently, compliant mechanisms became popular in the field of micro transmission mechanisms. Compliant transmission couplings [2] [3], micro motion converters [4], and compliant stroke multipliers are some of the few examples of compliant transmission mechanisms that exist in literature. Compliant mechanisms transmit and transform force and motion by undergoing elastic deformation of their flexible segments as opposed to rigid-body motions of traditional linkages. The monolithic nature of these mechanisms allows for miniaturisation. Therefore, this enables a compact system design by integration of the power transmission and actuation part. However, finite travel range of the rotational flexures is the main kinematic limitation in this type of mechanisms.

Here, we report a new method for the design of compliant frequency-multiplier transmissions, utilising a building block approach based on exploiting the singularity of the double-slider mechanism. The main advantage of this proposed movement is that the mechanism does not need full-cycle rotational joints or frictional contacts.

Method

A limited-cycle kinematic is proposed to increase the motion frequency within a finite travel range. This will eliminate the need for problematic continuous, infinite-travel-range, rotational joints or rigid contacts for frequency multiplication at micro-scale. A generalised input-output kinematic relationship for such a transmission mechanism is shown in Figure 1.

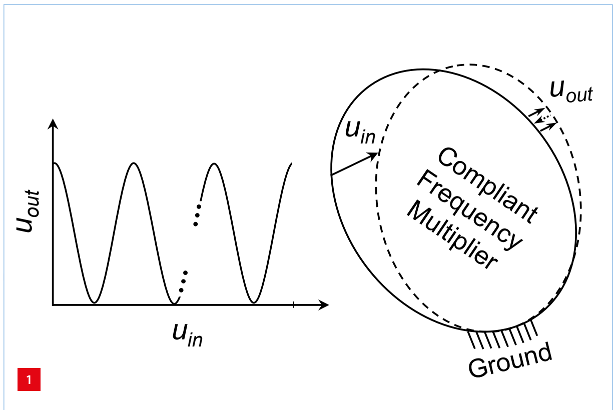

1

The generalised input-output displacement relationship of a compliant frequency multiplier.

AUTHORS' NOTE
Davood Farhadi Machekposhti, Just L. Herder and Nima Tolou are associated with the Department of Precision and Microsystems Engineering, Delft University of Technology, the Netherlands. Guy Semon works at the Department of Research and Development of TAG Heuer in La Chaux-de-Fonds, Switzerland.
d.farhadimachekposhti@tudelft.nl
www.pme.tudelft.nl
www.tagheuer.com

To increase the motion frequency, the direction of the output motion, u_{out}, needs to reverse while the input is subjected to the displacement u_{in}. This can be shown in the first kind of singularity in the rigid-body mechanisms. This type of kinematic singularity refers to a configuration where a kinematic chain reaches the boundary of the workspace. The input-output frequency-multiplication ratio can be identified based on the number of singularities of the first kind, m, in the kinematic chain within the considered range of motion, and can be given by:

$$f_{out} / f_{in} = m + 1 \tag{1}$$

Here f_{out} (in cycles per second, Hz) and f_{in} are the motion frequency of the output and the input members of the mechanism, respectively.

The proposed building block in this article is based on a four-bar linkage, where for a finite travel range there is only one configuration representing a singularity of the first kind. This can be shown in the double-slider four-bar mechanism (Figure 2a), which can be a favourable choice for MEMS devices due to the rectilinear input and output motions. Therefore, based on Equation 1, the mechanism can multiply the input motion frequency with a ratio of 2 (Figure 2b). As can be seen, the motion of the output slider u_{out} completes a full cycle while the input slider displaces with u_{in} from left to right, which is half a complete cycle.

Theoretically, a frequency-multiplier mechanism with the ratio of 2^n can be achieved by concatenating n number of frequency-doubler mechanisms, where $n = 1, 2, ..., N$. However, the output performs a small displacement compared to the input since the mechanism is working around the singularity. Therefore, this limits the use of this mechanism in a serial combination to reach higher multiplication ratios or a desired output displacement.

Two partial compliant frequency-doubler building blocks are proposed, shown in Figure 3. The stroke of the output is amplified by arranging two compliant equivalents of the double-slider mechanism in series with a shared input. The building block shown in Figure 3 can double the output frequency when a rectilinear cyclic motion with sinus or cosine function is subjected to the input, respectively.

The output displacement of the proposed frequency-doubler building blocks is limited by the maximum input displacement and the length of the beams. However, a compliant mechanical stroke amplifier can be paired with the output of the mechanism to amplify the displacement with a desired factor. Two different examples are presented herein, which illustrate the combination of the proposed compliant cycle doubler building blocks with different types of stroke amplifier concepts (Figure 4).

The output displacement from the cycle doubler building blocks, u_o^1, can be amplified to a desired output displacement, u_{out}, by a stroke amplifier. Case I comprises two sets of angled beams where their ends are constrained by a vertical beam, shown in Figure 4a. The first set, with the angle of α_1, is the cycle doubler mechanism, equivalent with the angled arrangement shown in Figure 4b. The second set, with the angle of α_2, acts as a stroke amplifier with the instant multiplication ratio of tan α_2, where the condition $\alpha_2 < 45°$ should be satisfied to get a stroke multiplication ratio higher than one. Case II, illustrated in Figure 4b, includes a compliant cycle doubler building block, equivalent with the arrangement shown in Figure 4a, paired with a lever arm as a stroke amplifier with an multiplication ratio of b_2 / b_1.

Design

A compliant frequency-quadrupler transmission mechanism has been designed based on the proposed

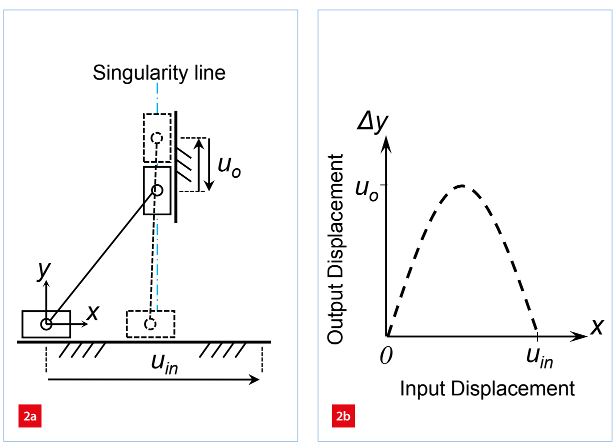

The double-slider four-bar mechanism.
(a) Rigid-body mechanism representation.
(b) The input-output displacement relationship.

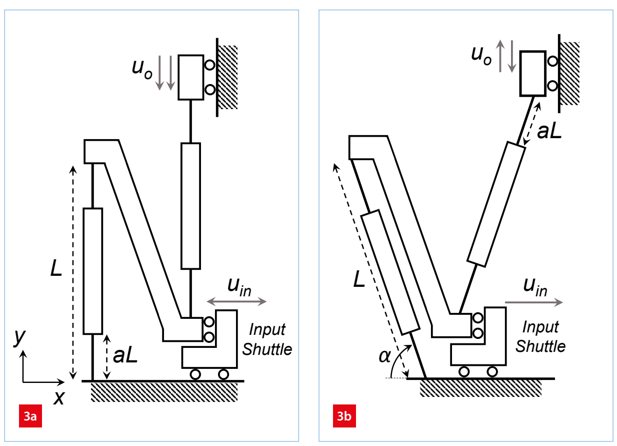

Partially compliant frequency-doubler building blocks, with two different initial shapes.
(a) At the singularity.
(b) At the angled arrangement.

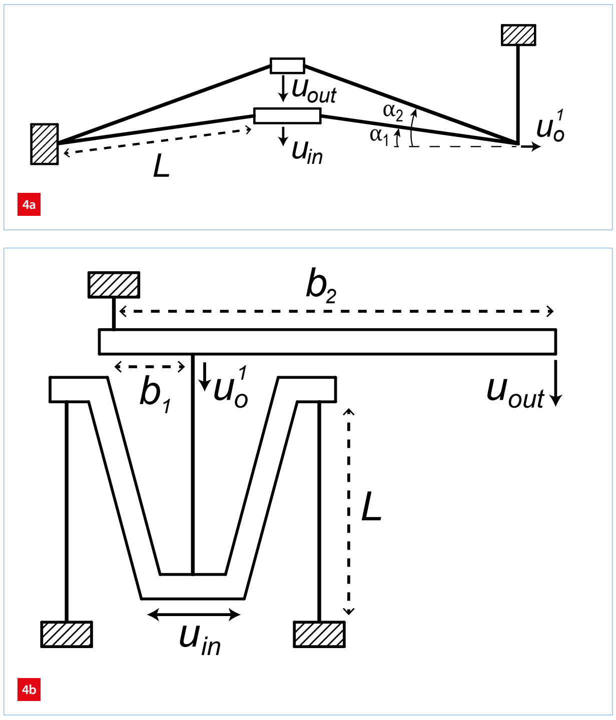

Combinations of frequency-doubler building block and different compliant stroke amplifier concepts.
(a) Double-slider mechanism (Case I).
(b) Lever mechanism (Case II).

method, shown in Figure 5. The set of design parameters are summarised in Table 1.

Furthermore, a constant thickness of t = 30 µm is considered in the drawing for all the flexures included in the design. The design is composed of two frequency-doubler building blocks, concatenated with a set of stroke amplifiers. The design comprises an input shuttle which can be subjected to a reciprocating input motion, and it is

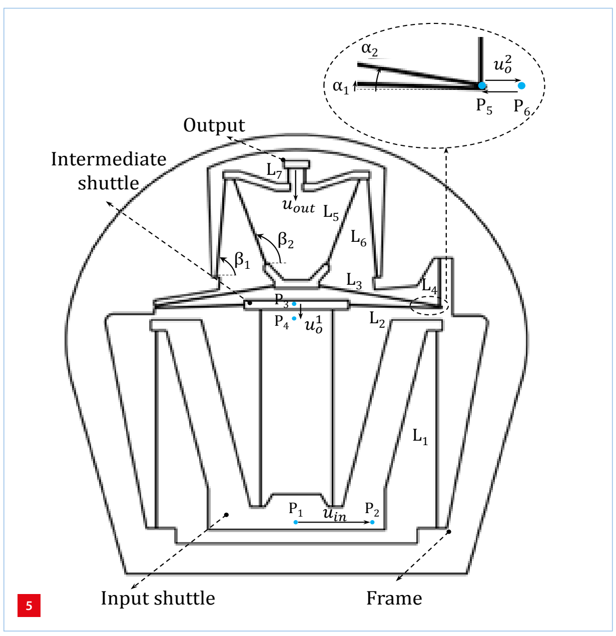

The design embodiment of a compliant micro frequency-quadrupler.

connected to the ground and an intermediate shuttle each with two parallel long-length flexures. This is a fully compliant equivalent of the building block shown in Figure 4a. For an input displacement of u_{in} towards the right (from point P_1 to point P_2), the intermediate shuttle moves downwards from point P_3 to point P_4.

Table 1
Design parameters for the micro frequency-quadrupler transmission mechanism.

Parameter	Value
L_1	13 mm
L_2	5.5 mm
L_3	7.5 mm
L_4	3 mm
L_5	6 mm
L_6	6.5 mm
L_7	1 mm
β_1	85°
β_2	110°
α_1	2.2°
α_2	10°

Besides, the intermediate shuttle follows similar movement when the input moves towards the left with a displacement of u_{in}. Therefore, the intermediate shuttle completes two cycles for a full cyclic movement of the input, which results in a frequency-multiplication factor of two. The intermediate shuttle is connected to the ground and a cantilever beam, equivalent to the concept of Figure 4a (Case I), via two angled long-length flexures, with the angle α_1. The endpoint P_5 travels to point P_6 and then returns back to the same point P_5 (a complete cycle), while the intermediate shuttle moves from P_3 to point P_4.

This provides another frequency-duplication effect, which results in an overall frequency-multiplication ratio of four between the input movement and the motion at point P_6. However, the stroke is small due to a consecutive combination of two motion frequency multipliers. Therefore, a stroke amplifier is connected to the output of the compliant frequency-quadrupler mechanism with a multiplication ratio of 1:19.

Fabrication and characterisation

A micro-device was fabricated in silicon using deep reactive ion etching (DRIE), shown in Figure 6.
The design was first patterned on a w = 525 µm thickness silicon wafer and then etched by DRIE. This was done with the basic Bosch plasma etching process, which includes

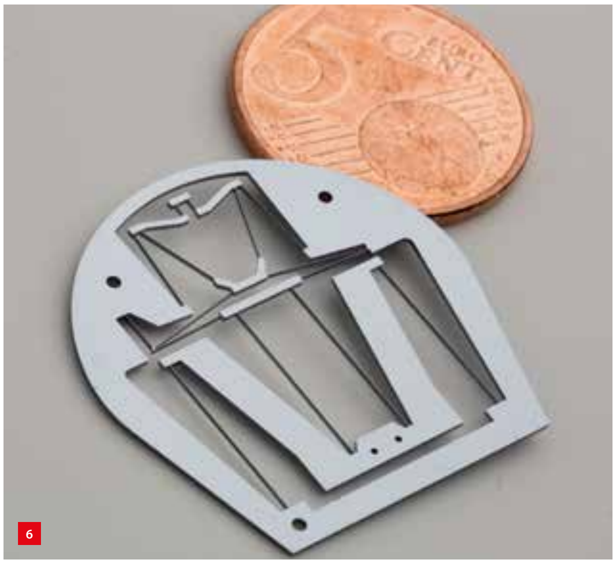

The prototype of the compliant frequency-quadrupler fabricated out of silicon using the DRIE process.

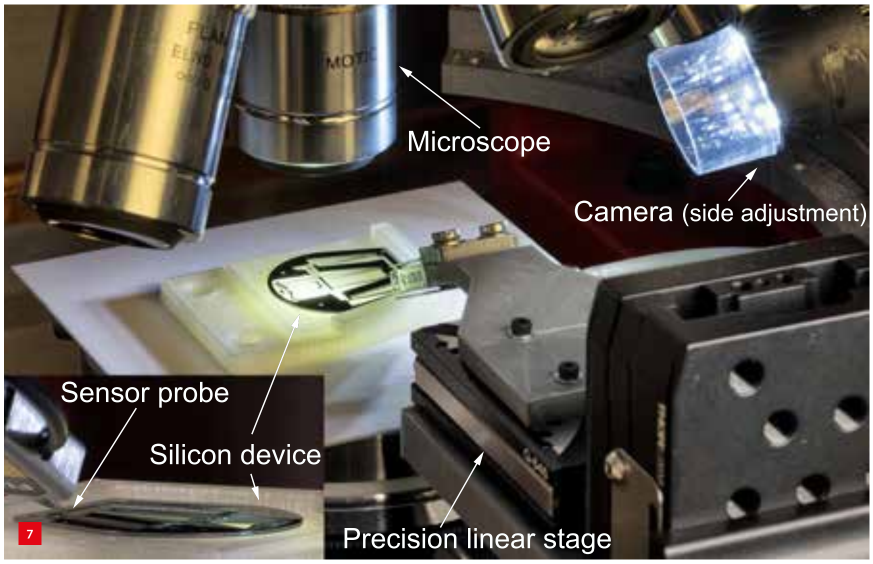

Experimental set-up to evaluate the actuation force, and the input-output kinematics of the compliant frequency-quadrupler.

two subprocesses: the etching and the passivation, to produce a device with a high aspect ratio.

A customised test set-up was constructed for testing the actuation stiffness and the input-output kinematics of the silicon device, shown in Figure 7. The force deflection of the device was measured using a 20-gram force sensor (FUTEK LSB200) with a resolution of 20 μN. The force sensor was mounted on a precision linear stage (PI Q-545), with a resolution of 1 nm and minimum incremental motion of 6 nm, to provide a rectilinear input motion. A displacement of 2 nm was applied to the input shuttle of the micro-device, and the movement of the output shuttle was simultaneously captured by an optical microscope (Keyence VHX-1000E). The displacement was analysed afterwards using image processing, where it was detected with 500-nm accuracy.

Performance

The optical displacement measurement, the finite-element model (FEM) and the pseudo-rigid-body model (PRBM) show the same behaviour and order of magnitude for the input-output kinematic relationship, shown in Figure 8a. As can be seen, the proposed compliant transmission mechanism multiplies the input motion frequency with a factor of four, and with a maximum output displacement of 120 μm. The PRBM shows a maximum of 6.7% discrepancy with the experimental results. This can be explained by the elastokinematic effects since the presented theoretical plot is based on the PRBM.

The force-deflection measurement is illustrated and compared to the FEM and the PRBM in Figure 8b. The results show a nonlinear correlation between the actuation force and the displacement, which can be explained by the nonlinear kinematics of the proposed compliant frequency-doubler building block. Clearly, by increasing the input displacement the compliant device is behaving as a linear spring, softening spring, and hardening spring, sequentially. Besides, it is shown that the results from the FEM and the PRBM are in agreement. The small discrepancy between these results, maximum 3.4%, illustrates the accuracy of the PRBM.

As can be seen in Figure 8b, the result from the measurement shows a more linear stiffness behaviour as compared to both the FEM and the PRBM. Besides, a 9,4% discrepancy is observed at maximum actuation force between the measurement and the PRBM. This can be explained by uncertainties in the thickness measurement by SEM, ±1.5 μm. A decrease in thickness t of 0,5 μm for flexible members with an initial average thickness of 21.25 μm results in a 7.8% decrease of the actuation force. Moreover, the difference in nonlinear stiffness behaviour, between the PRBM and the experiment, can be explained

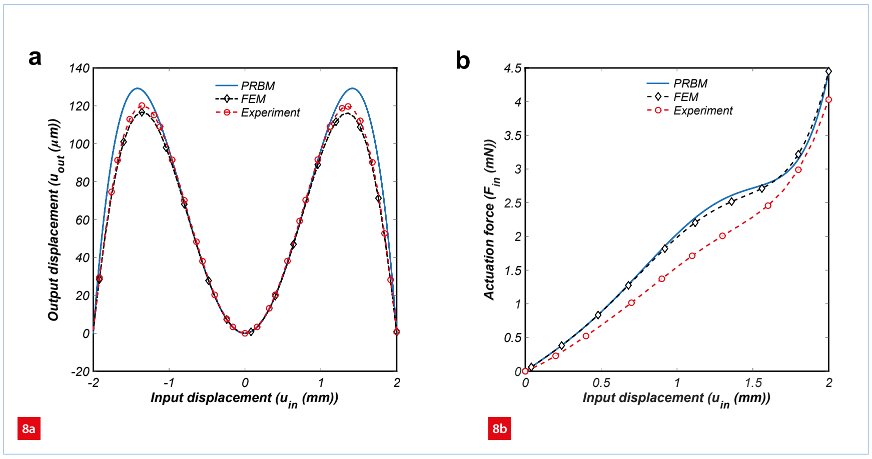

The results for the micro compliant frequency-quadrupler from the theoretical model (pseudo-rigid-body model, PRBM), finite-element model (FEM) and experiment.
(a) The input-output kinematics.
(b) Force-displacement characteristics.

by the stiffness of the compliant stroke amplifier, K_{SA}, in which a similar trend can be observed between the PRBM and the experiment, i.e. a 25% decrease in the actuation stiffness of the compliant stroke amplifier with an initial stiffness of K_{SA} = 8.8 N/mm.

As can be seen, based on the force-deflection results, there is a trade-off between adding compliant multipliers (frequency or stroke) and the additional motion stiffness that is associated with those. However, the principle of static balancing can be applied in each building block separately since the elastic force is a conservative force. For instance, a balancing segment (preloaded beams) which provides a negative stiffness can be added to cancel the positive stiffness of each compliant building block.

Future developments will focus on actuation force reduction using static balancing with preloaded beams. Moreover, it will also include the integration of an embedded actuator to study the kinematics of the proposed compliant micro-transmission in high-speed operation.

Conclusions

A monolithic micro transmission mechanism was presented that can multiply the frequency of a reciprocating input motion. The mechanism is based on a compliant version of the double-slider mechanism, taking advantage of its singularity properties. Furthermore, by concatenating multiple of these mechanisms in a building block approach it was shown that higher frequency-multiplication ratios can be generated.

REFERENCES

[1] Bell, D.J., Lu, T.J., Fleck, N.A., and Spearing, S.M., "MEMS actuators and sensors: observations on their performance and selection for purpose", *Journal of Micromechanics and Microengineering*, 15(7), p. S153, 2005.

[2] Machekposhti, D.F., Tolou, N., and Herder, J.L., "A fully compliant homokinetic coupling", *Journal of Mechanical Design*, 140(1), p. 012301, 2018.

[3] Machekposhti, D.F., Tolou, N., and Herder, J.L., "A statically balanced fully compliant power transmission mechanism between parallel rotational axes", *Mechanism and Machine Theory*, 119, pp. 51-60, 2018.

[4] Wessels, J., Machekposhti, D.F., Herder, J.L., Sèmon, G., and Tolou, N., "Reciprocating geared mechanism with compliant suspension", *Journal of Microelectromechanical Systems*, 26(5), pp. 1047-1054, 2017.

DELTAPATENTS

Specialist in protecting high-tech inventions

Precision engineering has developed into a core technology within the field of mechanical engineering, optics, mechatronics and other industrial applications. 'A fast and exciting development' according to Alex Hogeweg of DeltaPatents, 'but the IP field changes as a result. We are specialized in protecting software related inventions and are up-to-date with the legal provisions for such inventions'. Because of the amount of patent applications filed every year, freedom to operate gets more challenging.

European patent attorney Alex Hogeweg has nineteen years of experience with electrical and mechanical patents and is almost six years active at DeltaPatents. 'I have worked for many large companies in electronics and also in the mechanical field. This combination is actually a must to understand the inventions made by companies in the field of precision engineering. A large part of the inventions relate to software, which is used to control the (micro-) mechanical devices. Due to my years of experience I know which aspects of a development are patentable.'

Face to face

'For us, face to face contact is very important', according to Hogeweg. 'We work on the basis of a personal approach and like to support our customers in their decision making process. Especially when it comes to new high tech inventions, the market is more complex and it is important to have clarity about what a customer wants to patent, what value it will bring to his business and how his business may be affected by patents of others.'

Plastic cup

Hogeweg uses the plastic cup example to explain what he means. 'Let's assume that someone invents a plastic cup and he gets a patent granted for his invention. Then another party is not allowed to copy that same cup, but he can get his own patent for an improved version thereof. The first party may then not sell the improved version of his own invention. This is because a patent does not give you the right to use your own invention, it merely gives you the right to prohibit others to use your invention. Especially smaller companies are not always aware of the difference. You can have such a beautiful new invention, but if you do not have the freedom-to-operate, the value of your invention is affected.'

Time to market

DeltaPatents is aware of the problems of its clients. As you drive your innovation from idea to reality, there are many hurdles: solving technical problems, arranging financing, agreeing terms with business partners, sourcing manufacturers, and planning marketing campaigns. Intellectual Property (IP) discussions are frequently postponed until success is guaranteed, or until a conflict arises. By then it may be too late to protect your own IP. 'We can assist you in defining your IP strategy, identifying valuable inventions, suggesting ways of avoiding or overcoming potential risks, and drafting IP contracts. We can also help you in defending against rights of others.'

The field changes

The patent attorneys of DeltaPatents are up-to-date with changes in IP legislation and case law. 'Under political pressure, the patent friendliness has decreased. Long discussions have taken place on patentability of software-related inventions.
We have extensive experience in assessing if a software invention will be seen as technical and drafting a patent application according to the latest requirements, adequately substantiating your embodiments'.

Patent specialist and training institute DeltaPatents

DeltaPatents is a renowned IP training institute offering an extensive range of IP courses and seminars. 'We specialize in training your IP managers, coordinators and researchers, increasing the IP awareness in your company and contributing to cost-effective IP procedures.'

What is patentable?

The golden egg in the palm of the inventor symbolizes the invention that companies want to protect. According to the specialists of DeltaPatents it is important to know if an invention is seen as a technical system, does not yet exist, and whether there is freedom to operate. Applying for a patent starts with a detailed conversation about what a customer actually wants to protect. **More information can be found on www.deltapatents.com.**

LASERING E-CARS

Predictions say that by 2025 half of all new cars sold worldwide will be powered electrically. To be prepared, the automotive industry will have to set up mass production for battery packs and electric motors. Trumpf Lasertechnik in Ditzingen, Germany, is well ahead in preparing for this technological changeover, with laser-based scanner welding playing an important role.

FRANS ZUURVEEN

The making of car body parts, such as doors, from steel sheet bulk material involves precision technology. When assuming a tolerance field of 500 μm for the slits between body parts, the tools for making those sheet parts need to be accurate by more than a factor of 5 to 10, while the measuring machines for inspecting these tools require accuracies in the micrometer range.

In the drive towards improving the accuracy and reliability of car body joints, Trumpf Lasertechnik has helped car manufacturers to replace the traditional joining technology of resistance spot welding with the faster and more reliable process of scanner welding with a laser (see Figure 1). Now, the rise of e-cars adds new production challenges: battery packs and electric motors. In this application field, Trumpf lasers also can play a prominent part.

Battery cells

The rechargeable battery packs in electric vehicles consist of several battery modules, each comprising 9 to 12 battery cells of approx. 3.8 V each (see Figure 2). The current basic lithium-ion battery cells are built up in layers. They consist of copper foil and coated aluminium layered together with the electrode foils of lithium metal oxide (cathode) and graphite (anode). Each of these foils is only approx. 100 μm thick, and the easiest way to cut them is by applying a short-pulse laser.

The next fabrication step is adding liquid electrolyte: lithium salts in an organic solvent. The last step is sealing the cell with a cap and fitting a pressure-relief valve. It is crucial that the welds completely seal the cell, but they should not penetrate too deeply, as this will make the cell useless. The only solution for this dilemma is to use lasers with an accurate focusing spot of minimal dimensions (see Figure 3).

Depending on the application (materials to weld, welding speed, etc.), the dimension (diameter of the welding spot) is typically 0.1-0.4 mm. To guarantee a good welding result, accurate positioning of the parts to be welded is necessary. To this end, intelligent sensors are generally used to detect the correct welding position and provide the input for any adjustment; this is called scanner welding. The laser has an active power control to permanently guarantee that correct laser parameters are used and repeatable welding results are obtained.

1

Welding a steel sheet part with a Trumpf laser.

2

Packing individual battery cells into modules, which are combined in battery packs to be mounted into vehicles.

AUTHOR'S NOTE

Frans Zuurveen, former editor of Philips Technical Review, is a freelance writer who lives in Vlissingen, the Netherlands.

Precision laser welding of battery cells.

Battery modules

A battery module groups together the basic cells with interconnected terminals. For that purpose, thin metal strips are used, made from 0.3-mm thick copper or aluminium sheets. These current-carrying leads are welded in overlap. Creating such lead overlaps requires careful welding procedures. The weld should not extend into the chemical cell content and welding should not heat the cell above 80 °C.

The weld seam's main purpose is to create an efficient current flow and this requires a low electrical resistance obtained by creating a sufficiently large contact area. This is achieved by 'wobbling' a scanner-guided laser welding spot (see Figure 4). The scanner oscillates the beam over the metal strip, thus creating a very fine, very long seam producing a large contact area.

Complete battery pack

The combination of battery modules in a complete battery pack requires the creation of a busbar, which guides the electric power to the electric drive. Connecting the busbar contacts poses a problem similar to that of making the module leads, as creating a busbar often requires joining dissimilar materials: aluminium and copper. A problem is that the high reflectivity of aluminium causes back reflections. Here again, scanner-guided wobbled welding with a disk laser provides an ideal solution.

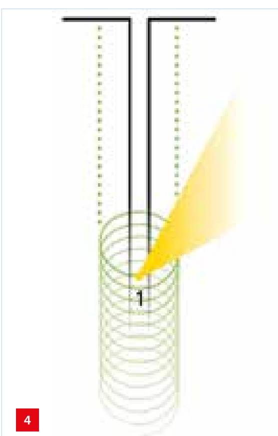

Wobbling a scanner-guided beam in a spiral-like pattern for creating a large contact area without filler material.

Ultimately, the battery pack has to be installed in the vehicle, ideally as low as possible to achieve the lowest centre of gravity, hence in a shallow compartment at the underbody of the car, one or two decimeters above the road surface. This compartment must be completely sealed to avoid any leakage and should be robust in the event of a crash.

Battery compartments are welded together from steel or aluminium sheet metals using highly productive disk lasers. Once the compartment is finished, the lid has to be glued onto the sheet-metal box. A laser is again used for cleaning and structuring the adhering surfaces.

Smart electric motors

For the faster and more efficient volume production of electric motors, car companies try to find alternatives for the traditional application of coils with windings of copper wire. Wrapping each individual slot in a rotor or stator with wire takes time and is difficult to automate.
That's why car makers have invented a new technology using 'hairpins'. This involves firing a hairpin-like rectangular copper wire straight into each slot. This much faster method completely fills the slot with copper, providing an extra advantage: improved motor efficiency. The protruding parts of the hairpin on both sides are pressed, jammed or twisted together using a kind of mask. The connected ends then have to be welded (see Figure 5), but are sometimes slightly out of alignment. This problem is solved by again using scanner welding. A camera in the laser optics determines the position of the point to be connected within a fraction of a second. The beam focus oscillates at the right place and finishes the weld.

To conclude

The advance of electric motors forces car manufacturers to meet the challenge of inventing new production methods. These are aimed at lower cost prices and better efficiency for electric components. Just as car manufacturers succeeded in reaching optimal machining technologies for complicated sheet metal components, they now have to scrutinise conventional methods for producing battery packs and electric motors. Hopefully, this process will result in widely affordable electric cars.

Literature

M. Kirchhoff and M. Reinhard, "It's heading this way", *Trumpf Laser Community*, nr. 26, April 2018.

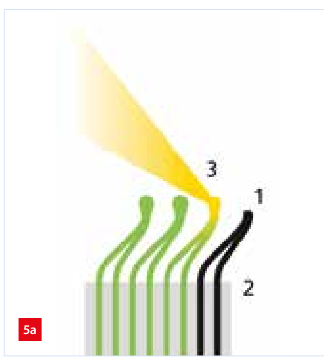

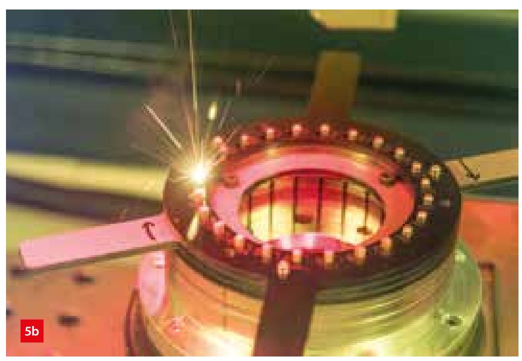

Laser welding 'hairpins'.
(a) Schematic: Hairpin-like windings (1) made from rectangular copper wire inserted in a stator (2). The protruding ends are pressed together and laser welded with a scanner system (3).
(b) Practice.

BIG SCIENCE IN THE SPOTLIGHT

On 14 and 15 November 2018, the eighteenth edition of the Precision Fair will once again be the annual, international meeting point for precision technology. At this free event visitors can visit some 300 stands of exhibitors (specialised companies and knowledge institutions), among which 50 DSPE members. The Big Science congress programme will highlight the challenges and opportunities offered by the Dutch national science agenda and the large international research projects.

The heart of the Precision Fair in the NH Conference Centre Koningshof in Veldhoven, the Netherlands, is the exhibition. It covers a wide array of fields, including optics, photonics, calibration, linear technology, measuring equipment, micro-assembly, motion control, piezo technology, precision tools, sensor technology, software and vision systems. A few innovations on display are presented on the following pages.

The two-day lecture programme comprises over fifty presentations, including a Big Science programme, featuring big science projects such as CERN (nuclear research) and ESO (European Southern Observatory), and the Dutch national science agenda. International top speakers from various research institutes will talk about recent developments and forthcoming tenders. The International Meet & Match Event will be hosted on both fair days as well.

Awards

At the end of each fair day, event partner DSPE will organise an award ceremony. On Wednesday 14 November, the Ir. A. Davidson Award will be presented to a young precision engineer who has worked for some years in a company or institute and who has a demonstrable performance record. On Thursday 15 November, the Wim van der Hoek Award will be presented to the person with the best graduation project in the field of design in mechanical engineering at one of the Dutch or Belgian universities of technology or applied sciences. The nominations are presented on page 45 ff.

Mikroniek will report on the highlights of the Precision Fair 2018 in its December issue.

Visit DSPE members exhibiting at the Precision Fair 2018

Stand	Number	Stand	Number
169	BKB Precision	203	MI-Partners
64	Brainport Industries	17	Mitutoyo Nederland
162	Bronkhorst Nederland	135	MKS Instruments
126	Ceratec Technical Ceramics	77	Molenaar Optics
93	Connect 2 Cleanrooms	177	MTA
130	Demcon	27	NTS-Group
275	Dutch Society for Precision Engineering	238	Oude Reimer
57	Ertec	43	Pfeiffer Vacuum Benelux
139	Etchform	138	PI Benelux
40	Festo	159	Settels Savenije Precision Parts
4	Fontys Hogeschool Centre of Expertise HTSM	104	Sioux CCM
103	Frencken Europe	119	Sumipro
34	Heidenhain Nederland	81	Technobis Group
105	Hembrug Machine Tools	50	Teesing
40	Hittech Group	141	Tegema
51	Holland Innovative	101	Ter Hoek
136	IBS Precision Engineering	276	The House of Technology
293	Inholland Delft Precision Engineering	290	TNO
277	Janssen Precision Engineering	286	TU Delft
292	Leidse Instrumentmakers School	288	TU/e High Tech Systems Center
80	MathWorks	231	UCM
5	Maxon Motor Benelux	112	VDL ETG & VDL GL Precision
267	Mecal	60	Veco Precision
129	MEVI Fijnmechanische Industrie	145	VSL
68	Mikrocentrum	19	Zeiss

1
Impression of the Big Science programme at the Precision Fair 2017. (Photo: Mikrocentrum)

Ecoclean GmbH | UCM AG

Mr. Roger Kohnen
T +32 (0)474-45 79 39
E info@ucm-ag.com
www.ecoclean-group.net
www.ucm-ag.com 231

VDL GL Precision

Herman Rusch
T +31 (0)40-29 22 055
E sales@vdlglprecision.nl
www.vdlglprecision.nl
112

VDL ETG

Sven Breuls
T +31 (0)40-26 38 666
E info@vdletg.com
www.vdletg.com
112

TNO

Wouter Jonker
T +31 (0)6 22 5
E wouter.jonker
www.tno.nl

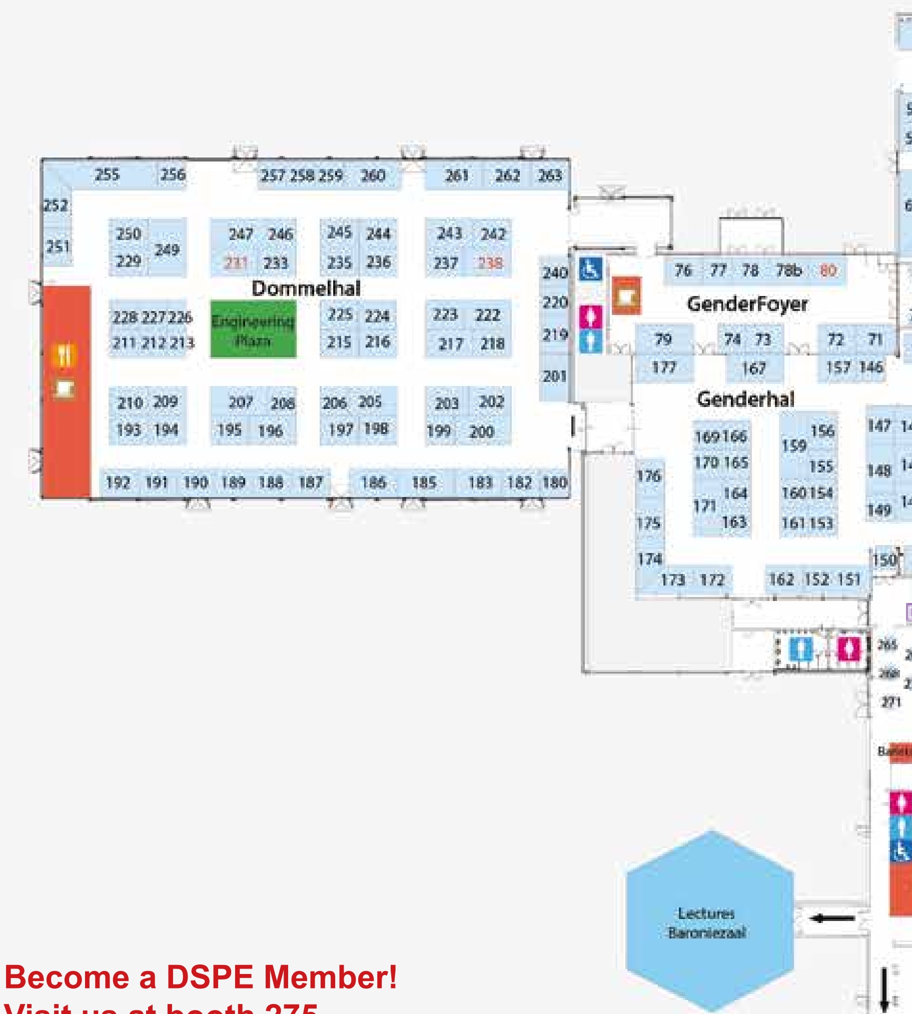

Festo BV

Martijn Borsboom
T +31 (0)15-25 18 890
E martijn.borsboom@festo.com
www.festo.nl
140

Frencken Group
Lieke Mehagnoul
T +31 (0)40-25 07 507
E sales.office@
frenckengroup.com
www.frenckengroup.com
103

Groneman B.V.

André Lammertink
T+31 (0)74-25 51 140
E info@groneman.nl
www.groneman.nl
37

HEIDENHAIN NEDERLAND B.V.

Maarten Kok
T +31 (0)318-58 18 00
E info@heidenhain.nl
www.heidenhain.nl 34

IBS Precision Engineering

Dirk Smits
T +31 (0)40-29 01 270
E info@ibspe.com
www.ibspe.com
136

JANSSEN PRECISI

Huub Janssen
T +31 (0)43-35
E huub.janssen
www.jpe.nl

innovation
for life

5 88 89
@tno.nl
290

Ter Hoek Vonkerosie Rijssen BV

Peter Sanders
T +31 (0)548-54 08 07
E sales@terhoek.com
www.terhoek.com **101**

Technobis Group BV

T +31 (0)72-30 20 040
E info@technobis.com
www.technobis.com
81

MOTION | POSITIONING

Infinite possibilities in precision motion at booth no.**138**

www.pi.ws/benelux

Precision Fair 2018

Precision Fair 2018

Wednesday 14th and Thursday 15th November 2018

OUDE REIMER BV
machines en gereedschappen voor de metaalindustrie

T +31 (0)35-64 60 920
E info@oudereimer.nl
www.oudereimer.nl **238**

NTS-Group
Accelerating your bussiness

T +31 (0)40-25 97 200
E info@nts-group.nl
www.nts-group.nl
27

Newport Spectra-Physics B.V.

Jorg Bos
T +31 (0)6-15 22 28 86
E jorg.bos@newport.com
www.ophiropt.com/photonics
www.newport.com **135**

PERTS IN
OSITIONING
ON ENGINEERING

85 777
@jpe.nl
277

The MathWorks B.V.

T +31 (0)40-21 56 700
E info@mathworks.nl
www.mathworks.nl
80

maxon motor

Manon Nijenhuis
T +31 (0)53 744 0 744
E info@maxonmotor.nl
www.maxonmotor.nl
5

Mitutoyo BeNeLux

Mr. Werner De Ridder
T +31 (0)318-53 49 11
E info@mitutoyobenelux.com
www.mitutoyobenelux.com
17

Exhibitors

Stand number	
160	2-S BV
249	4JET MICROTECH GMBH & CO. KG
255	AALBERTS ADVANCED MECHATRONICS
207	ACE STOßDÄMPFER GMBH
70c	ADRUU BV
02	ADVANCED CHEMICAL ETCHING
157	AEROTECH LTD
114	AJB INSTRUMENT BV
271	ALPHA TECHNIEK BV
154	ALUMECO NL BV
196	AMADA MIYACHI EUROPE
91	AMMERTECH BV
229	ANALIS NV
14	ANDES MEETTECHNIEK BV
133	ANTERYON BV
26	ART CCG CAULIL CYLINDRICAL GRINDING BV
266	ATG EUROPE BV
127	ATTOCUBE SYSTEMS AG
73	AVERNA
106	AXXICON EINDHOVEN
78	AZBIL EUROPE NV
109	B&S TECHNOLOGY BV
186	BALLUFF BV
92	BEARING DESING AND MANUFACTURING BV
76	BETECH GROUP
169	BKB PRECISION
123	BKL ENGINEERING BV
116	BOA NEDERLAND BV
251	BOUMAN HIGH TECH MACHINING
71	BRABANT ENGINEERING
64	BRAINPORT INDUSTRIES
162	BRONKHORST NEDERLAND BV
279	BRUKER
260	C3 TOOLING BV
198	CAPABLE BV
260	CCC PROJECTS & ENGINEERING
249	CDL-PRÄZISIONSTECHNIK GMBH & CO. KG
71	CEMATEC ENGINEERING BV
126	CERATEC TECHNICAL CERAMICS BV
261	CERATIZIT NEDERLAND BV
246	COLANDIS GMBH
288b	COMATE BVBA
93	CONNECT 2 CLEANROOMS LTD
183	CONWAY NEDERLAND BV
03	CUSTOM SPECIAL TOOLS BV
57	D&M VACUÜMSYSTEMEN BV
24	DCD TECHNOLOGY BV
190	DE RIDDER
156	DE ROOY SLIJPCENTRUM BV
25	DEKRACOAT BV
175	DEMACO
263	DEMATECH PARTS & PROJECTS
130	DEMCON
87	DIAMOND KIMBERLIT BV
205	DIXI POLYTOOL BV
100	DMS
115	DOEKO BV
39	DORMAC CNC SOLUTIONS
70d	DRALINE BV
150	DUTCH PRECISION TECHNOLOGY
275	DUTCH SOCIETY FOR PRECISION ENGINEERING
231	ECOCLEAN GMBH
143	EDMUND OPTICS GMBH
193	ELTREX MOTION
84	EMS BENELUX
215	ENCOMA CNC SOLUTIONS BV
291	ENTERPRISE EUROPE NETWORK / KAMER VAN KOOPHANDEL
287	ERIKS BV
235	ERNST & ENGBRING GMBH
224	EROWA AG
257	ERTEC BV
139	ETCHFORM
29	ETE PRODUCTIE TECHNIEK
65	EUSPEN
195	FAES CASES BV
53	FARO BENELUX BV
90	FAULHABER BENELUX BV
244	FEINMECHANIK ULRICH KLEIN GMBH
140	FESTO BV
181	FIJNMECHANISCHE INDUSTRIE GOORSENBERG BV
120	FMI HIGHTECH SOLUTIONS
294	FONTYS HOGESCHOOL CENTRE OF EXPERTISE HTSM
28	FORMATEC CERAMICS BV
47	FRAUNHOFER PROJECT CENTER
103	FRENCKEN EUROPE
249	FRT FRIES RESEARCH & TECHNOLOGY GMBH
249	GBM - GESELLSCHAFT FÜR BILDANALYSE UND MESSWETERFASSUNG MBH
04	GELDERBLOM CNC MACHINES BV
228	GENTEC BENELUX
07	GERMEFA BV
257	GF MACHINING SOLUTIONS INTERNATIONAL SA
92	GIBAC CHEMIE BV
56	GIBAS
240	GIMEX TECHNISCHE KERAMIEK BV
147	GLYNWED BENELUX BV
27b	GOM OPTICAL METROLOGY
237	GORE, W.L. & ASSOCIATES
37	GRONEMAN BV
55	HAUCK HEAT TREATMENT EINDHOVEN BV
34	HEIDENHAIN NEDERLAND BV
258	HELIOTIS AG
151	HEMABO PRECISIE KUNSTSTOFFEN
105	HEMBRUG MACHINE TOOLS
16	HEXAGON MANUFACTURING INTELLIGENCE
289	HIGH TECH MAINTENANCE NEDERLAND
40	HITTECH GROUP
194	HIWIN GMBH
22	HOGETEX
51	HOLLAND INNOVATIVE BV
180	HOSITRAD VACUUM TECHNOLOGY
136	IBS PRECISION ENGINEERING BV
192	ICHOR PRECISION MACHINING
134	IKO NIPPON THOMPSON EUROPE BV
142	ILT FINEWORKS BV
225	IMPA PRECISION
293	INHOLLAND DELFT PRECISION ENGINEERING
200	IPS TECHNOLOGY
227	ISP SYSTEM
277	JANSSEN PRECISION ENGINEERING BV
185	JENAER ANTRIEBSTECHNIK GMBH
208	JEOL
89	JEVEKA BV
118	JOB PRECISION
08	JOHAN FISCHER ASCHAFFENBURG GMBH & CO. KG
82	KEYTEC NETHERLANDS BV
38	KISTLER BENELUX
49	KMWE
70b	KMWE TOOLMANAGERS BV
274	KNF VERDER BV
18	KUSTERS GOUMANS BV
58	KUSTERS PRECISION PARTS
173	LAB MOTION SYSTEMS
201	LANDES HIGH END MACHINING BV
153	LARSEN & BUHL
210	LASER TECHNOLOGY JANSSEN BV
86	LASERTEC BV
95	LASOS LASERTECHNIK GMBH
226	LEERING HENGELO BV
45	LEMO
247	LEYBOLD NEDERLAND BV
188	LIAD ELECTRONICS
187	LIGHTHOUSE WORLDWIDE SOLUTIONS BENELUX BV
283	LIGHTMOTIF BV
217	LM SYSTEMS BV
137	LOUWERSHANIQUE
189	LUCASSEN GROEP BV
209	MACHINNO
202	MAGISTOR BV
20	MAKE! MACHINING TECHNOLOGY BV
245	MARPOSS GMBH
176	MASÉVON TECHNOLOGY GROUP
110	MAT-TECH BV
05	MAXON MOTOR BENELUX BV
259	MAZAK
267	MECAL HIGH-TECH / SYSTEMS
102	MELOTTE
70	METAALHUIS
42	METRICCONTROL
129	MEVI FIJNMECHANISCHE INDUSTRIE BV
243	MICRO-EPSILON MESSTECHNIK GMBH & CO. KG
09	MIFA ALUMINIUM BV
68	MIKROCENTRUM
213	MINIMOTOR BENELUX BVBA
203	MI-PARTNERS
17	MITUTOYO NEDERLAND BV
135	MKS INSTRUMENTS
09	MOGEMA BV
77	MOLENAAR OPTICS VOF
177	MTA BV
12	MTRC SPECIAL PLATING BV
171	MTSA TECHNOPOWER BV
199	MULTIVALENT PLATING & ETCHING BV
32	MURAAD BV
125	MYTRI BV
212	NB EUROPE BV
278	NEBO SPECIAL TOOLING BV
128	NEWAYS TECHNOLOGIES BV
30	NIJDRA GROUP BV
108	NIKON METROLOGY EUROPE NV
249	NMWP.NRW
27	NTS-GROUP
124	OERLIKON BALZERS
88	OLYMPUS NEDERLAND BV
238	OUDE REIMER
107	OWIS GMBH
122	PARKER HANNIFIN BV
43	PFEIFFER VACUUM BENELUX BV
138	PI BENELUX
281	PIEZOSYSTEM JENA GMBH
152	PINK GMBH VAKUUMTECHNIK
33	PM BV
219	PMP LICHTENVOORDE BV

242	POELMAN PRECISION BV	165	SMINK GROUP BV	132	TRESCAL
250	POLYTEC GMBH	44	SMS	286	TU DELFT
108b	POLYWORKS BENELUX	220	SOLID POINT PRECISION MANUFACTURING SDN BHD	284	TU/E HIGH TECH SYSTEMS CENTER
268	PQ+ NETHERLANDS BV	70e	SPARTNERS	231	UCM AG
11	PRECISION MICRO	265	SPECIAL TOOLS BENELUX BV	222	VACOM VACUUM COMPONENTS & METROLOGY BVBA
295	PROCLEANROOM	10	STEMMER IMAGING BV	46	VACUTECH BV
146	PROMIS ELECTRO-OPTICS BV	292	STICHTING LIS-TOP	211	VAN DEN AKKER FLUID SERVICE BV
262	PULSAR PHOTONICS GMBH	170	STT PRODUCTS BV	70a	VAN DER HOORN BUIGTECHNIEK
269	QSO INTERFEROMETER SYSTEMS AB	119	SUMIPRO BV	70h	VAN HOOF GROEP BV
270	QUANTUMCLEAN	70g	TB PRECISION PARTS BV	155	VAN HOORN CARBIDE NEDERLAND BV
256	RAYTECH BVBA	216	TBP ELECTRONICS	164	VARIASS GROUP
149	RELIANCE PRECISION LTD	95	TE LINTELO SYSTEMS	121	VARIODRIVE
288	RENA TECHNOLOGIES GMBH	81	TECHNOBIS GROUP	112	VDL ETG & VDL GL PRECISION
167	RENISHAW BENELUX BV	07	TECHNOLOGY TWENTE	66	VDMA ELECTRONICS, MICRO AND NANO TECHNOLOGIES
262	RJ LASERTECHNIK	206	TECHNOLUTION BV	60	VECO PRECISION
54	RODRIGUEZ GMBH	148	TECNOTION	176	VERNOOY VACUUM ENGINEERING BV
272	ROMEX BV	50	TEESING	70f	VIA ENGINEERING DEURNE BV
85	SALOMON'S METALEN BV	141	TEGEMA	48	VIRO
96	SBN NEDERLAND BV	23	TELMASTAAL BV	174	VOSSEBELT PRECISIEBEWERKING BV
79	SCHAEFFLER NEDERLAND BV	101	TER HOEK	145	VSL BV
41	SCHNEEBERGER GMBH	163	TEVEL TECHNIEK BV	35	WEISS NEDERLAND BV
01	SCHUT GEOMETRISCHE MEETTECHNIEK BV	276	THE HOUSE OF TECHNOLOGY	78B	WEISS TECHNIK NEDERLAND BV
144	SENTECH BV	80	THE MATHWORKS BV	98	WERTH MESSTECHNIK GMBH
191	SERVOMETER, A MW INDUSTRIES COMPANY	197	THK GMBH	249	WFMG
113	SERVOTRONIC BVBA	280	THORLABS	233	WIJDEVEN INDUCTIVE SOLUTIONS BV
159	SETTELS SAVENIJE PRECISION PARTS	290	TNO	72	WILL-FILL BVBA
15	SIGMACONTROL BV	172	TONASCO MALAYSIA SDN BHD	21	WILTING
104	SIOUX CCM	236	TOOLING SPECIALIST DERKSEN BV	223	WZW OPTIC AG
218	SKF BV, AFD. L&AT	31	TOTAL SUPPORT GROUP	19	ZEISS
74	SMARACT GMBH	260	TOWA EUROPE BV	249	ZENIT GMBH
166	SMC	222	TREAMS GMBH	161	ZME FIJNMECHANISCH ATELIER BV

BRECON GROUP

IPA Fraunhofer TESTED® DEVICE
Brecon Group
Brecon Cassette Panel System
Report No. BR 1804-1024

Brecon Cassette Panel System (BCPS) certified

Innovative modular building system tested for GMP- EHEDG- ISO 14644-1 facilities

The Brecon Group, 'preferred cleanroom supplier' since the early 90's to ASML, has developed a revolutionary new building system: the modular Brecon Cassette Panel System. This completely prefab wall and ceiling system, including windows and doors, makes the assembly of cleanrooms considerably more efficient and affordable. Thanks to the pre-made building elements, doors and windows,the building process is not only faster, but also much cleaner!

In addition, this system also offers the highest quality. The Fraunhofer Institute in Germany is the largest organisation for applied research in Europe.
For controlled environment applications, the hygienic design and a number of characteristics of the applied materials of the BCPS building system assessed according to the GMP Annex 1, EHEDG and ISO 14644-1 standards and guidelines have been tested by the Fraunhofer-IPA business unit. The BCPS is now the only cleanroom building system supplied in the Netherlands that is IPA tested and included in the data file tested-device.com

Can be implemented up to the highest level
The final assessment has led to a classification of the Brecon system according to ISO 14644-1 class 3 and GMP starting from the highest class A and lower. This means that the building system can be implemented up to the highest level in the pharmaceutical, medical device, food and cosmetic industries and the semi-conductor related sector.

With conventional building techniques, a frame construction is first made onto which plasterboard is usually attached as a foundation for PHL adhesion.
The Modular BCPS Cleanroom System is a more considered approach. The prefab panels of this system are made prefab in the factory. They can be supplied in HPL as well in Steel. Both final finishes are certified.
At the building site, the panels are assembled according to the click & fixed principle and then the cleanroom is further assembled. This offers many advantages: there are far fewer work activities on site and the throughput times at the project are much shorter. With renovations, the shutdown period is reduced considerably.
The modular panels are also ideally suited for re-use.

The new Brecon system is the result of extensive research into materials. We were also faced with the challenge of developing the right profiles and constructive composition of the doors, windows and ultimately the entire building system, the assessment of the correct parts and the search for innovative solutions concerning air transport... plus a list of hundreds of topics.
The certification is an important end result, of course, especially considering this intensive and complex development process. Best of all, the first results can be seen in the compounding pharmacy of the new Princess Maxima Centre in Utrecht, the MSD Pharmacist in Boxmeer, foods producer Nutricia in Zoetermeer and at MJN (Mead Johnson Nutrition) in Nijmegen.

For more information, please visit
www.brecon.nl

Droogdokkeneiland 7 - 5026 SP Tilburg - T 076 504 70 80 - www.brecon.nl

INNOVATIONS ON DISPLAY

Etchform (stand number 139)
Titanium etching

Titanium is difficult to etch. As standard, hydrofluoric acid (HF) is used for this. Depending on the concentration, this acid is considered either toxic or highly toxic and therefore use in a production environment is not advisable. That is why, over 15 years ago, Etchform developed its own process, which can be used safely in a production environment as it does not carry the risk of skin burns or even fatal incidents. This does not affect the results; the very accurate production technology delivers high-end, high-quality finished products.

Titanium is strong, light and biocompatible. It is so corrosion-resistant that it is often compared to precious metals in that aspect; the very stable oxide film makes titanium almost impenetrable to chemicals. Titanium is not magnetic either. Add the proper thermal conductivity to that, and the popularity of titanium has been fully explained.

Titanium parts are used in the medical sector, among others. Parts produced by Etchform include detector foils for proton irradiation, implants for facial reconstruction and dentistry, membranes for hearing aids, parts for microdosing, and collector grids for pacemaker batteries. Etchform also delivers titanium cooling plates and parts applied in electron microscopes and the aerospace industry.

WWW.ETCHFORM.COM

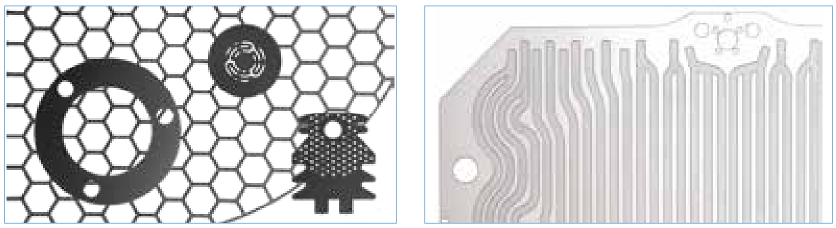

Various titanium parts.

Mitutoyo (stand number 17)
Novelties celebrating 50 years in Europe

The future of precision measurements lies in innovative software solutions that bring out the full potential of measuring hardware. The Internet of Things (IoT) connects a variety of machines to the network, enabling production processes to be continuously monitored in real time. On-site digitisation, automation and virtualisation boost work efficiency. With this idea, Mitutoyo BeNeLux presents several novelties.

MiSCAN
The brand-new MiSCAN multi-sensor vision system combines highly accurate non-contact vision measurements with tactile measuring, applying either the SP25M touch probe or Mitutoyo's newly developed MPP-NANO scanning probe. The SP25M provides accurate scanning measurements with high throughput while the MPP-Nano is specifically designed for high-accuracy scanning measurements of minute parts.

TAG-Lens
This lens uses ultrasonic sound waves to modulate light and is able to change the focus within nanoseconds. The ultra-fast depth-of-field control ensures that you can focus very quickly. It offers a new dimension for applications where fast 3D imaging is important.

Mach Ko-ga-me with robot
Accelerating and automating measurement procedures is important both in the measuring room and the production environment. The compact and fast in-line CMM Mach Ko-ga-me with robot set-up qualifies for obtaining extremely qualitative and accurate measuring results.

U-Wave fit
A newly developed system for the transfer of Digimatic calipers' and micrometers' measuring results to a PC via a receiver. The transmission unit's dimensions are smaller than the instrument's display size. The U-Wave fit sets an end to cumbersome cable connections and allows the connection of a multitude of measuring instruments with a single PC system.

Measurlink8
This advanced statistical platform provides real-time data and comprehensive quality reporting. It offers a good view of the inspection process and measurement results for successfully managing process improvement and defect prevention.

WWW.MITUTOYOBENELUX.COM

The MiSCAN multi-sensor vision system.

The U-Wave fit system enables measurement data transfer.

SIOS (Te Lintelo Systems, stand number 95)

The universal interferometer of the SP-NG series

The basic system of the SP-NG series is based on the proven concept of the compact single-beam laser interferometer from SIOS Messtechnik. These interferometers are distinguished by the fact that only one measuring beam, which is reflected by the measuring reflector back into itself, is used for the interferometric length measurement. This results in a defined sensing point on the measurement object. Therefore, it is possible to design the metrological arrangement so that the laser beam is exactly aligned with the measuring axis. This minimises the Abbe error that is a typical source of error in all length measurements. With a small reflector that can tilt up to ±12.5°, measurement set-ups can be quickly and easily calibrated.

The measuring principle of the interferometer also allows the use of a simple plane mirror as a reflector if there is considerable transverse displacement of the measurement object along the beam direction in the set-up. With the environmentally corrected light wavelength of a stabilised He-Ne laser as a highly stable natural measuring standard, these sensors have nanometer accuracy and excellent linearity. The light source is located outside the sensor in the evaluation electronics and the light is generally supplied via fibre-optic cables. As a result, the very compact size of the sensor head is determined only by optical elements.

For length measurements over longer distances, the SP-NG interferometers are equipped with a highly accurate environmental compensation, which is crucial for the measurement deviation. For short measuring distances, the standard version of the SP-NG interferometer has built-in alignment optics.

WWW.SIOS.DE

The compact SP-NG interferometer for a diagonal measurement in a machining centre.

Tecnotion (stand number 148)

New online direct-drive motor selection & simulation tool

With the new online calculation tool, replacing Tecnotion's offline tool, the user can simulate direct-drive motor behaviour under different conditions and with different movement profiles. At all times movement profiles, application parameters and motor types can be changed to explore options for maximum velocity, maximum efficiency or cost effectiveness. In this way, users can experiment with different scenarios and quickly find the one that best suits their application.

To start the simulation, a specific motor type and series have to be selected; then, a specific motor that is suitable, based on the necessary force. As a third step, one or more movement profiles are added, in order to reflect real-life movement, and the application data can be changed, to play, for example, with thermal and mechanical properties. Finally, the tool will show a graph with every relevant parameter, and a table with the relevant values of these parameters. You can see in an instant whether the motor is suitable or not. The inserted data can be adjusted easily.

Not only the usability of the tool has been increased, also a lot of new features have been adopted. For example, all motors that can be found in the Tecnotion catalogues – iron core, ironless and torque – are now available. Moreover, it is possible to save all the created simulations inside the tool, and adjust them in a later stage. In the torque motor simulations, there is an option to switch between degrees, radians and revolutions. For American users, there is a possibility to use imperial units, instead of SI units.

WWW.TECNOTION.COM/SIMTOOL

Four steps to use the tool.

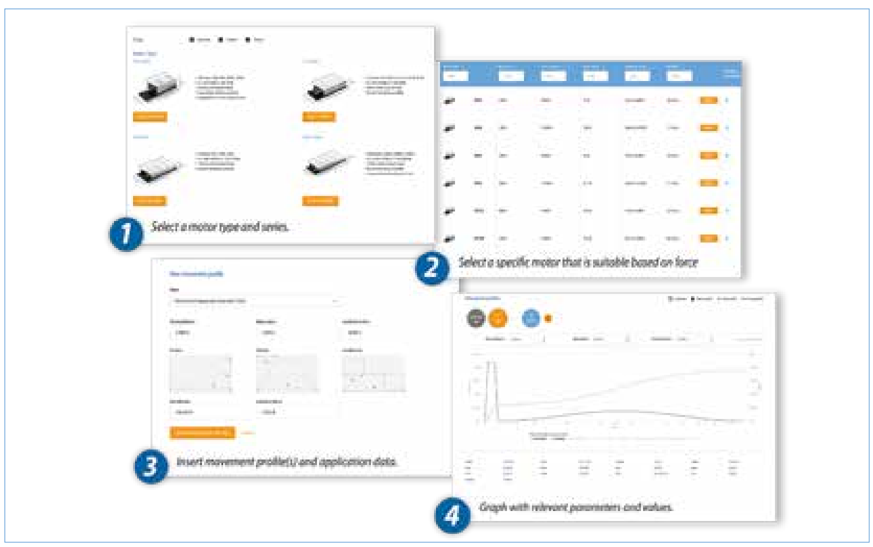

Jeveka (stand number 89)

The small screw for large cleanroom and vacuum applications

Vacuum is a challenging branch of sport. In the vacuum industry you often co-engineer with the customer. Screws and nuts that are still somewhere on the shelf are often unsuitable for building a vacuum installation. Those screws are greasy, which reduces friction during assembly, but contaminates vacuum. In addition, the alloy of the metal may contain unwanted elements that exhibit outgassing. Also, when assembling, gas residues can be trapped between the screw thread and behind the fastening article. This can result in 'untraceable' virtual leaks that ruin ultra-high and ultra-clean vacuum. Through collaboration, Jeveka has developed a new brand: Jeclin. Jeclin is a comprehensive range of fasteners especially for cleanroom and vacuum applications.
For vacuum applications, Jeveka makes vented screws with a hole drilled in the longitudinal direction. In this way the air behind the screw can be evacuated and virtual leaks are prevented. This enables shortening the pumping time needed for achieving the desired final pressure; consequently, production can start earlier.

The products have been on the market for some time, now the program is well established so that it can live on under its own brand name. In the name, Jeclin, Jeveka remains recognisable as sender (Je ~) and emphasis is on 'clean' (~ clin). The main difference between Jeclin and other fasteners for cleanroom and vacuum applications is the basic material.

For Jeclin, standard stainless steel A4-80 (1.4432) is used, i.e a higher strength class compared to many other screws.
In addition to the development of the vented screw, Jeveka provides all kinds of process steps for improving the material properties. Jeveka does not improve the material properties themselves, but it does happen under their control. One step in improving the material properties is electrolytic polishing. This reduces the surface roughness, so that less pollution can remain behind during the process. Then the stainless steel will not exhibit galling ('cold welding'). As little as possible material is removed in order to maintain the mechanical properties of the screw.
All super-clean fasteners are packaged in special polyamide bags.
As a result, the material is not exposed to plasticisers. Next, residual gas analyses are carried out and the products are validated, certified and coded with a certificate number. In this way, all products are traceable and their quality is monitored at all times.

Examples of Jeclin vented screws for vacuum applications.

TU/e High Tech Systems Center (HTSC) drives in depth research focusing on complex equipment with the emphasis on systems design and multidisciplinary approach. With a strong link between academia and industry HTSC is currently building consortia in the fields of (a.o.):

- Industrial Internet of Things
- AgriFoodTech
- Additive Manufacturing
- Digital Engineering
- Scientific Instrumentation
- Plasma Technology

Stay informed about building consortia and other developments of TU/e HTSC, and:

- Sign in for the HTSC newsletter and/or HTSC Research Meets via htsc@tue.nl
- Follow us on Twitter @TUeHTSC or LinkedIn https://www.linkedin.com/company/hightechsystemscenter/

Meet us at the Precision Fair on November 14 and 15, Baronie zaal, stand 284 (Koningshof, Veldhoven)

MICRO-OPTOFLUIDICS FOR MEDICAL DIAGNOSTICS

Renal disease patients need periodic haemodialysis to remove unwanted salts from their blood, and the efficiency of this process is dependent on the composition of the dialysis fluid. Knowing this composition, i.e. the relevant electrolyte concentrations, may also prevent fluid being thrown away after a single use, allowing it to be used on several occasions. At Eindhoven University of Technology in the Netherlands, Manoj Sharma has developed a smart micro-optofluidic sensor to measure the sodium-salt content in dialysis fluid.

FRANS ZUURVEEN

Manoj Sharma (B.Sc. in Electronics and Communication Engineering from M.S. Ramaiah Institute of Technology, India, and M.Sc. in Nanotechnology from KTH, Sweden) obtained his Ph.D. at Eindhoven University of Technology (TU/e) in the Netherlands on the topic of micro-optofluidics. His research at the TU/e Department of Mechanical Engineering involved developing a microfluidic device for electrolyte monitoring in dialysis. Figure 1 shows Manoj Sharma with the tiny lab-on-a chip. His interest in the use of microsystem technologies for medical applications led him to work on facilities for haemodialysis.

Diagnosis for dialysis

The advances in haemodialysis (HD) have saved the lives of millions of patients with kidney failure. HD is based on the convection and diffusion of ions between blood and dialysis fluid, also called dialysate. HD machines use a dialyser, a semi-permeable membrane, which allows solutes with a size smaller than the pore size in the membrane filter to move between blood and dialysate. This results in returning the blood plasma composition to normal values.

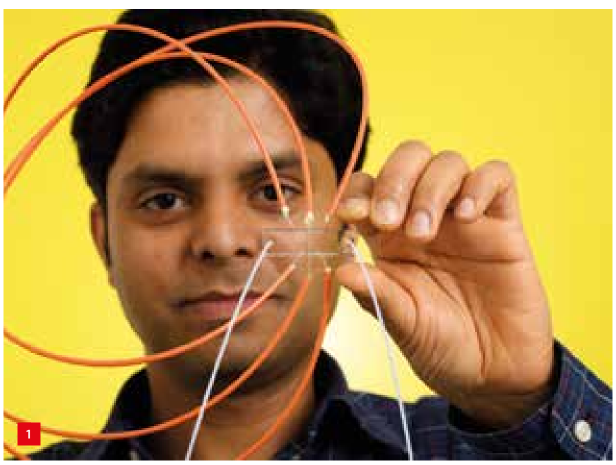

1 *Manoj Sharma with his lab-on-a-chip for measuring sodium ion concentration in dialysis fluid. (Photo: Bart van Overbeeke)*

AUTHOR'S NOTE

Frans Zuurveen, former editor of Philips Technical Review, is a freelance writer who lives in Vlissingen, the Netherlands.

A problem with the current HD method is that every patient has a different individual concentration of Na^+, K^+ and Ca^{2+} ions in their plasma, yet the standard concentration of these respective salts in dialysates is fixed. This one-size-fits-all approach might be contributing to cardiovascular complications, thus a reliable method for measuring salt concentrations in blood and dialysate is desired.

The rather simple method of measuring the fluid's electrical conductivity might offer some help, but it does not give values that can be contributed to the different kinds of salts mentioned above. Therefore, the TU/e research group concentrated on a different method: the molecular fluorescence measurement principle. Sensors based on this principle use PET molecules (PET = photoinduced electron transfer).

PET sensor molecules

Sharma explains the functioning of PET with the help of Figure 2: "The PET sensor consists of a fluorophore linked to an ionophore [or receptor] via a spacer and hence is called a fluoroionophore. The fluorophore part, also known as signalling part, acts as a transducer. The ionophore, also known as 'guest-binding' site, is responsible for the selectivity and efficiency of the binding of ions. The act of analyte binding at the ionophore is transmitted across the spacer to cause a change in photophysical properties of the fluorophore."

In the absence of an analyte, the HOMO (Highest Occupied Molecular Orbital) of the excited fluorophore is lower than the HOMO of the unbound receptor. This energy difference causes an electron transfer from the receptor (ionophore) to the fluorophore in the excited state, thus 'quenching' the fluorescence process. This state is also known as off-state.

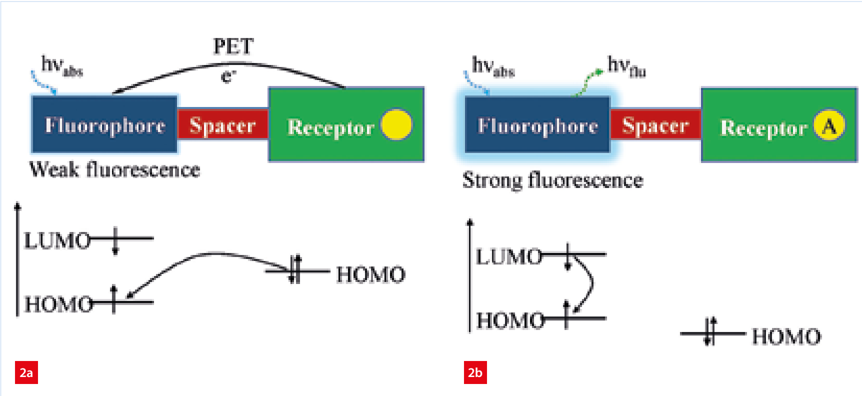

Diagram illustrating the principle of the signalling process of photoinduced electron transfer (PET), based on an 'on/off' switching mechanism through fluorescence or quenching light emission. HOMO = Highest Occupied Molecular Orbital, LUMO = Lowest Unoccupied Molecular Orbital. See text for further explanation.
(a) Unbound receptor (empty yellow circle in the green Receptor box).
(b) Bound receptor (yellow circle in the green Receptor box filled with an A, which stands for analyte).

When the receptor is bound to an analyte, the energy level of the excited fluorophore is higher than the HOMO of the receptor. Therefore, it is not energetically favourable for an electron to transfer from receptor to fluorophore. This leads to the relaxation of the excited electron from the LUMO (Lowest Unoccupied Molecular Orbital) to the ground state (HOMO), resulting in fluorescence emission. This is known as on-state. The on/off switching mechanism of the sensor molecule results in an intensity-based sensor upon ion binding.

In practice, the PET sensor molecules are surface-coated on the inner walls of the microchannel of the device; see the discussion below.

The optofluidic device

The PET-based micro-optofluidic chip is fabricated in a PDMS-substrate. PDMS (polydimethylsiloxane) is an optically clear and non-toxic kind of silicon plastic, ideally suited for making a microchannel for fluid flow. Figure 3a shows the schematics of the optofluidic chip, Figure 3b the real device. The microchannel is 500 μm wide and 225 μm high and has micropillars of 100 μm diameter at the detection region to increase the active surface area.

A photolithographic technique was used to make the chip after spin-coating a 225-μm thick negative photoresist layer on a standard silicon wafer. The photoresist was covered with a polymeric photomask and then exposed to UV light. After developing, the result was a master mould for making the microfluidic channels and the fibre coupling groove. This was followed by casting a PDMS mixture in a curing agent onto the master mould. After curing, the PDMS layer was peeled away from the mould. Inlet and outlet ports were then punched using a circular 1.2-mm diameter tool. A light microscope was used to align the fibre in the fibre coupler groove with respect to the PDMS microchannel.

Figure 4 shows the interrogation area, where the fluid under investigation meets the PET molecules. These can only be bound (using 'click chemistry') in the PDMS channel after first integrating NH_2-groups in the microchannel wall with a special chemical procedure. After this, a solution with the PET dye coats PET molecules onto the inner walls of the microchannel. Checking the outcome of these complicated chemical processes is performed by excitation with blue light of 470 nm wavelength and then observing the emitted 530 nm green light, as shown in the figure.

System design

The PET sensor described here is used by Sharma to measure sodium ion concentrations, but can also be modified (by changing the receptor) to measure potassium and calcium ion concentrations. Figure 5 shows the experimental set-up. A diode-pumped solid-state laser generates light with a wavelength of 450 nm. The PET-based micro-optofluidic device is placed between the laser light source and a spectrometer, which allows the recording of the device's output signal. A syringe pump controls the flow of dialysate or blood. Figure 6 demonstrates the effectiveness of the experimental

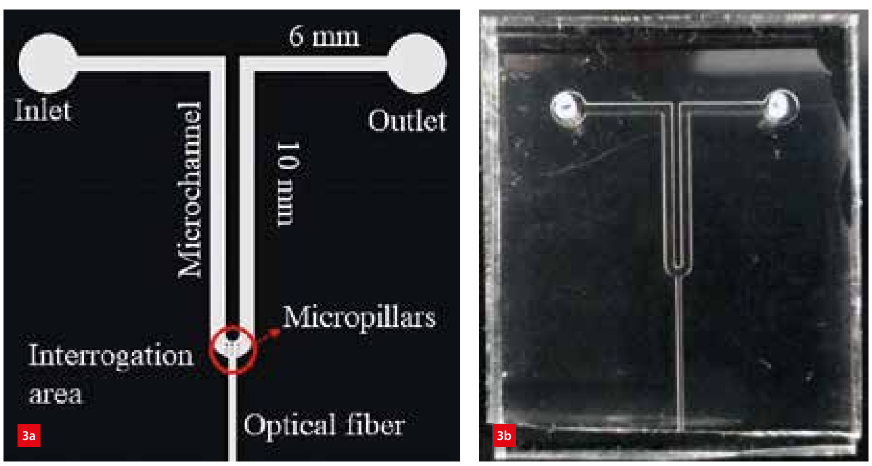

The microfabricated PET sodium ions measuring device.
(a) Schematic.
(b) Realisation, with a channel width of only 500 μm.

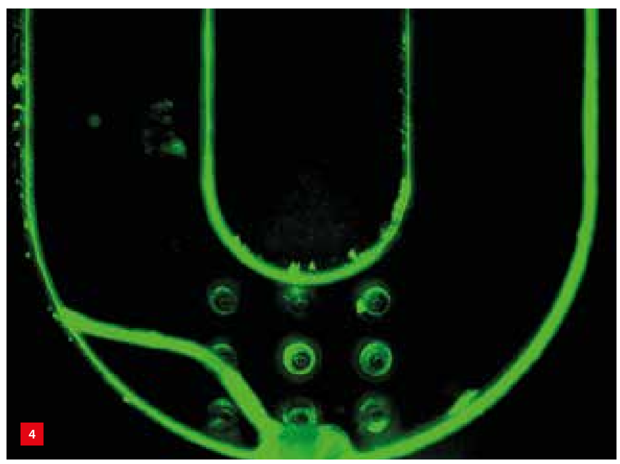

Fluorescence microscope image of the interrogation area of the micro-optofluidic chip. In green is the lighting of PET-molecules after excitation with blue light. The nine points are pillars for enlarging the active surface.

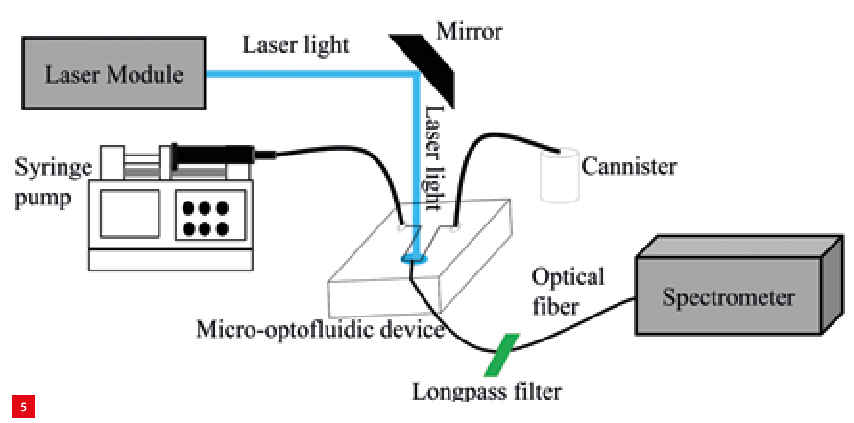

5

The experimental set-up with a laser-light source, a micro-optofluidic chip with integrated fibres and a spectrometer for measuring the intensity of emitted light.

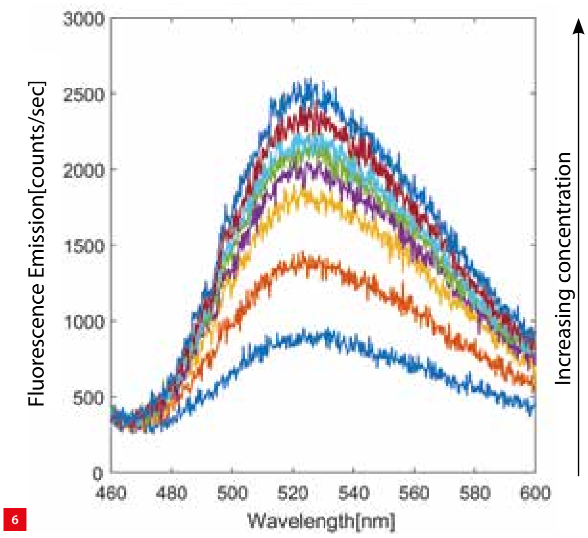

6

Fluorescence emission spectra of the micro-optofluidic device at various sodium concentrations (represented by different colours).

set-up. It shows the fluorescence emission as a function of the wavelength of the light measured by the spectrometer at different sodium concentrations (sodium chloride was used as a source of sodium ions). Taking the maximum of each curve in Figure 6 delivers the position of the points in Figure 7: peak fluorescence intensity as a function of sodium concentration.

Figure 7 proves the excellent functioning of the device developed by Manoj Sharma and his colleagues in the 0-10 mM concentration range as a proof-of-concept for the use of optical sensors for real-time monitoring of electrolytes. The typical (extracellular) concentration of, e.g., sodium in blood, however, is 130-140 mM. To measure such concentrations requires some modification of the receptor part of the current PET sensor, i.e. it needs additional binding sites to reach the physiologically relevant range of 130-150 mM.

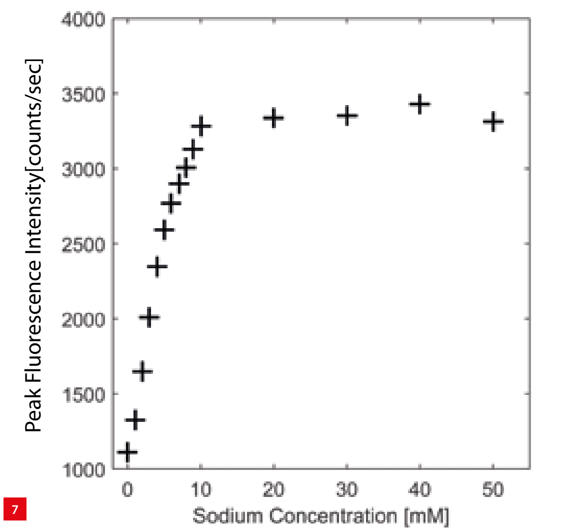

7

Intensity response of the micro-optofluidic device as a function of sodium concentration.

To conclude

A lot of work has to be done before medical laboratories can avail themselves of such a practical instrument for the measuring of salt contents in dialysis fluid and blood. It is quite certain, however, that such a device will improve dialysis procedures and save dialysis fluid, thus helping renal patients as well as the environment.

Literature

- M.K. Sharma, R. Göstl, A.J.H. Frijns, F.K. Wieringa, J.P. Kooman, R.P. Sijbesma and D.M. Smeulders, "A fluorescent micro-optofluidic sensor for in-line ionselective electrolyte monitoring", *IEEE Sensors Journal*, vol. 18 (10), pp. 3946-3951, 2018.
- M.K. Sharma, A.J.H. Frijns, R. Mandamparambil, J.P. Kooman and D.M. Smeulders, "Ion-selective optical sensor for continuous on-line monitoring of dialysate sodium during dialysis", *Optical Fibers and Sensors for Medical Diagnostics and Treatment Applications XVII, Proc. of SPIE*, vol. 10058, pp. 1005804-1 to 8, 2017.

FOCUS ON PRECISION IMAGINEERING

The two-day DSPE Conference on Precision Mechatronics 2018 in Sint Michielsgestel, the Netherlands, featured the theme of 'Precision Imagineering', representing the combination of precision, imagination and engineering. This report will focus on the exciting keynote presentations and the award-winning contributions. The biennial conference once again attracted a lot of young participants, so the dream of a bright precision engineering future lives on.

Talking about a bright perspective, the fine weather – the date of the conference was changed from early October to early September – helped to create a pleasant atmosphere with a lot of informal contacts outdoors on the very nice premises of the conference hotel. Figure 1 gives some impressions of the overall conference atmosphere. Indoors, intriguing posters and demos were presented (Figure 2).

This year's conference theme, 'Precision Imagineering', represented the combination of precision, imagination and engineering. An enterprise may start with a dream or 'imagination', but it takes 'engineering' skills in the broadest sense to actually transform an initial idea into a successful product, service or business. This was indeed reflected by the programme. All participants contributing an oral presentation, demo or poster presented top-of-the-bill, highly interesting material. A summary of all this can be found in the conference preview in the June issue of Mikroniek and on the conference website.

Guest keynotes

*Smart*light: a table-top synchrotron for the investigation of art objects*
Joris Dik, Antonie van Leeuwenhoek professor at Delft University of Technology, the Netherlands, gave a very nice overview of looking behind the visible part of art paintings with the aid of X-rays. Due to the presence of all sorts of pigments (meanwhile mostly forbidden because of their heavy metal content) hidden layers behind the visible art work can be discovered. Also the age of paintings can be determined accurately by detecting the elements and their relative amounts, and combining that information with the periods when the specific pigments were applied.

In this way, art history is being strongly pushed forward by technology. Nevertheless, the X-ray sources suffer from limitations in terms of low intensity, coherence and tuneability of energy. A synchrotron source overcomes this problem, but until recently there was no chance that they could be mobile and be made available on the museum site. New developments in ultra-low-emittance electron guns, compact X-band accelerator technology and high-power pulsed lasers will enable the development of a very compact synchrotron X-ray source with the possibility of carrying out very precise in-depth material analysis while the work of art can stay in the museum conservation studio.

Advancing precision in additive manufacturing
John Taylor, adjunct professor Center for Precision Metrology, University of North Carolina at Charlotte (USA), discussed the outcome of the Advancing Precision in Additive Manufacturing (AM) conference (Berkeley California, July 2018), which he had co-chaired (see also the September issue of Mikroniek). Taylor gave an extensive description of the latest developments in AM, together with their relationship to precision engineering. His main message in this lecture was that the transition towards precision AM can be made with the aid of determinism.

AUTHOR'S NOTE

Jos Gunsing is a technology innovator at MaromeTech and DSPE board member.

jos.gunsing@marometech.nl
www.marometech.nl


1
Conference impressions.

A selection of the demos.
(a) An overconstrained compliant mechanism, presented by TU Delft and UT.
(b) A set-up for bi-directional micrometer-accuracy film positioning, presented by Nexperia.
(c) A positioning stage, presented by Frencken.

With determinism he means: Solving problems of mankind using applied science, which means commitment to ensuring results with high certainty or known uncertainty. The implication is that results must be predictable, repeatable, quantifiable and measurable.

Taylor compared the AM development roadmap with, for example, that of diamond turning in earlier days. The big difference with many other manufacturing technologies is that the engineer is much more closely involved in the art and science of creating material properties; metallurgy, (crystal) structure, porosity, etc. AM is making very good progress but there is still a long way to go to be fully deployed in the precision engineering field

Note: John Taylor was also one the two presenters (the other being Hans Vermeulen of ASML and the TU/e High Tech Systems Center) in the mini-seminar "Precision engineering in the last 40 years", which was held the day after the conference, 6 September 2018, at Eindhoven University of Technology (TU/e). There he unveiled the impact of the search for determinism in precision engineering on his projects and his career.

Printing of lenses – from imagination to imagineering
Joost van Abeelen, COO of Luxexcel, based in Turnhout (Belgium), really showed a quest for the proper technology-market combination with the right products. Luxexcel started with the development of a process for printing lenses based on additive manufacturing. A lot of problems have been overcome, such as yellowing due to UV light; a treatment with a specific wavelength for 24 hours bleaches the lens to complete transparency.

The market that Luxexcel is now focusing on is that of ophthalmic lenses (in this case special/non-standard eye correction) where planoconvex or planoconcave lenses are possible (Figure 3). An adjacent market is that of electronic switchable sunglasses with a much better response time than the currently available electrochromatic lenses. A bit further in the future, applications with augmented reality are likely to emerge. Van Abeelen's lecture gave an interesting inside look into the struggle of a company not only to get the technology in place, but even more how to find the right market that fits in with the maturity level of its technology.

Awards

At the end of the conference awards were presented for the best presentation, demo and poster, selected by a panel of judges (Figure 4).

Presentation award
Jan Huang of ASML held an inspiring lecture on a completely new design for an in-vacuum linear stage with 30g acceleration capacity. Instead of increasing actuator size he took advantage of designing a resonant moving system, thus keeping the actuator for controlling the movement small and light. He applied magnetic springs at both ends

Ophthalmic lenses that were 3D-printed using Luxexcel technology.


4

The panel of judges had a challenging task in selecting the award-winning presentation, demo and poster. But it was fun, also during the award presentations.

of the moving stage. For the guiding of the stage he did not select magnetic but rather air bearings. The air is kept away from the vacuum by using scavenging grooves.

Huang came up with a smart design in which a hollow air-bearing shaft is used as a vacuum outlet gas pipe to the pump. Furthermore, a moving chamber on the stage connects the air-bearing scavenging grooves and the gas inlet to the shaft. In this way, the ambient pressure groove is kept away from the ultra-high vacuum in the process room and particle contamination is avoided.

The presentation of Jan Huang was not only interesting from a purely technical point of view; with his almost unlimited enthusiasm he entertained the audience and kept them engrossed, which was quite a challenge just before dinner.

Demo award

Lukas Kramer and his colleagues from the TNO Department of Optomechatronics demonstrated their nano-precision multi-agent Maglev positioning platform. The development of this device was triggered by the previous development of a multi-AFM platform (AFM = atomic force microscopy). By applying up to 50 free-moving agents (e.g. the AFMs) sitting on as many separate carriers freely moving over a Hallbach magnet array (Figure 5), the scanning AFMs can be moved in order to do their job independently.

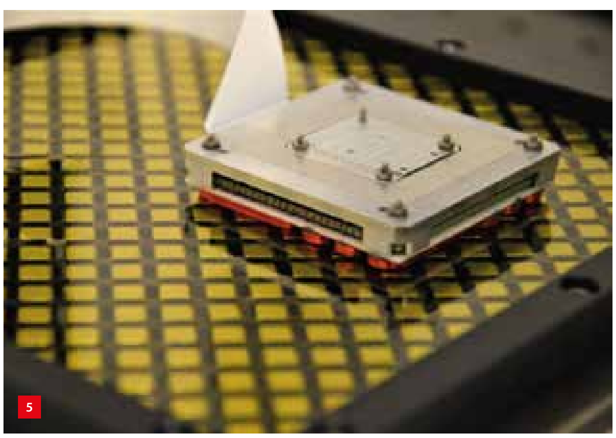
5

Realisation of a 50x50mm carrier with moving coils on a Hallbach array of magnets.

The carriers will be independently operated mini-systems which contain coils, Hall sensors and a controller/amplifier. In the future, wireless communication and energy transfer is foreseen to obtain the necessary autonomy. The carrier motion performance was demonstrated in this first demo set-up, which was still fitted with wired communication and a power supply. The applications/agents (in particular the AFMs) will be developed in parallel.

Poster award

Jaap Brand and his colleagues from VDL ETG Technology and Development presented a poster entitled "Lumped parameter model of vacuum flow, using 20SIM". An interesting modelling approach of complex vacuum systems, containing many discrete volumes and interconnections, was presented to simulate the pressure gradients and outgassing rates as a function of time. The vacuum architecture of complex systems can thus be predicted and optimised. The system was transformed into a lumped-parameter model and the simulation was carried out with the 20-sim program. Experimental results were used to match successfully with the model.

Conclusion

The DSPE Conference 2018 fulfilled all of its promises, with precision, engineering and imagination combined in the various contributions. This is no surprise considering the involvement of so many full-bred precision technologists, including those in the audience. We will now have to wait for the next DSPE Conference in 2020.

A special word of thanks goes to Annemarie Schrauwen and Adrian Rankers for organising the DSPE Conference already for the fourth time, to all program committee members and last but not least to all contributors of a presentation, demo or poster.

INFORMATION
INFO@DSPE-CONFERENCE.NL
WWW.DSPE-CONFERENCE.NL

SmartBin

exclusivey at **Jeveka**

- Continuous insight with stock on weight sensors
- Automated inventory keeping
- Proven technology
- Lower cost of ownership
- From bins to pallets

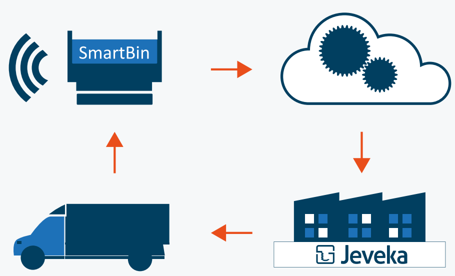

www.smartbin.nl

Jeclin

cleanroom & vacuum fasteners

developed by **Jeveka**

Jeclin, an extensive range of products for vacuum and cleanroom applications, was originally co-engineered for the semiconductor industry by Jeveka. Today, these fasteners are used in a wide range of applications that depend on vacuum or cleanroom technology, such as aerospace industry, solar systems and health technology.

- Available from stock
- Small packages and sales units
- Electro polishing, for reducing friction and particles
- Kolsterising, for preventing galling
- Cleanroom packaging for minimizing contamination
- Stainless steel A4-80
- Inconel and Titanium (grade 2 and 5)

www.jeclin.com

Jeveka

keeping it together

+31(0)36 303 2000
www.jeveka.com

Precision Fair 2018

Find us at stand 89

Also at our stand:

- Jextar SST fasteners > 900 N/mm²
- KATO inserts & tools
- Unbrako
- Specials
- Pepernoten

THE GLUEBUSTER SUCCESS

In 2016, SUSS MicroTec Photomask Equipment, a leading supplier of photomask process equipment, engaged Eindhoven-based engineering and high-tech manufacturing specialist KMWE for support in developing its MaskTrack X GlueBuster process station. Following the successful completion of the initial project in 2018, SUSS MicroTec has now expanded the scope of its initial engagement with KMWE to include complete assembly of the MaskTrack X GlueBuster module.

Early 2018, SUSS MicroTec launched its new pellicle glue removal system, the MaskTrack X GlueBuster, to support the maintenance of 193i lithography photomasks. Pellicles are used to prevent particles from contaminating the pattern area of a lithography mask during transport, storage and use. These pellicles consist of thin membranes, which are transparent at the exposure wavelengths. The membranes are stretched across an aluminium frame, which is then glued-on to the mask surface.

While pellicles provide protection from exogenous particles, masks must still be re-cleaned from time to time. This is primarily due to contamination that grows on the mask surface around the pellicle frame and underneath the pellicle membrane. This contamination can originate from airborne molecular contamination, residual mask surface contamination and even outgassing of pellicle materials.

Prior to cleaning these masks, the used pellicles must be removed. This removal process typically leaves behind residual glue where the frame was once attached to the mask surface. Before a new pellicle may be installed, this residual glue must be removed without damaging the pattern area. In the past this was not possible, and removal of the glue residue was limited to highly aggressive chemicals. Today, elimination of these aggressive chemicals is possible following the development of the MaskTrack X GlueBuster.

EDITORIAL NOTE

This article was based on interviews with Davide Dattilo, process scientist and project manager at SUSS MicroTec Photomask Equipment, Martin Samayoa, jr. director at SUSS MicroTec, Maarten Coolen, sr. design engineer at KMWE, and Peter Veldkamp, account manager at KMWE.

1 *SUSS MicroTec's MaskTrack X photomask cleaning platform.*

The GlueBuster module is now available for stand-alone operation or it can also be clustered with the MaskTrack X photomask cleaning platform, which can perform a variety of fully-automated mask cleaning operations (Figure 1).

Localised cleaning

The MaskTrack X GlueBuster performs localised pellicle glue removal by combining tightly controlled physical forces with an innovative delivery method of specifically-selected chemicals. By acting on the glue residue itself, the process chemicals and its by-products are constrained to an area that lies outside of the pattern area, which serves to ensure its cleanliness and integrity. This localised approach also reduces the total volume and cost of process chemicals.

Track record

The GlueBuster is the outcome of a development project that started in 2016 to meet industry's demand for a solution to the pellicle glue removal problem. After the project was approved at SUSS, the decision was made to outsource engineering of the new process station while retaining some of the standard assemblies and architectures for the new module.

After evaluating various candidates, KMWE was selected due to its well-fitted expertise and excellent track record in the semiconductor and aerospace markets, its competences in mechanical design, value-add engineering, and its extensive manufacturing capabilities (CNC machining and additive manufacturing). SUSS also considered its past 10-year collaboration with KMWE in other projects, such as the re-engineering of a mask aligner which demonstrated KMWE's potential in generating designs and delivering products based on functional specifications.

Challenge

One of the requirements for the process station was a precise alignment of the mask's edges to the movement of a highly innovative process arm. Other requirements included integrating a compact multi-cavity media dispense and suck-back system, an adjustable contact force system, and a running wiper tape system to the process arm itself. Aside from the mechanical challenges, the engineering group at KMWE had to venture into other areas to complete the design, such as chemistry, ergonomics, health and safety. Figure 2 provides an impression of the complexity of the design, without going too much into detail, for confidentiality reasons.

Design topics

The main feature of the MaskTrack X GlueBuster system is containment of the cleaning action. This is not limited to the physical contact between the wiper tape and surface, but also pertains to the process chemistry and even the fumes in proximity to the process area. This was achieved by integrating a highly innovative nozzle which allows media dispense and suck-back surrounding the wiper tape.

The process arm itself is attached to a programmable X/Y-stage which is equipped with a programmable surface contact force control system. While the surface contact force has to be high enough to enable efficient cleaning, it must also be controlled within tight boundaries to avoid damaging the mask surface. The surface contact force is frequently monitored by a load-cell and automatically adjusted if needed. After removal of the residual glue along one edge of the mask, the chuck holding the substrate is rotated 90 degrees, to consecutively position all edges of the mask with respect to the cleaning head. This reduces the degrees of freedom and the complexity of the process arm design and motion control.

Another critical component is the nozzle for dispensing the process chemicals. Its design determines the maximum achievable cleaning speed. This required a special configuration for the flow distribution channels inside the nozzle, which could only be realised by additive manufacturing (AM). Based on prior experiences with the shared AddLab research facility, KMWE designed the nozzle and printed it in the AddFab printing factory (*www.addfab.nl*). The development process addressed issues such as the fragile nature of a thin-walled product and the required post-processing for achieving an acceptable surface roughness.

With exceptionally high cleanliness requirements, the process station incorporates 'clean' inox steel and technical polymer materials. To prevent friction that generates particle contamination, bearings and bushings were positioned as far from the process area as possible.
The process area is also covered by a hood to provide a guarded, 'clean' environment which encompasses an opening for loading and unloading the masks. The hood also serves to confine chemical fumes if they would ever be present in this area, which is not the case in normal operation, provided they are evacuated by the suck-back function in the cleaning nozzle.

Partners

SUSS MicroTec

The SUSS MicroTec Group, headquartered in Garching, Germany, is a leading supplier of equipment and process solutions for micro-structuring applications with more than sixty years of engineering and manufacturing experience. The portfolio covers a comprehensive range of products and solutions for back-end lithography, wafer bonding and photomask processing, complemented by micro-optical components.

In close cooperation with research institutes and industry partners SUSS MicroTec contributes to the advancement of next-generation technologies such as 3D integration, EUV, and nanoimprint lithography, as well as key processes for WLP (wafer-level packaging), MEMS and LED manufacturing. With nearly 800 employees and a global infrastructure for applications and service, SUSS MicroTec supports more than 8,000 installed systems worldwide.

KMWE

Headquartered in Eindhoven, the Netherlands, KMWE is specialised in high-mix, low-volume, high-complexity products that involve machining of complex, functionally critical components, and high-quality (cleanroom) assembly and engineering of fully-tested mechatronic modules and systems for the aerospace & defence, semiconductor, medical and industrial markets. With over sixty years of experience, an international supplier network and more than 600 employees, KMWE is a global player with offices and partnerships in the Netherlands, Malaysia and India.

The capabilities of KMWE include engineering, machining, assembly of complex mechatronic systems in a cleanroom environment, additive manufacturing, sheet metal fabrication and thermal spraying.

WWW.SUSS.COM
WWW.KMWE.COM

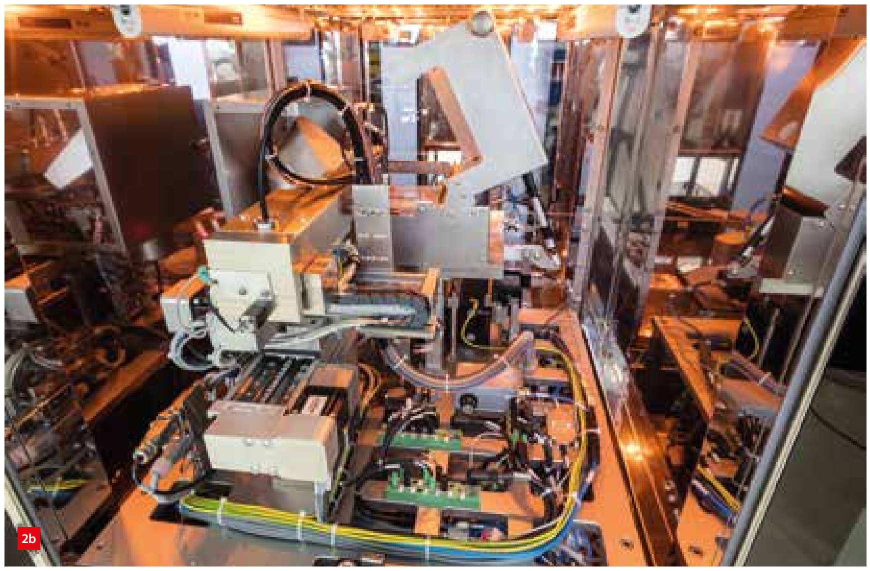

Close-ups of the MaskTrack X GlueBuster system.
(a) View of the process arm, engineered by KMWE, in the upper half of the photo, with the nozzle head on the left side.
(b) View of the X/Y-stage, which is used to position and move the nozzle as required to remove the pellicle glue residue without impacting the mask pattern area.

Another important design requirement was the operation of the cleaning wiper tape and the cassette from which it is dispensed. For moving the tape smoothly, in both directions, the effects of wetting and friction had to be taken into account. An innovative clamping mechanism featuring two spline axes was also designed, for rapid manual exchange of the tape cassettes.

Timeline

KMWE first engineered a functional alpha process station – a small-scale, table-top model comprising the mechanical parts of the process arm – which was delivered to SUSS in 2016, for preliminary testing and proof-of-concept. Based on the learnings from the alpha process station, a beta process station was then engineered in 2017 and assembled in close collaboration with SUSS. The beta module was later evaluated at a customer site in the USA. Most recently, a gamma process station, representing the first production-series version, has been delivered to SUSS for integration into the module. After final testing by SUSS, KMWE will complete the technical product documentation for the process station.

Future

At the time this article is being edited, three KMWE engineers are assisting SUSS engineers at its Sternenfels site with the assembly of a complete MaskTrack X Glue Buster photomask cleaning module (see Figure 3). This will provide KMWE the necessary experience and also assist in the creation of assembly documentation, covering the integration of the process station into the complete MaskTrack X GlueBuster module. KMWE may be contracted to assemble all future HVM MaskTrack X GlueBuster systems at one of its facilities, while pursuing continuous improvement and conducting value engineering to further enhance functional and cost performance.

This illustrates the close partnership and successful collaboration between SUSS and KMWE, which can be attributed to KMWE's technical capability and its ability to satisfy the customer's needs.

The SUSS-KMWE team at the SUSS MicroTec Photomask Equipment site in Sternenfels, Germany, working on the assembly of a MaskTrack X GlueBuster photomask cleaning platform.

Dynetics – dynamic in mechatronics

Dynetics specialises in high-quality, high-precision mechatronic components and helps customers economise their designs by offering solutions with an optimum price-performance ratio. Most of its products can be customised to the client's specific needs.

Dynetics, founded in 1994 and with offices in Germany and the Netherlands, assists engineers in selecting the most suitable motor for their mechatronic assignment. Dynetics represents leading manufacturers such as Nidec Servo, KSS, Nippon Pulse Motor (NPM) and Elmo, and offers a wide range of small rotating motors (up to 200 W) and high-precision linear motors (up to 100,000 N) with various technologies (piezo, brush, brushless, coreless), together with peripherals like ultra-high-precision lead screws, miniature ball screws, gearboxes, electronics and so on.

Many of the motors supplied by Dynetics can be customised. Examples of such include a double shaft or modified shafts, encoders and different windings. All fans and motors can be fitted with connectors as per customer request.

Portfolio

The products in the Dynetics portfolio can be roughly divided into five groups:

1. Rotating solutions in different technologies:
   - stepping motors (PM or hybrid);
   - brush and brushless AC, and PMDC-motors (with or without gear head);
   - coreless motors;
   - piezo motors;
   - options like gearheads and encoders.

2. Linear solutions in different technologies:
   - linear servo motors (actuators, cylinders and stages);
   - precision lead screws and miniature ball screws.

3. Motion controllers (ASIC, PCB and box level).

4. Fans and blowers.

5. Customised solutions.

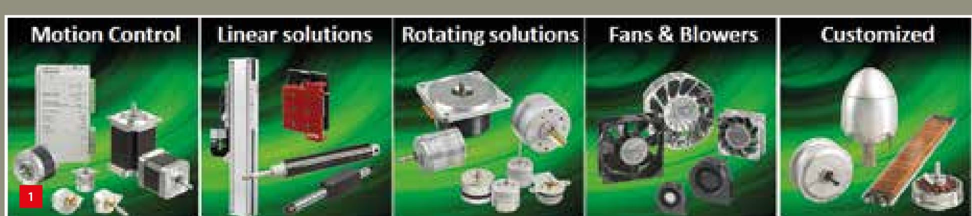

An overview of the Dynetics portfolio.

Logistics and service

Dynetics offers a comprehensive logistic system with a central warehouse in Best, the Netherlands, for optimal supply chain management. While the main focus is on the European market, Dynetics has customers around the world. As it understands that local presence is sometimes required, Dynetics also works with an extensive reseller network that is able to provide customers with the best possible service, as reflected in its motto: "Dynetics is a reliable partner with a long-term commitment focus".

Compact linear servo motors supplied by Dynetics for high-power-density applications.

INFORMATION
WWW.DYNETICS.EU


Efficient Solutions for Precision Parts Cleaning
www.ucm-ag.com
Experience UCM at the Precision Fair 14-15 November 2018 at the NH Conference Center Koningshof, Veldhoven, Dommelhal Booth 231
UCM supplies machinery for ultrasonic precision parts cleaning applications. Its globally leading solutions help companies around the world in achieving highest cleanliness requirements. From the High Tech and High Purity industries, through manufacturers of optical and medical components to precision parts from the tools and automotive industries, UCM always offers the right solution. UCM's success is based on innovation, efficiency, sustainability and technology that inspires!
SBS ECOCLEAN GROUP
UCM
technology that inspires


maxon motor
ϕ 266
Turning ideas into solutions together.
Visit us at the Precision Fair
Booth 05 | 14-15 November
www.maxonmotor.nl

UPCOMING **EVENTS**

4-9 November 2018, Las Vegas (NV, USA)

33th ASPE Annual Meeting

Meeting of the American Society for Precision Engineering, introducing new concepts, processes, equipment, and products while highlighting recent advances in precision measurement, design, control, and fabrication.

WWW.ASPE.NET

12-16 November 2018, Kamakura (JP)

17th International Conference on Precision Engineering

Conference, organised by the Japan Society for Precision Engineering, featuring digital design and manufacturing systems, non-traditional machining and additive manufacturing, robotics and mechatronics, and ultra-precision control.

WWW.SCOOP-JAPAN.COM/KAIGI/ICPE2018

14-15 November 2018, Veldhoven (NL)

Precision Fair 2018

Eighteenth edition of the trade fair and conference on precision engineering, organised by Mikrocentrum. See the preview on page 39 ff.

Precision Fair

WWW.PRECISIEBEURS.NL

21 November 2018, Utrecht (NL)

Dutch Industrial Suppliers & Customer Awards 2018

Event organised by Link Magazine, with awards for best knowledge supplier and best logistics supplier, and the Best Customer Award.

WWW.LINKMAGAZINE.NL

27-29 November 2018, Paris-Saclay (FR)

Special Interest Group Meeting: Structured & Freeform Surfaces

A special focus will be given to research fields in the following topics: replication techniques, structured surfaces to effect function, precision freeform surfaces, large-scale surface structuring, and surfaces for nano-manufacturing and metrology.

WWW.EUSPEN.EU

11-12 December 2018, Amsterdam (NL)

International MicroNanoConference 2018

Organ-on-chip, microfluidics, biosensing, and functional surfaces and interfaces are main topics of this industry- and application-oriented conference, exhibition and demo event.

WWW.MICRONANOCONFERENCE.ORG

12-13 December 2018, Den Bosch (NL)

AgriFoodTech 2018

Third edition of event featuring innovations within the agri and food sectors, such as sensors, drones, autonomous robots, smart farming, big data, vision technology and smart LEDs. The focus is on efficient, effective and sustainable production, in machine design and food processing as well as in the field.

WWW.AGRIFOODTECH.NL

22-23 January 2019, Sheffield (UK)

Integrated Metrology for Precision Manufacturing Conference

The first of two conferences being held as part of a roadmapping project to define the future of integrated metrology in advanced manufacturing in the UK.

WWW.NOTTINGHAM.AC.UK/CONFERENCE/FAC-ENG/METMAP-2019

13-14 March 2019, Veldhoven (NL)

RapidPro 2019

The annual event showcasing solutions for prototyping, product development, customization and rapid, low-volume & on-demand production.

Rapid Pro

WWW.RAPIDPRO.NL

13-14 March 2019, Sheffield (UK)

Lamdamap 2019

Thirteenth edition of this event, focused on laser metrology, coordinate measuring machine and machine tool performance.

WWW.LAMDAMAP.COM

19-22 March 2019, Ede/Veenendaal (NL)

Demoweek 2019

Eight companies demonstrate their automation offerings for the metalworking industry: software, robotisation, control, measurement, 3D printing and machining.

DeMO WeeK

WWW.DEMOWEEK.NL

25 March 2019, Düsseldorf (GE)

Gas Bearing Workshop 2017

Third edition of the initiative of VDE/VDI GMM, DSPE and the Dutch Consulate-General in Düsseldorf (Germany), focused on gas bearings as important components or integral technology of most advanced precision instruments and machines.

WWW.GAS-BEARING-WORKSHOP.COM

11 April 2019, Eindhoven (NL)

High-Tech Systems 2019

One-day conference and exhibition with the focus on high-end system engineering and disruptive mechatronics in for instance smart manufacturing, thermal design, smart logistics, scientific instruments, design principles and medical system.

WWW.HIGHTECHSYSTEMS.EU

3-7 June 2019, Bilbao (ES)

Euspen's 19th International Conference & Exhibition

This event features latest advances in traditional precision engineering fields such as metrology, ultra-precision machining, additive and replication processes, precision mechatronic systems & control and precision cutting processes. Furthermore, topics will be addressed covering robotics and automation, Industry 4.0 for precision manufacturing, precision design in large-scale applications, and applications of precision engineering in biomedical sciences.

WWW.EUSPEN.EU

HIGH-QUALITY NOMINATIONS FOR THE 2018 **WIM VAN DER HOEK AWARD**

For years the high-tech industry has been in dire need of technical talent. The good news is that the influx of technical students at the higher education level is increasing and that the outflux is of high quality. This last observation is once again evidenced by the nominations for the 2018 Wim van der Hoek Award. A total of five nominations, including one duo nomination, were received from universities of technology and applied sciences in the Netherlands and Belgium by the jury for this award, which will be presented in mid-November for the thirteenth time, under the auspices of DSPE, at the Precision Fair.

Candidates

Bart Cornelissen & Nick Toonen (AVANS Hogeschool 's-Hertogenbosch)

COO reduction by controlling leakage issue

"Students graduating in duo is customary at AVANS Hogeschool 's-Hertogenbosch. The report of Bart & Nick concerns modifications to a food processing machine. The existing design exhibited leakage during cleaning. After systematically excluding potential causes, and investigating possible problems, a new design was made that is likely to produce a significant improvement. Thanks to the structured approach, the commissioning company has so much confidence in the design that it decided to actually build the modified machine and test and monitor it under production conditions. Bart and Nick are serious go-getters with a good working attitude. Diving into a difficult problem they have shown inventiveness and focus and used a structured solution method, which has led to a well-founded design, taking into account the existing construction in the field. In doing so, they not only considered the technical aspects but also took a commercial view (cost of ownership reduction)."

Jens de Goeij (UAS Utrecht)

Het ontwerp van de verticaal translerende beweging van een wafer handler transport robot

"Jens had the very complex challenge of redesigning the vertical translating movement of a wafer-handler transport robot, because it was overdimensioned and the reliability left something to be desired. With his unique combination of practical experience and physical insights, Jens searched for the right solution in a very structured manner. In doing so, he took into account the fact that the robot arm had to fit into a very small space, had to be able to position itself with a high degree of accuracy and at a low contamination level. Jens considered various construction principles and thoroughly tested his design. As a result of the tests, various adjustments have been made and this has led to a well-founded concept. Jens is good at receiving and processing feedback and is willing to communicate in an open and direct way."

Bert Van Raemdonck (KU Leuven)

Design and tuning of an elastic inflatable actuator with a non-linear response

"Bert has shifted the scientific boundaries concerning inflatable flexible actuators. In essence, he developed a new type of balloon actuator with unseen nonlinear properties, which are not only scientifically interesting, but also extremely useful for applications in medical surgery. Whereas researchers and engineers often try to avoid nonlinear behaviour, Bert has shown that these characteristics are the key to hardware intelligence in soft robotics, which until now seemed far-off. With a thorough analysis, Bert managed to capture the foundations of these nonlinearities, which he later verified with tests on prototype actuators. The combination of an excellent analytical capacity with an excellent practical insight is an extremely desirable combination that makes Bert an engineer who has already made his mark on science and technology."

Roy Jacobs (TU Eindhoven)

Design and analysis of a passive vibration isolation system using negative stiffness
"Roy has come up with a new approach to reduce the pneumatic stiffness in air mounts, viz. by integrating an additional negative stiffness mechanism. Based on first principles in literature, and after studying magnetic and pneumatic alternatives, he designed and analysed an adjustable non-linear compliant mechanism, which allows for accurately tuning the required isolation frequency independent of the load distribution in the optical system. The concept design is patent pending. Roy has demonstrated very good engineering skills, not only in utilising and further developing design principles, but also bridging towards other domains. He works in an independent, systematic manner, both in an academic and industrial environment."

Martin Kristelijn (TU Eindhoven)

Design of a motion compensation mechanism for offshore load transfer
"With his proposed design for a motion compensation and load transfer mechanism, Martin has demonstrated his broad talent in mechanical engineering, both in kinematics and structural design and analyses at the component level, including cost assessment. His novel concept for offshore load transfer that is based on a Roberts straight-guide mechanism, is modular and rather compact, and was designed for minimal parasitic platform motion and high stability. Martin possesses good analytical and communication skills and works very independently."

PIB DAY AT **PUNCH POWERTRAIN**

On 4 October 2018, Punch Powertrain in Eindhoven, the Netherlands, hosted a DSPE Precision in Business day (PiB day). Whereas most PiB days are organised at manufacturers of high-tech machinery, this time the focus was on the automotive branch, although one could assert that cars are high-tech machines nowadays. Punch Powertrain is an independent developer and manufacturer of automatic transmissions, electric and hybrid powertrains for passenger cars. In the development of new product lines, Punch Powertrain prioritises minimal fuel consumption and low emissions.

Jeroen van Assen, director of New Product Development DCT (Dual Clutch Transmission) of Punch Powertrain, welcomed the DSPE party, counting nearly thirty participants, and outlined his route from high-tech machinery to automotive. He derived his motivation from his personal interests matching the mission of Punch Powertrain: "Punch intends to become the leading independent provider of innovative clean powertrain technologies for car manufacturers."

Van Assen sketched the history of Punch Powertrain, starting as a supplier for DAF transmissions and, after the bankruptcy of DAF, continuing as an independent separate company, Punch Powertrain. In addition to that, at the beginning of this century three Ph.D. graduates from Eindhoven University of Technology started their own company, Drivetrain Innovations. They continued their development and in 2013 were taken over by Punch Powertrain. Their location is now Punch's Eindhoven branch.

Automatic transmissions
Punch specialises in automatic transmissions (continuously variable transmissions, CVTs) and these days transmissions for electric cars are its fastest growing market. Therefore, the focus is on developing transmissions for this market, with the latest goal being to develop a new transmission for Peugeot (PSA), the DT2. In China, Punch is the second largest automatic transmission supplier. And 4% of all automatic transmissions are Punch CVTs. Of all CVTs in China, 80% come from Punch. In Europe, however, these products are not available on the market.

This spring, Groupe PSA selected Punch Powertrain technology for its future electrified transmission systems. Punch Powertrain is to supply its newest generation of patented e-DCT systems by 2022, as part of Groupe PSA's electrification push. This electrified Dual Clutch Transmission – hybrid DT2 – with a 48V motor will equip Mild Hybrid Electric Vehicles.

Koen van Diepen, Product Architect of Punch, continued with a presentation about the system principles, as far as these were not confidential. He started with the explanation why you actually need a transmission in your car: with a combustion engine your traction is not constant. And to have good traction for the entire range of speeds, you need to shift gear. There are various options to address the gearing challenge and Van Diepen explained the differences between the classic manual transmission, and dual clutch transmission (DCT).

He focused his presentation on a DCT system, DT1. Development started with making a choice between two systems: AMT (automated manual transmission) and DCT. The advantages and disadvantages of both options were assessed and Punch combined the best of both worlds: good performance, low cost, good drivability, ... A major issue is always the reduction of cost and complexity. One way of achieving this is by reducing the number of parts of a system. They investigated the possibilities and took into account the inevitable downside of parts reduction. In this case, for instance, the number of gears had to be reduced. Luckily this did not compromise performance.

A crucial question in transmission development is always the optimisation of the transmission ratios. This depends on the car's applications, for example on the motorway, in commuter traffic, inner-city driving, and traffic jams. As the transmission is a mechatronic system, there is active clutch control, by the TCU (transmission control unit).

Systems engineering

To conclude, Van Diepen focused on the system approach to the development of a new transmission. The systems engineering group within Punch Powertrain combines three system aspects: purpose (to the customer/end-user), elements (structure, boundaries) and interaction (interfaces, behaviour). Therefore, they organised a 3D matrix of structure, behaviour and requirements. They use the well-known V-model with a PCP (product creation process) that is divided into seven target goals. The V-cycle is run at various levels: Business, Application, Transmission, Modules, and Components. There is a breakdown from one level to the next: first the requirements, and after the development and building of the system, a validation of all the components and the system is required.

Requirements management

Related to systems engineering is requirements management: how to deal with and satisfy the requirements? Systems engineer Rainier Brouwer, who has gained experience with this in start-ups and mature organisations (Philips, Bosch, DAF), gave a presentation about the historical perspective and how requirements management is conducted within Punch. From the historical perspective, the complexity of systems has increased enormously. The same applies to the requirements. For the sake of clarity, Punch split up the related activities into requirements management and requirements engineering.

Going from your requirements to making design decisions, how does that work? According to Rainier Brouwer it might be as simple as: common sense. This works with low as well as high complexity, but the tools to be used for the different cases vary. As Punch develops very complex systems, they acquired a Requirements Management System (RMS), Polarion. For the development of the DT1 system, the RMS divides the system into layers, domains and modules in order to obtain a product breakdown system.

The structured way of working was an advantage in closing the deal with PSA. Besides Punch's own requirements for DT1, PSA formulated many additional requirements. It appeared that the different languages used (French and English) could lead to misunderstanding: the requirements were written in French, and the translation into English was not always optimal. This inspired a lot of discussions about the requirements. The various system levels are reflected in the requirements: Business, Application, Product and Modules.

After the requirements ('reqs') have been defined and the design has been finished, it has to be verified that the design satisfies the reqs. Naturally, Punch shares all the information with clients like PSA. Together they decide whether a req has been met or not. It is therefore possible that a req has to be adjusted. This can have a lot of consequences for the total system, and all the reqs involved. The systems engineer must consequently be aware of these kinds of changes, to help the design team to do the right things. Which brings Rainier Brouwer back to his Rule #1: Use your common sense.

This concluded the DSPE PiB day at Punch Powertrain. DSPE wishes to thank Punch for hosting this informative and entertaining event.

Impression of the tour of the Punch Powertrain premises in Eindhoven during the PiB day.

(report by Marty van de Ven)

WWW.PUNCHPOWERTRAIN.COM

ECP² COURSE CALENDAR

COURSE (content partner)	ECP² points	Provider	Starting date
FOUNDATION			
Mechatronics System Design - part 1 (MA)	5	HTI	8 April 2019
Fundamentals of Metrology	4	NPL	to be planned
Mechatronics System Design - part 2 (MA)	5	HTI	to be planned
Design Principles	3	MC	13 March 2019
System Architecting (S&SA)	5	HTI	11 March 2019
Design Principles for Precision Engineering (MA)	5	HTI	26 November 2018
Motion Control Tuning (MA)	6	HTI	6 February 2019
ADVANCED			
Metrology and Calibration of Mechatronic Systems (MA)	3	HTI	6 November 2018
Surface Metrology; Instrumentation and Characterisation	3	HUD	to be planned
Actuation and Power Electronics (MA)	3	HTI	20 November 2018
Thermal Effects in Mechatronic Systems (MA)	3	HTI	13 March 2019
Summer school Opto-Mechatronics (DSPE/MA)	5	HTI	-
Dynamics and Modelling (MA)	3	HTI	26 November 2018
Manufacturability	5	LiS	to be planned
Green Belt Design for Six Sigma	4	HI	to be planned
RF1 Life Data Analysis and Reliability Testing	3	HI	5 November 2018
SPECIFIC			
Applied Optics (T2Prof)	6.5	HTI	to be planned
Applied Optics	6.5	MC	28 February 2019
Machine Vision for Mechatronic Systems (MA)	2	HTI	to be planned (Q2 2019)
Electronics for Non-Electronic Engineers – Analog (T2Prof)	6	HTI	7 January 2019
Electronics for Non-Electronic Engineers – Digital (T2Prof)	4	HTI	4 February 2019
Modern Optics for Optical Designers (T2Prof)	10	HTI	to be planned (Q3 2019)
Tribology	4	MC	12 March 2019
Basics & Design Principles for Ultra-Clean Vacuum (MA)	4	HTI	20 November 2018
Experimental Techniques in Mechatronics (MA)	3	HTI	to be planned (Q2 2019)
Advanced Motion Control (MA)	5	HTI	5 November 2018
Advanced Feedforward Control (MA)	2	HTI	to be planned
Advanced Mechatronic System Design (MA)	6	HTI	to be planned (Q3/4 2019)
Finite Element Method	5	ENG	in-company
Design for Manufacturing – Design Decision Method	3	SCHOUT	in-company
Precision Engineering Industrial Short Course	5	CRANF	11 February 2019

ECP² program powered by euspen

The European Certified Precision Engineering Course Program (ECP²) has been developed to meet the demands in the market for continuous professional development and training of post-academic engineers (B.Sc. or M.Sc. with 2-10 years of work experience) within the fields of precision engineering and nanotechnology. They can earn certification points by following selected courses. Once participants have earned a total of 45 points, they will be certified. The ECP² certificate is an industrial standard for professional recognition and acknowledgement of precision engineering-related knowledge and skills, and allows the use of the ECP² title.

ECP2EU.WPENGINE.COM

Course providers

- Engenia (ENG)
  WWW.ENGENIA.NL
- The High Tech Institute (HTI)
  WWW.HIGHTECHINSTITUTE.NL
- Mikrocentrum (MC)
  WWW.MIKROCENTRUM.NL
- LiS Academy (LiS)
  WWW.LISACADEMY.NL
- Schout DfM (SCHOUT)
  WWW.SCHOUT.EU
- Holland Innovative (HI)
  WWW.HOLLANDINNOVATIVE.NL
- Cranfield University (CRANF)
  WWW.CRANFIELD.AC.UK
- Univ. of Huddersfield (HUD)
  WWW.HUD.AC.UK
- National Physical Lab. (NPL)
  WWW.NPL.CO.UK

Content partners

- DSPE
  WWW.DSPE.NL
- Mechatronics Academy (MA)
  WWW.MECHATRONICS-ACADEMY.NL
- Technical Training for Prof. (T2Prof)
  WWW.T2PROF.NL
- Systems & Software Academy (S&SA)

Lightmotif OP3 machine installed at Philips

Philips in Drachten, the Netherlands, put a new OP3 machine from Lightmotif, based in Enschede, the Netherlands, into operation during the first half of 2018. This 5-axis laser micromachining system is used for rapid prototyping of shaving systems, as well as for machining of tooling and micro-texturing of moulds. The machine uses an ultrashort-pulse laser (picosecond laser), capable of precise machining of various materials without negative heat-related effects, by so-called ablation processes (local evaporation of material). With this new capabilities Philips's aim is to improve existing processes and to develop new applications.

The machine delivered by Lightmotif has been specifically developed for laser micro-milling and laser micro-texturing of flat and curved surfaces. With laser milling micrometer-accurate pockets can be machined into any material, irrespective of its hardness. This technique is for example used for machining accurate 3D-shaped metal prototypes or tooling. Laser micro-texturing is used for example to apply very fine textures to surfaces of (curved) injection moulds, which isn't possible by other techniques. These fine textures can add new functional properties to surfaces of materials, such as reduced friction or super-hydrophobicity.

With the investment in the OP3 a close collaboration was started between Philips and Lightmotif. Lightmotif will help the application engineers of Philips in developing new processes and applications, and Philips will provide valuable user feedback to Lightmotif supporting continuous improvement of the machines and software.
Lightmotif, a spin-off company of the University of Twente and the M2i institute, develops production solutions for micromachining based on the use of ultrashort-pulse lasers. Since the launch of the company in 2008, they invested heavily in R&D, which resulted in a flexible machine concept and control software specifically designed for laser micromachining. For this, Lightmotif was rewarded with the Laser Innovation Award in April 2018.

Lightmotif's OP3 machine installed at Philips in Drachten.

A 10-mm diameter steel sphere with a pyramid texture (0.2 × 0.2 mm raster, 100 μm high). Behind that a 50 mm diameter steel sphere with a negative pyramid texture (0.5 × 0.5 mm raster, 40 μm deep).

WWW.LIGHTMOTIF.NL

Brecon Cassette Panel System certified

The Brecon Group, 'preferred cleanroom supplier' since the early 90s to ASML, has developed a revolutionary new building system: the modular Brecon Cassette Panel System. This completely prefab wall and ceiling system, including windows and doors, makes the assembly of cleanrooms considerably more efficient and affordable. Thanks to the pre-made building elements, doors and windows, the building process is not only faster, but also much cleaner.

The innovative modular building system was tested for GMP- EHEDG- ISO 14644-1 facilities. The final assessment has led to a classification of the Brecon system according to ISO 14644-1 class 3 and GMP starting from the highest class A and lower. This means that the building system can be implemented up to the highest level in the pharmaceutical, medical device, food and cosmetic industries and the semiconductor-related sector.

The new Brecon system is the result of extensive research into materials. Brecon was also faced with the challenge of developing the right profiles and constructive composition of the doors, windows and ultimately the entire building system, the assessment of the correct parts and the search for innovative solutions concerning air transport... plus a list of hundreds of topics. The certification is an important end result, of course, especially considering this intensive and complex development process.

WWW.BRECON.NL

The right time for etching titanium

The application of titanium and its alloys has seen rapid growth over the last few decades, mainly as a result of the metal's high strength and low density. The density of titanium is almost half that of copper and less than 60% of the density of stainless steel. The tensile and yield strengths of titanium are comparable to those of most stainless steels. The resulting high strength-to-weight ratio accounts for the widespread use of titanium; most notably in the aerospace industry (nearly 80% of titanium is used in the aerospace industry).

Thanks to their biocompatibility, corrosion resistance and mechanical strength, titanium alloys have also found widespread use in medical applications, such as in medical implants. Chemical processing is another area where titanium is used due to its outstanding resistance to aggressive chemical environments.

Wet photochemical etching can be used to produce patterns and features from metal sheets, including titanium alloys. Etching works by selectively dissolving the metal using an oxidising chemical reagent. Areas where etching of the metal is required are left exposed to the etching solution, while the rest of the metal surface is covered with a protective polymeric film known as the photoresist. It is essential that the photoresist remains attached to the metal areas where etching is not required.

Etching of titanium is conventionally carried out using hydrofluoric acid (HF) or a mixture of hydrofluoric and nitric acids. The effective etching reagent is hydrofluoric acid while the optional nitric acid is used mainly to reduce hydrogen absorption and therefore hydrogen embrittlement in the final part. However, there are two major issues associated with using HF and nitric acid. Firstly, HF is a major health and safety hazard. Secondly, both HF and nitric acid tend to attack most types of photoresists, ultimately causing detachment of the photoresist.

Advanced Chemical Etching (ACE), based in Telford, UK, specialises in photo-chemical etching and aims at advancing the state of this industry.

Photochemically etched products; 'TiME' indicated the titanium products.

(to be continued on the next page)

Innovations can have a huge impact on industries which use chemically etched components in the manufacture of their products, such as the medical, electronic, automotive and aerospace industries. Advances in etching technologies will allow more complex and intricate geometries to be produced and will make it possible to etch new materials that are difficult to etch using conventional methods.
Therefore, ACE invested in an intensive R&D programme to develop a non-HF process for the etching of titanium alloys. This resulted in the TiME™ process for etching titanium as well as nickel-titanium alloys. The new process uses a unique chemistry that is safer than conventional HF-based solutions. The process also includes a pre-treatment step to improve photoresist adhesion to the metal, as well as a post-etch treatment process to achieve the required surface finish.
Etching can produce complex features and geometries in titanium sheets. Sheet sizes of up to 330 x 1,000 mm and thicknesses ranging from 70 µm to 1.0 mm can be processed using the new process. Moreover, the process does not affect the chemical and mechanical properties of the metal.
The recent expansion of the company to double its previous size was driven in part by the success of the new TiME process. In the Benelux, Advanced Chemical Etching is represented by Cumatrix.

WWW.ACE-UK.NET
WWW.CUMATRIX.COM

Mikroniek on ResearchGate

In 2014, Mikroniek published a series of three articles, "Introduction to Frequency Response Function measurements – Part 1, 2 and 3" (volume 54, issues 2, 3 and 4, respectively). The authors were Pieter Nuij and David Rijlaarsdam from NTS Systems Development (and Maarten Steinbuch (TU/e) and Johan Schoukens (VUB) for Part 3). The articles were posted on ResearchGate, a professional network for scientists and researchers, with over 15 million members from all over the world using it to share, discover, and discuss research. Since then, the article series has generated over 1,100 reads.

Other Mikroniek articles can also be found on ResearchGate. Mikroniek authors are invited to post their publications.

WWW.RESEARCHGATE.NET

MathWorks expands deep learning capabilities

Last month, MathWorks introduced Release 2018b of MATLAB and Simulink. The release contains significant enhancements for deep learning, along with new capabilities and bug fixes across the product families. The new Deep Learning Toolbox, which replaces Neural Network Toolbox, provides engineers and scientists with a framework for designing and implementing deep neural networks. Now, image processing, computer vision, signal processing, and systems engineers can use MATLAB to more easily design complex network architectures and improve the performance of their deep learning models.

As deep learning becomes more prevalent across multiple industries, there is a need to make it broadly available, accessible, and applicable to engineers and scientists with varying specialisations, according to MathWorks. "Now, deep learning novices and experts can learn, apply, and conduct advanced research with MATLAB by using an integrated deep learning workflow from research to prototype to production."

WWW.MATHWORKS.COM

Air Bearings

AeroLas GmbH
Grimmerweg 6
D-82008 Unterhaching
Germany

T +49 89 666 089-0
F +49 89 666 089-55
E info@aerolas.de
W www.aerolas.de

AeroLas is world leader in air bearing technology strengthening the customer´s competitive advantage with customized air-guided products and solutions.

Automation Technology

Festo BV
Schieweg 62
2627 AN DELFT
The Netherlands
T +31 (0)15-2518890
E sales@festo.nl
W www.festo.nl
Contact person:
Mr. Ing. Richard Huisman

Festo is a leading world-wide supplier of automation technology and the performance leader in industrial training and education programs.

member DSPE

Cleanrooms

Brecon Group
Droogdokkeneiland 7
5026 SP Tilburg
T +31 (0)76 504 70 80
E brecon@brecon.nl
W www.brecon.nl

Brecon Group can attribute a large proportion of its fame as a cleanroom builder to continuity in the delivery of quality products within the semiconductor industry, with ASML as the most important associate in the past decades.

Brecon is active with cleanrooms in a high number of sectors on:
* Industrial and pharmaceutical
* Healthcare and medical devices

member DSPE

Connect 2 Cleanrooms BV
Newtonlaan 115
Zen Building
3584 BH Utrecht
Nederland
T +31 (0)30 210 60 51
E info@connect2cleanrooms.com
W www.connect2cleanrooms.nl

Our cleanroom solutions are bespoke and scalable, encouraging efficiency through flexible design. We help organisations reduce failure rates by getting it right first time.

member DSPE

Development

TNO
T + 31 (0)88-866 50 00
W www.tno.nl

TNO is an independent innovation organisation that connects people and knowledge in order to create the innovations that sustainably boosts the competitiveness of industry and wellbeing of society.

member DSPE

Development and Engineering

Segula Technologies Nederland B.V.
De Witbogt 2
5652 AG Eindhoven
T +31 (0)40 8517 500
W www.segula.nl

SEGULA Technologies Nederland BV develops advanced intelligent systems for the High Tech and Automotive industry. As a project organisation, we apply our (engineering) knowledge to non-linear systems. This knowledge is comprised of systems architecture and modelling, analysis, mechanics, mechatronics, electronics, software, system integration, calibration and validation.

member DSPE

Education

Leiden school for Instrumentmakers (LiS)
Einsteinweg 61
2333 CC Leiden
The Netherlands
T +31 (0)71-5681168
E info@lis.nl
W www.lis.nl

The LiS is a modern level 4 MBO school with a long history of training Research instrumentmakers. The school establishes projects in cooperation with industry and scientific institutes thus allowing for professional work experience for our students. LiS TOP accepts contract work and organizes courses and summer school programs for those interested in precision engineering.

member DSPE

Electrical Discharge Machining (EDM)

CVT BV
Heiberg 29C
5504 PA Veldhoven
The Netherlands
T +31 (0)497 54 10 40
E info@cvtbv.nl
W www.heinmade.com

Partner high tech industry for wire EDM precision parts. Flexible during day shifts for prototyping. Outside office hours low cost unmanned machining. Call and enjoy our expertise!

member DSPE

Ter Hoek Vonkerosie
Propaanstraat 1
7463 PN Rijssen
T +31 (0)548 540807
F +31 (0)548 540939
E info@terhoek.com
W www.terhoek.com

INNOVATION OF TOMORROW, INSPIRATION FOR TODAY
Staying ahead by always going the extra mile. Based on that philosophy, Ter Hoek produces precision components for the high-tech manufacturing industry.

We support customers in developing high-quality, custom solutions that can then be series-produced with unparalleled accuracy. That is what makes us one of a kind.
It is in that combination of innovative customization and repeated precision that we find our passion. Inspired by tomorrow's innovation, each and every day.

member DSPE

Lasers, Light and Nanomotion

Laser 2000 Benelux C.V.
Voorbancken 13a
3645 GV Vinkeveen
Postbus 20, 3645 ZJ Vinkeveen
T +31(0)297 266 191
F +31(0)297 266 134
E info@laser2000.nl
W www.laser2000.nl

Laser 2000 Benelux considers it her mission to offer customers the latest photonics technologies available.
Our areas of expertise are:
- Lasers, scanners and laser machines for industry and research
- Light metrology instruments for LED and luminaire industries
- Light sources for scientific applications
- Piezo- and stepper motion products for nano- and micro positioning
- Inspection and research grade high speed cameras
- Laser safety certified products

Te Lintelo Systems B.V.
Mercurion 28A
6903 PZ Zevenaar
T +31 (0)316 340804
E contact@tlsbv.nl
W www.tlsbv.nl

Photonics is our passion!
Our experienced team is fully equipped to assist you with finding your best optical business solution.
For over 35 years TLS represent prominent suppliers in the photonics industry with well-educated engineers, experience and knowledge.
Over the years we became the specialist in the field of:
- Lasers
- Light metrology,
- Opto-electronic equipment,
- Positioning equipment
- Laser beam characterization and positioning,
- Interferometry,
- (Special) Optical components,
- Fiber optics,
- Laser safety

Together with our high end suppliers we have the answer for you!

Mechatronics Development

SOURCE OF YOUR TECHNOLOGY

Sioux CCM
De Pinckart 24
5674 CC Nuenen
T +31 (0)40 2635000
F info.ccm@sioux.eu
W www.sioux.eu

Sioux CCM is a technology partner with a strong focus on mechatronics.
We help leading companies with the high-tech development, industrialization and creation of their products, from concept stage to a prototype and/or delivery of series production.
Commitment, motivation, education and skills of our employees are the solid basis for our business approach

Sioux CCM is part of the Sioux Group.

member DSPE

CREATING MACHINES TOGETHER

Manufacturing Technical Assemblies (MTA) b.v.
Waterbeemd 8
5705 DN Helmond
T +31 (0)492 474992
E info@m-t-a.nl
W www.m-t-a.nl

MTA is an high-tech system supplier specialized in the development and manufacturing of mechatronic machines and systems.
Our clients are OEM s in the Packaging, Food, Graphics and High-tech industries.

member DSPE

Mechatronics Development

PARTNERS IN MECHATRONIC INNOVATION

MI-Partners
Dillenburgstraat 9N
5652 AM Eindhoven
The Netherlands
T +31 (0)40 291 49 20
F +31 (0)40 291 49 21
E info@mi-partners.nl
W www.mi-partners.nl

MI-Partners is active in R&D of high-end mechatronic products and systems. We are specialised in concept generation and validation for ultra-fast (>10g), extremely accurate (sub-nanometers) or complex positioning systems and breakthrough production equipment.

member DSPE

Metal Precision Parts

ETCHFORM METAL PRECISION PARTS

Etchform BV
Arendstraat 51
1223 RE Hilversum
T +31 (0)35 685 51 94
F info@etchform.com
W www.etchform.com

Etchform is a production and service company for etched and electroformed metal precision parts.

member DSPE

Micro Drive Systems

maxon motor
driven by precision

Maxon Motor Benelux

The Netherlands

Head Office
maxon motor benelux bv
Josink Kolkweg 38
7545 PR Enschede

South
High Tech Campus 9
5656 AE Eindhoven
T +31(053) 744 0 744
E info@maxonmotor.nl
W www.maxonmotor.nl

Belgium / Luxembourg

maxon motor benelux bv
Schaliënhoevedreef 20C
2800 Mechelen - Belgium
T +32 (15) 20 00 10
F +32 (15) 27 47 71
E info@maxonmotor.be
W www.maxonmotor.be

maxon motor is the worldwide leading supplier of high precision drives and systems. When it really matters! Try us.

member DSPE

Micro Drive Systems

FAULHABER Benelux B.V.
Drive Systems
High Tech Campus 9
5656 AE Eindhoven
The Netherlands
T +31 (0)40 85155-40
E info@faulhaber.be
E info@faulhaber.nl
W www.faulhaber.com

FAULHABER specializes in the development, production and deployment of high-precision small and miniaturized drive systems, servo components and drive electronics with output power of up to 200 watts. The product range includes brushless motors, DC micromotors, encoders and motion controllers.
FAULHABER also provides customer-specific complete solutions for medical technology, automatic placement machines, precision optics, telecommunications, aerospace and robotics, among other things.

Physik Instrumente (PI) Benelux BV
Hertog Hendrikstraat 7a
5492 BA Sint-Oedenrode
The Netherlands
T +31 (0)499-375375
F +31 (0)499 375373
E benelux@pi.ws
W www.pi.ws

PI is the world's leading provider of nanopositioning products and systems. All key technologies are developed, manufactured and qualified in-house by PI: Piezo components, actuators and motors, magnetic drives, guiding systems, nanometrology sensors, electronic amplifiers, digital controllers and software.

member DSPE

Motion Control Systems

Aerotech United Kingdom
The Old Brick Kiln
Ramsdell, Tadley
Hampshire RG26 5PR
UK
T +44 (0)1256 855055
F +44 (0)1256 855649
W www.aerotech.co.uk

Newport Spectra-Physics B.V.
Vechtensteinlaan 12 - 16
3555 XS Utrecht
T +31 (0)30 6592111
E netherlands@newport.com
W www.newport.com

Newport Spectra-Physics B.V. is a subsidiary of Newport, a leader in nano and micro positioning technologies with an extensive catalog of positioning and motion control products. Newport is part of MKS Instruments Inc., a global provider of instruments, subsystems and process control solutions that measure, control, power, monitor, and analyze critical parameters of advanced processes in manufacturing and research applications.

member DSPE

Motion Control Systems

Physik Instrumente (PI) Benelux BV
Hertog Hendrikstraat 7a
5492 BA Sint-Oedenrode
The Netherlands
T +31 (0)499-375375
F +31 (0)499 375373
E benelux@pi.ws
W www.pi.ws

PI is the world's leading provider of nanopositioning products and systems. All key technologies are developed, manufactured and qualified in-house by PI: Piezo components, actuators and motors, magnetic drives, guiding systems, nanometrology sensors, electronic amplifiers, digital controllers and software.

member DSPE

Optical Components

Molenaar Optics
Gerolaan 63A
3707 SH Zeist
T +31 (0)30 6951038
E info@molenaar-optics.nl
W www.molenaar-optics.eu

Molenaar Optics is offering optical engineering solutions and advanced products from world leading companies OptoSigma, Sill Optics and Pyser Optics.

member DSPE

Piezo Systems

HEINMADE BV
Heiberg 29C
NL - 5504 PA Veldhoven
T +31 (0)40 851 2180
E info@heinmade.com
W www.heinmade.com

As partner for piezo system solutions, HEINMADE serves market leaders in the high tech industry. Modules and systems are developed, produced and qualified in-house. HEINMADE distributes Noliac piezo components.

member DSPE

Piezo Systems

Physik Instrumente (PI) Benelux BV
Hertog Hendrikstraat 7a
5492 BA Sint-Oedenrode
The Netherlands
T +31 (0)499-375375
F +31 (0)499 375373
E benelux@pi.ws
W www.pi.ws

PI is the world's leading provider of nanopositioning products and systems. All key technologies are developed, manufactured and qualified in-house by PI: Piezo components, actuators and motors, magnetic drives, guiding systems, nanometrology sensors, electronic amplifiers, digital controllers and software.

member DSPE

Ultra-Precision Metrology & Engineering

IBS Precision Engineering
Esp 201
5633 AD Eindhoven
T +31 (0)40 2901270
F +31 (0)40 2901279
E info@ibspe.com
W www.ibspe.com

IBS Precision Engineering delivers world class measurement, positioning and motion systems where ultra-high precision is required. As a strategic engineering partner to the world's best manufacturing equipment and scientific instrument suppliers, IBS has a distinguished track record of proven and robust precision solutions. Leading edge metrology is at the core of all that IBS does. From complex carbon-fibre jet engine components to semiconductor chips accurate to tens of atoms; IBS has provided and engineered key enabling technologies.

member DSPE

ADVERTISERS INDEX


If you can sketch it,
we can etch it.
ETCHFORM
METAL
PRECISION
PARTS
ETCHING
& ELECTROFORMING
www.etchform.com - info@etchform.com


HEIDENHAIN
4714-1211